Theoretical Studies for Nuclear Magnetic Shieldings in Solution

YAMAZAKI Takeshi

DOCTOR OF PHILOSOPHY

Department of Functional Molecular Science
School of Mathematical and Physical Science
The Graduate University for Advanced Studies

2001

Acknowledgment

This thesis is a summary of my studies from 1999 to 2001 at the Department of Functional Molecular Science, the Graduate University for Advanced Studies. This work has been carried out under the supervision of Professor Fumio Hirata at Institute for Molecular Science. I would like to express my gratitude to him who has given me a chance to study the electronic structure theory in solution here, has supported me constantly in the research environment, and has given me many fruitful suggestions. I also would like to thank Dr. Hirofumi Sato for his constant guidance, criticism, and encouragement. I am thankful to all the members of the Hirata group and my friends for their kindness. It should be emphasized that this work could not be carried out without their support. I am most thankful to my parents for their support, understanding, and encouragement. Finally, it should be added that I thank to all people who are kindly patient with my bad drunk attitudes.

Contents

Chapter 1

Introduction

Nuclear magnetic resonance (NMR) spectroscopy[1] measures the transitions between energy levels of the nuclear magnetic moment split by the external magnetic field. This spectroscopy principally has three features as follows. First, the nuclear magnetic moment is a very sensitive and site-specific probe of microscopic environment in which the nucleus is situated. Second, perturbation due to the NMR measurement is very small relative to other spectroscopies. While the resonance frequency of NMR spectroscopy is approximately 10^{-19} erg in energy, for example, the energy of the X-ray is about 10^{-9} erg. The system in question, thus, is not affected much by NMR observation. Finally, unlike other experimental methods(UV, Raman, IR, and neutron scattering), NMR directly probes the electron density at a nucleus. In other words, NMR can measure how a nucleus is shielded by electrons in its vicinity. Owing to these features, NMR spectroscopy in solutions occupies a unique position for studying the structure and dynamics of materials in areas of chemistry, biology and medicine.[2]

I Principles of Nuclear Magnetic Resonance

In this section, the principle of NMR is reviewed briefly. Any nucleus with a non-zero spin quantum number, **I**, has a magnetic moment, **m**, associated with it, which can interact

with an applied external magnetic field, $\mathbf{B}$. This interaction can be represented as follows

$$\begin{aligned} \mathcal{H} &= -\gamma\hbar\mathbf{I}\cdot\mathbf{B} \\ &= -\mathbf{m}\cdot\mathbf{B}, \end{aligned} \tag{1.1}$$

where γ is the magnetogyric ratio. $\hbar$ is equal to $\frac{h}{2\pi}$, where h is the Planck's constant. The interaction energy, E, associated with the above Hamiltonian is,

$$E = -\gamma\hbar B m_I, \tag{1.2}$$

where B is the strength of the magnetic field applied along the z-axis and m_I is the magnetic spin quantum number which can have any of the following values

$$m_I = I, I-1, I-2, \cdots, -I+2, -I+1, -I. \tag{1.3}$$

In the case of proton which has $I = \frac{1}{2}$, m_I can either be $+\frac{1}{2}$ or $-\frac{1}{2}$. The energy difference, ΔE, called as the Zeeman energy, is

$$\Delta E = \mid \hbar\omega_0 \mid, \tag{1.4}$$

where ω_0 is the resonance frequency called as the Larmor frequency:

$$\omega_0 = \gamma B. \tag{1.5}$$

A transition between these two energy levels can be induced by applying a second field, $\mathbf{B}'$, perpendicular to $\mathbf{B}$ and oscillating at the resonance frequency ω_0. Since each nucleus has its own characteristic magnetogyric ratio, distinctive frequencies for each type of nuclei at a given static field $\mathbf{B}$, can be detected. This leads to the nuclear-specificity of NMR spectroscopy. Nuclei normally find themselves among electrons which are continuously in motion in an atom or a molecule. The applied magnetic field causes currents of electrons which, in turn, induce a secondary local magnetic field at any given nuclear site. Thus a nucleus in a molecule sees a local field that may be less(shielded) or greater(deshielded) in magnitude as compared with the applied field, depending on the behavior and distribution

of the electrons in its immediate vicinity. The local or actual magnetic field, $\mathbf{B}^{\text{local}}$, experienced by the nucleus can be expressed as

$$\mathbf{B}^{\text{local}} = (1 - \boldsymbol{\sigma})\mathbf{B}, \tag{1.6}$$

where $\boldsymbol{\sigma}$ is the nuclear magnetic shielding tensor reflecting the molecular electronic properties specific to a given nuclear site. In liquid, gas-phase, or solution NMR, only one value of the shielding property is observed owing to the free tumbling motion of molecules which results in averaging of the shielding tensor over all orientations of the molecule with respect to the applied magnetic field. In most cases, molecules do not prefer a single orientation so the averaging which takes place is isotropic. The observed value referred to as the isotropic shielding value is the average of the principle components

$$\sigma_{\text{iso}} = \frac{\sigma_{11} + \sigma_{22} + \sigma_{33}}{3}, \tag{1.7}$$

and from now on, only the isotropic shielding value is considered in this thesis. As can be readily seen from eq. (1.6), σ is the index of shielding referenced to the bare nucleus. Usually, certain compounds are chosen as convenient references or standards. For example, in the case of proton NMR, tetramethylsilane (TMS) is chosen as the reference. The normally reported quantity is defined as

$$\begin{aligned} \delta &= \frac{\nu - \nu^{\text{ref}}}{\nu^{\text{ref}}} \\ &= \frac{\sigma^{\text{ref}} - \sigma}{1 - \sigma^{\text{ref}}}, \end{aligned} \tag{1.8}$$

where $\nu = \frac{\omega_0}{2\pi}$ is the resonance frequency in Hertz, directly measured in the NMR spectroscopy. Since $\sigma \ll 1$, δ can be rewritten as

$$\delta = \sigma^{\text{ref}} - \sigma. \tag{1.9}$$

δ is called as the chemical shift, and this is a significant part of the NMR spectral information. It is noted that the chemical shift is in an opposite direction compared with shielding. Positive chemical shift indicates more deshielded environment than in the case of reference.

II Experimental Motivations

Chemical shifts have long been used as tools for covalent structural analysis, and it has recently played an especially important role in structural understanding of proteins and nucleic acids. An application of the method to protein structure by utilizing the high resolution-high pressure NMR spectroscopy[3] is a good example of those studies. In that study, proton chemical shifts of a protein in solution are measured with varying pressure. From a set of the chemical shifts resolved for each amino acid residue, it has been concluded that pressure induces important substates of protein ranging from native to completely denatured, which can be regarded as conformational fluctuations of the molecule in ambient pressure. In other words, the free energy landscape of a protein could have been realized by applying pressure as an order parameter, and the site-specific information of the NMR chemical shift has made the realization possible. The NMR chemical shift can also provide detailed information about intermolecular interaction in solution. Hydrogen bonds, for example, are one of the most important interactions in solution, and the proton chemical shift is most widely used for investigating the interaction.

Study of the hydrophobic hydration[4, 5] is of particular importance due to its relation with stability of biomolecules in aqueous solution. The major emphasis of the studies has been put on determining the structuring or destructuring effect on water around an apolar solute, i.e., on determining whether hydrogen bonds between water molecules around the solute are enhanced or not. The proton chemical shift, which is a direct measure of the hydrogen bond, has been utilized in this problem in company with some thermodynamic measurements. In general, low-field chemical shifts of water in solution have been interpreted as structuring of water, i.e., increased strength or number of water-water hydrogen bonds, by apolar solutes. Decrease in structure would reduce hydrogen bonds, cause more shielding of a hydrogen nucleus, and thus give rise to a high-field shift. Although both chemical shifts and thermodynamic measurements have provided profitable information, current understanding of the hydrophobic hydration is far from complete. This originates

from the two difficulties. First, the difficulty in connecting two properties: the chemical shift as microscopic properties in one hand and macroscopic thermodynamic properties on the other hand. Second, the difficulty in understanding the chemical shift in solution. The chemical shift in solution is determined by two contributions: contribution from the change in the molecular structure due to solvation, and contribution from solvation structure around the molecule. If there would be a theory which can give thermodynamic properties, solvation structures, and chemical shifts consistently and nonempirically, it could provide valuable insight into a mechanism of the hydrophobic hydration. Obviously, the two difficulties mentioned above are generally true for all studies in solution utilizing the NMR chemical shift. Such consideration has motivated the present study to build up a theory of the NMR chemical shift in solution.

III Theories of Chemical Shift in Solution

Theories of the chemical shift in solution have not been well developed due to a number of reasons: the most important has been the lack of a theory to describe the electronic structure of a molecule in solution. As can be readily understood, the electronic structure is of primary significance in determining the magnetic shielding of a nucleus. However, the electronic structure is modified largely by solvent when the molecule is in solution. Such effects manifested in the effective charge of atoms amount to 10 - 40 % sometimes, and it can never be neglected. In addition, the NMR chemical shift is a very sensitive and site-specific probe of environment as mentioned above. Therefore, a successful theory to describe the NMR chemical shift should be able to treat the microscopic solvent effect on the electronic structure.

Approaches based on the continuum model have been used for various problems in solutions, and have given reasonable agreements with experimental data despite of its model for over simplified solvent. Recently, the continuum model was extended for calculating the chemical shift,[6, 7, 8] and qualitatively correct results were obtained. However,

the chemical shift is a microscopic probe which is highly sensitive not only to the structure of the molecule in question but to the microscopic intermolecular interactions such as hydrogen bonds. The description due to the oversimplified solvent model may mislead to wrong conclusions with respect to the microscopic process occurring in solution.

The approaches based on the molecular simulations[9, 10] seem to be promising for studying the NMR chemical shifts in solutions, since it is capable of taking the molecular details of solvent into account. However, the approach in the current stage requires some empirical processes to obtain the NMR chemical shift, which casts a shadow on its predictability. Owing to the development of computer, the NMR chemical shift has been obtained by carrying out the *ab initio* calculation for molecular clusters selected from the configuration space sampled by the molecular simulation.[11, 12] The cluster approach is indeed attractive because the intermolecular interactions can be treated entirely with quantum chemistry. A problem inherent to this approach is the convergence: it will be extremely difficult to find out how many samples (configurations) of a cluster and how many molecules for a cluster are needed for convergence of the physical properties in question. If the convergence is very slow, the computational load will become a serious problem.

Very recently, the QM/MM method was extended for calculating the chemical shifts,[13] and the effect of solvation on the chemical shift was studied using solvent configurations obtained by the molecular dynamics simulation. The QM/MM approach is superior to the cluster approach in the sense that the former includes the effect from bulk solvent. However, this method has the same problem as the cluster approach: how many samples of a cluster and how many molecules for a cluster are needed for convergence of the physical properties in question.

IV Purpose

In this thesis, in order to understand the relation between the NMR chemical shift and the solvation structure, a new theory for treating the nuclear magnetic shieldings in solutions

is proposed, based on the *ab initio* electronic structure theory combined with the reference interaction site model[14, 15] in statistical mechanics for molecular liquids(RISM-SCF[16, 17]). The RISM-SCF method treats both solute and solvent molecules in atomic level, and determines the solute electronic structure and the statistical solvent distribution in a self-consistent manner. Thus, the method provides a microscopic picture for the solvent effect on the electronic structure of a solute molecule within reasonable computation cost. Furthermore, this approach is suitable for studying the relationship between the chemical shifts and solute-solvent interactions, because the RISM-SCF method treats a solute-solvent system, in which a solute molecule is at infinite dilution in solvents.

In chapter 2, the theoretical background to treat the magnetic shielding in solution are reviewed briefly. In chapter 3, the theory for the magnetic shielding in solution is presented. In chapter 4, preliminary results for the chemical shifts of a water molecule solvated in water are shown, and the results for the proton chemical shifts of a water molecule solvated in various solvents are discussed. Furthermore, the effect of the overlap of electron clouds between solute and solvent on the chemical shift, which is disregarded in the present framework, is discussed briefly using molecular cluster. The conclusions are presented in chapter 5.

References

[1] For example: (a)M. Hirota, *NMR NYUMON* (Tokyo Kagaku Dojin, 1994) (in Japanese). This is the translation of *NMR and Chemistry* written by J. W. Akitt (Chapman & Hall, London, 1992). (b)K. Akasaka and T. Imoto, *PARUSU OYOBI FURIE HENKAN NMR* (Yoshioka, 1990) (in Japanese). This is the translation of *Pulse and Fourier Transform NMR* written by T. C. Farrar and E. D. Becker (Academic Press, 1971). (c)M. Kotani and K. Kobe, *BUSSHITSU NO DENKI BUNKYOKU TO JISEI* (Yoshioka, 1974). This is the translation of *The Theory of Electric and Magnetic Susceptibilities* written by J. H. van Vleck (Oxford University Press, 1932). (d)Y. Arata, *NMR NO SHO* (Maruzen, 2000) (in Japanese). (e)J. K. M. Sanders and B. K. Hunter *Modern NMR Spectroscopy* (Oxford University Press, New York, 1987). (f)C. P. Slichter, *Principle of Magnetic Resonance* (Springer-Verlag, Berlin, 1978).

[2] *Encyclopedia of Nuclear Magnetic Resonance*, edited by D. M. Grant and R. K. Harris (Wiley, New York, 1996).

[3] K. Akasaka and H. Yamada, in *Methods in Enzymology*, edited by T. L. James, V. Dötsch, and U. Schmitz, (Academic Press, New York, 2001), vol. 338, p. 134.

[4] A. Ben-Naim, *Hydrophobic Interactions*, (Plenum, New York,1980).

[5] C. Tanford, *The Hydrophobic Effect* 2nd Ed., (Wiley, New York, 1980).

[6] D. Cremer, L. Olsson, F. Reichel, and E. Kraka, Isr. J. Chem. **33**, 369 (1993).

[7] K. V. Mikkelsen, P. Jørgensen, K. Ruud, and T. Helgaker, J. Chem. Phys. **106**, 1170 (1997).

[8] R. Cammi, B. Mennucci, and J. Tomasi, J. Chem. Phys. **110**, 7627 (1999).

[9] I. M. Svishchev and P. G. Kusalik, J. Am. Chem. Soc. **115**, 8270 (1993).

[10] T. M. Nymand, P.-O. Åstrand, and K. V. Mikkelsen, J. Phys. Chem. B **101**, 4105 (1997).

[11] D. B. Chesnut and B. E. Rusiloski, J. Mol. Struct.: THEOCHEM **314**, 19 (1994).

[12] V. G. Malkin, O. L. Malkina, G. Steinebrunner, and H. Huber, Chem. Eur. J. **2**, 452 (1996).

[13] Q. Cui and M. Karplus, J. Phys. Chem. B **104**, 3721 (2000).

[14] D. Chandler and H. C. Andersen, J. Chem. Phys. **57**, 1930 (1972).

[15] F. Hirata and P. J. Rossky, Chem. Phys. Lett. **83**, 329 (1981).

[16] S. Ten-no, F. Hirata, and S. Kato, J. Chem. Phys. **100**, 7443 (1994).

[17] H. Sato, F. Hirata, and S. Kato, J. Chem. Phys. **105**, 1546 (1996).

Chapter 2

Background Theory

In this chapter, I describe our theory of the NMR chemical shift in solutions, which are founded on three theoretical elements: the quantum chemistry of NMR chemical shift,[1] the statistical mechanics of molecular liquids,[2] and the electronic structure theory of a molecule in solution.[3] In the next chapter, I combine those elements to describe solvent effect on the chemical shift in solution.

I Theory of NMR Shielding Constant in Gas Phase

The electronic Hamiltonian describing a closed shell molecule in the magnetic field composed of an uniform external magnetic field $\mathbf{B}$ and the dipole fields arising from nuclear magnetic moments $\mathbf{m}$ situated at fixed nuclear positions has the form (in atomic units)

$$\mathcal{H}(\mathbf{B},\mathbf{m}) = \frac{1}{2}\sum_j\{-i\nabla_j + \frac{1}{c}\mathbf{A}(\mathbf{r}_j)\}^2 - \sum_j\sum_N \frac{Z_N}{r_{jN}} + \sum_{j<l}\frac{1}{r_{jl}} + \sum_{N<N'}\frac{Z_N Z_{N'}}{R_{NN'}}. \quad (2.1)$$

Here, c is the velocity of light, $\sum_j$ is a sum over all electrons and $\sum_N$ is a sum over all nuclei. The last three terms represent the electron-nucleus, electron-electron and nucleus-nucleus contribution to the potential energy, respectively. The vector potential describing the interaction between the total magnetic field and jth electron, $\mathbf{A}(\mathbf{r}_j)$, is given by

$$\mathbf{A}(\mathbf{r}_j) = \frac{1}{2}\mathbf{B}\times\mathbf{r}_j + \sum_N \frac{\mathbf{m}^N \times \mathbf{r}_{jN}}{r_{jN}^3}, \quad (2.2)$$

where $\mathbf{r}_j$ is the position of an electron with respect to an arbitrarily chosen gauge origin, and $\mathbf{r}_{jN}$ is the position of an electron relative to the position $\mathbf{R}_N$ at which the nucleus with

charge Z_N is located. $\mathbf{r}_{jl}$ and $\mathbf{R}_{NN'}$ are the vectors $\mathbf{r}_j - \mathbf{r}_l$ and $\mathbf{R}_N - \mathbf{R}_{N'}$, respectively. The energy $E(\mathbf{B}, \mathbf{m})$ associated with this Hamiltonian can be found by solving the Schrödinger equation

$$\mathcal{H}(\mathbf{B}, \mathbf{m})\Psi(\mathbf{B}, \mathbf{m}) = E(\mathbf{B}, \mathbf{m})\Psi(\mathbf{B}, \mathbf{m}), \tag{2.3}$$

where $\Psi(\mathbf{B}, \mathbf{m})$ is the wavefunction describing the molecular electronic state in the presence of $\mathbf{B}$ and $\mathbf{m}$. $E(\mathbf{B}, \mathbf{m})$ can be expanded in a Taylor series of the magnetic fields $\mathbf{B}$ and $\mathbf{m}$ about their zero-field values:

$$\begin{aligned} E(\mathbf{B}, \mathbf{m}) &= E^{(0)} + \sum_{\alpha} (E^{(1,0)})_{\alpha} B_{\alpha} + \sum_{N} \sum_{\alpha} (E^{(0,1)})^{N}_{\alpha} m^{N}_{\beta} \\ &\quad + \frac{1}{2} \sum_{\alpha} \sum_{\beta} B_{\alpha} (E^{(2,0)})_{\alpha\beta} B_{\beta} + \sum_{N} \sum_{\alpha} \sum_{\beta} B_{\alpha} (E^{(1,1)})^{N}_{\alpha\beta} m^{N}_{\beta} \\ &\quad + \frac{1}{2} \sum_{N} \sum_{N'} \sum_{\alpha} \sum_{\beta} m^{N}_{\alpha} (E^{(0,2)})^{NN'}_{\alpha\beta} m^{N'}_{\beta} + \cdots, \end{aligned} \tag{2.4}$$

where $E^{(0)}$ indicates the energy without external fields, and $(E^{(i,j)})_{\alpha\beta}$ are for example,

$$(E^{(1,0)})_{\alpha} = \left. \frac{\partial E(\mathbf{B}, \mathbf{m})}{\partial B_{\alpha}} \right|_{\mathbf{B}=0}, \tag{2.5}$$

$$(E^{(1,1)})^{N}_{\alpha\beta} = \left. \frac{\partial^2 E(\mathbf{B}, \mathbf{m})}{\partial B_{\alpha} \partial m^{N}_{\beta}} \right|_{\mathbf{B},\mathbf{m}=0}, \tag{2.6}$$

where α and β are the subscripts referring to x, y, z-components, respectively. N indicates the nucleus.

In the framework of the perturbation theory, the nuclear magnetic shielding tensor of nucleus X is defined as the mixed second derivative of the energy with respect to the external magnetic field and the nuclear magnetic moment :

$$\sigma^{X}_{\alpha\beta} = (E^{(1,1)})^{X}_{\alpha\beta}. \tag{2.7}$$

Note that $\sum_{\alpha} B_{\alpha} (E^{(1,1)})^{X}_{\alpha\beta}$ in eq. (2.4) corresponds to the secondary magnetic field at the nucleus X due to the electronic currents. Thus the total magnetic field experienced by

the nucleus X which is measured by the NMR machine as resonance frequency is given by $\mathbf{B}(1-\boldsymbol{\sigma}^X)$.

In the SCF perturbation theory one seeks a solution $\Psi(\mathbf{B},\mathbf{m})$ to eq. (2.3) as a single determinant of molecular orbitals(MOs), $\phi_i(\mathbf{B},\mathbf{m})$. In the absence of magnetic field, it is usual to represent each MO as a linear combination of atomic orbitals(AOs), where the AOs are taken in the real form. On the other hand, in the presence of magnetic field, AOs should be taken in the complex form to obtain the magnetic shielding constants which are independent of the gauge of the vector potential. Therefore, each MO is expressed as:

$$\phi_i(\mathbf{B},\mathbf{m}) = \sum_{\nu} c_{i\nu}(\mathbf{B},\mathbf{m})\chi_v(\mathbf{B}), \tag{2.8}$$

where

$$\begin{aligned}\chi_\nu(\mathbf{B}) &= \exp\left(-\frac{i}{c}\mathbf{A}_\nu\cdot\mathbf{r}\right)\varphi_\nu \\ &= f_\nu\varphi_\nu.\end{aligned} \tag{2.9}$$

$\chi_v(\mathbf{B})$ is called as the gauge-invariant AO(GIAO), and the method calculating the magnetic shielding constant using the GIAO is referred as the GIAO method. In eq. (2.9), $\mathbf{A}_\nu = \frac{1}{2}\mathbf{B}\times\mathbf{R}_\nu$ is the value of the vector potential at the nucleus position $\mathbf{R}_\nu$ of the real atomic orbital φ_ν. $\mathbf{r}$ is the position vector of an electron. The Hartree-Fock-Roothaan equation in the presence of magnetic field is lead from the usual variational procedure:

$$\sum_{\lambda}\left[F_{\nu\lambda}(\mathbf{B},\mathbf{m}) - \epsilon_j(\mathbf{B},\mathbf{m})S_{\nu\lambda}(\mathbf{B})\right]c_{j\lambda}(\mathbf{B},\mathbf{m}) = 0, \tag{2.10}$$

where the Fock matrix elements $F_{\nu\lambda}(\mathbf{B},\mathbf{m})$ are given by

$$F_{\nu\lambda}(\mathbf{B},\mathbf{m}) = H_{\nu\lambda}(\mathbf{B},\mathbf{m}) + G_{\nu\lambda}(\mathbf{B},\mathbf{m}). \tag{2.11}$$

The one and two electron terms are given by

$$H_{\nu\lambda}(\mathbf{B},\mathbf{m}) = \langle\chi_\nu \mid \frac{1}{2}\{-i\nabla + \frac{1}{c}\mathbf{A}(\mathbf{r})\}^2 - \sum_N \frac{Z_N}{r_N} \mid \chi_\lambda\rangle, \tag{2.12}$$

$$G_{\nu\lambda}(\mathbf{B},\mathbf{m}) = \sum_{\varsigma\xi} P_{\varsigma\xi}(\mathbf{B},\mathbf{m})\{(\chi_\nu\chi_\lambda|\chi_\varsigma\chi_\xi) - \frac{1}{2}(\chi_\nu\chi_\xi|\chi_\varsigma\chi_\lambda)\}, \tag{2.13}$$

respectively. $S_{\nu\lambda}(\mathbf{B})$ is the overlap integral and $P_{\nu\lambda}(\mathbf{B},\mathbf{m})$ is the density matrix element. $\epsilon_j(\mathbf{B},\mathbf{m})$ is the MO energy. The total energy $E(\mathbf{B},\mathbf{m})$ is written by

$$E\left(\mathbf{B},\mathbf{m}\right)=\sum_{\nu\lambda}P_{\nu\lambda}\left(\mathbf{B},\mathbf{m}\right)\left\{H_{\nu\lambda}\left(\mathbf{B},\mathbf{m}\right)+\frac{1}{2}G_{\nu\lambda}\left(\mathbf{B},\mathbf{m}\right)\right\}. \tag{2.14}$$

Note that $c_{j\lambda}(\mathbf{B},\mathbf{m})$ and $P_{\nu\lambda}\left(\mathbf{B},\mathbf{m}\right)$ can be expanded as

$$c_{j\lambda}(\mathbf{B},\mathbf{m})=c_{j\lambda}^{(0)}+\sum_{\alpha}i\left(c_{j\lambda}^{(1,0)}\right)_{\alpha}B_{\alpha}+\sum_{N}\sum_{\alpha}i\left(c_{j\lambda}^{(0,1)}\right)_{\alpha}^{N}m_{\alpha}^{N}+\cdots, \tag{2.15}$$

$$P_{\nu\lambda}(\mathbf{B},\mathbf{m})=P_{\nu\lambda}^{(0)}+\sum_{\alpha}i\left(P_{\nu\lambda}^{(1,0)}\right)_{\alpha}B_{\alpha}+\sum_{N}\sum_{\alpha}i\left(P_{\nu\lambda}^{(0,1)}\right)_{\alpha}^{N}m_{\alpha}^{N}+\cdots. \tag{2.16}$$

Differentiating eq. (2.14) with respect to m_{β}^{X} leads to

$$\begin{aligned}\left.\frac{\partial E\left(\mathbf{B},\mathbf{m}\right)}{\partial m_{\beta}^{X}}\right|_{\mathbf{m}=0} &= \sum_{\nu\lambda}\frac{\partial}{\partial m_{\beta}^{X}}\left\{P_{\nu\lambda}\left(\mathbf{B},\mathbf{m}\right)\left(H_{\nu\lambda}\left(\mathbf{B},\mathbf{m}\right)+\frac{1}{2}G_{\nu\lambda}\left(\mathbf{B},\mathbf{m}\right)\right)\right\}\Bigg|_{\mathbf{m}=0}\\ &= \sum_{\nu\lambda}\left.\frac{\partial P_{\nu\lambda}\left(\mathbf{B},\mathbf{m}\right)}{\partial m_{\beta}^{X}}\right|_{\mathbf{m}=0}\left(H_{\nu\lambda}\left(\mathbf{B},\mathbf{m}\right)+G_{\nu\lambda}\left(\mathbf{B},\mathbf{m}\right)\right)|_{\mathbf{m}=0}\\ &\quad+\sum_{\nu\lambda}P_{\nu\lambda}\left(\mathbf{B},\mathbf{m}\right)|_{\mathbf{m}=0}\left.\frac{\partial H_{\nu\lambda}\left(\mathbf{B},\mathbf{m}\right)}{\partial m_{\beta}^{X}}\right|_{\mathbf{m}=0},\end{aligned} \tag{2.17}$$

where the relation

$$G_{\nu\lambda}\left(\mathbf{B},\mathbf{m}\right)=\sum_{\varsigma\xi}P_{\varsigma\xi}\left(\mathbf{B},\mathbf{m}\right)\left\{(\chi_{\nu}\chi_{\lambda}|\chi_{\varsigma}\chi_{\xi})-\frac{1}{2}(\chi_{\nu}\chi_{\xi}|\chi_{\varsigma}\chi_{\lambda})\right\} \tag{2.18}$$

and the fact that the GIAOs do not depend on the nuclear magnetic moment were used. This expression can be simplified by using the fact that the solutions of eq. (2.10) are constrained to be normalized for all values of $\mathbf{B}$ and $\mathbf{m}$

$$\sum_{\nu\lambda}c_{j\nu}^{*}\left(\mathbf{B},\mathbf{m}\right)S_{\nu\lambda}\left(\mathbf{B}\right)c_{j\lambda}\left(\mathbf{B},\mathbf{m}\right)=1. \tag{2.19}$$

Summing up over j, differentiating with respect to m_{β}^{X}, and using eq. (2.15), we obtain the following equation from eq. (2.19)

$$\begin{aligned}&\sum_{j}\sum_{\nu\lambda}\left\{\frac{\partial c_{j\nu}^{*}\left(\mathbf{B},\mathbf{m}\right)}{\partial m_{\beta}^{X}}S_{\nu\lambda}\left(\mathbf{B}\right)c_{j\lambda}\left(\mathbf{B},\mathbf{m}\right)\Big|_{\mathbf{m}=0}+c_{j\nu}^{*}\left(\mathbf{B},\mathbf{m}\right)S_{\nu\lambda}\left(\mathbf{B}\right)\left.\frac{\partial c_{j\lambda}\left(\mathbf{B},\mathbf{m}\right)}{\partial m_{\beta}^{X}}\right|_{\mathbf{m}=0}\right\}\\ &=\sum_{\nu\lambda}\left\{\left.\frac{\partial P_{\nu\lambda}\left(\mathbf{B},\mathbf{m}\right)}{\partial m_{\beta}^{X}}\right|_{\mathbf{m}=0}S_{\nu\lambda}\left(\mathbf{B}\right)\right\}\\ &=0.\end{aligned} \tag{2.20}$$

Since this relation holds for any $S_{\nu\lambda}$,

$$\left.\frac{\partial P_{\nu\lambda}(\mathbf{B},\mathbf{m})}{\partial m_\beta^X}\right|_{\mathbf{m}=0} = 0, \tag{2.21}$$

and therefore,

$$\left.\frac{\partial E(\mathbf{B},\mathbf{m})}{\partial m_\beta^X}\right|_{\mathbf{m}=0} = \sum_{\nu\lambda} P_{\nu\lambda}(\mathbf{B},\mathbf{m})|_{\mathbf{m}=0} \left.\frac{\partial H_{\nu\lambda}(\mathbf{B},\mathbf{m})}{\partial m_\beta^X}\right|_{\mathbf{m}=0}. \tag{2.22}$$

Differentiating eq. (2.22) with respect to B_α gives the expression for the nuclear magnetic shielding tensor of nucleus X as

$$\sigma_{\alpha\beta}^X = \sum_{\nu\lambda}\left\{P_{\nu\lambda}^{(0)}\left(H_{\nu\lambda}^{(1,1)}\right)_{\alpha\beta}^X + \left(P_{\nu\lambda}^{(1,0)}\right)_\alpha \left(H_{\nu\lambda}^{(0,1)}\right)_\beta^X\right\}. \tag{2.23}$$

In the above equation, for example,

$$\left(P_{\nu\lambda}^{(1,0)}\right)_\alpha = \left.\frac{\partial P_{\nu\lambda}}{\partial B_\alpha}\right|_{\mathbf{B},\mathbf{m}=0}, \tag{2.24}$$

$$\left(H_{\nu\lambda}^{(1,1)}\right)_{\alpha\beta}^X = \left.\frac{\partial^2 H_{\nu\lambda}}{\partial B_\alpha \partial m_\beta^X}\right|_{\mathbf{B},\mathbf{m}=0}. \tag{2.25}$$

Working in the Coulomb gauge, $\nabla\cdot\mathbf{A}=0$, and using the commutator

$$[-i\nabla + \frac{1}{c}\mathbf{A}(\mathbf{r}), \exp(-\frac{i}{c}\mathbf{A}_\lambda\cdot\mathbf{r})] = -\frac{1}{c}\mathbf{A}_\lambda \exp(-\frac{i}{c}\mathbf{A}_\lambda\cdot\mathbf{r}), \tag{2.26}$$

we can obtain the one electron term $H_{\nu\lambda}$ as follows:

$$\begin{aligned}
H_{\nu\lambda} &= \langle f_\nu^* f_\lambda \varphi_\nu \mid \frac{1}{2}\{-i\nabla + \frac{1}{c}\mathbf{A}(\mathbf{r}_\lambda)\}^2 - \sum_N \frac{Z_N}{r_N} \mid \varphi_\lambda\rangle \\
&= \langle f_\nu^* f_\lambda \varphi_\nu \mid \frac{1}{2}\{-\nabla^2 + \frac{1}{4c^2}(\mathbf{B}\times\mathbf{r}_\lambda)^2 + \frac{1}{c^2}\sum_N \frac{(\mathbf{m}^N\times\mathbf{r}_N)^2}{r_N^6} \\
&\quad - \frac{i}{c}(\mathbf{B}\times\mathbf{r}_\lambda)\cdot\nabla - \frac{2i}{c}\sum_N(\frac{\mathbf{m}^N\times\mathbf{r}_N}{r_N^3})\cdot\nabla \\
&\quad + \frac{1}{c^2}\sum_N(\mathbf{B}\times\mathbf{r}_\lambda)\cdot(\frac{\mathbf{m}^N\times\mathbf{r}_N}{r_N^3})\} - \sum_N \frac{Z_N}{r_N} \mid \varphi_\lambda\rangle,
\end{aligned} \tag{2.27}$$

where r_λ and r_N indicate the position of an electron relative to the position $\mathbf{R}_\lambda$ and $\mathbf{R}_N$, respectively. Differentiating eq. (2.27) with respect to B_α and m_β^X and with respect to

m_β^X gives

$$\left(H_{\nu\lambda}^{(0,1)}\right)_\beta^X = -\frac{i}{c}\langle\varphi_\nu \mid \frac{L_\beta^X}{r_X^3} \mid \varphi_\lambda\rangle, \tag{2.28}$$

$$\left(H_{\nu\lambda}^{(1,1)}\right)_{\alpha\beta}^X = \frac{1}{2c^2}\langle\varphi_\nu \mid \frac{\mathbf{r}_\lambda \cdot \mathbf{r}_X \delta_{\alpha\beta} - r_{\lambda\alpha} r_{X\beta}}{r_X^3} \mid \varphi_\lambda\rangle + \frac{1}{2c^2}\langle(\mathbf{R}_{\nu\lambda} \times \mathbf{r})_\alpha \varphi_\nu \mid \frac{L_\beta^X}{r_X^3} \mid \varphi_\lambda\rangle, \tag{2.29}$$

where L_β^X is the orbital angular momentum operator. $\mathbf{R}_{\nu\lambda}$ is the separation between $\mathbf{R}_\nu$ and $\mathbf{R}_\lambda$. $P_{\nu\lambda}^{(0)}$, $\left(H_{\nu\lambda}^{(1,1)}\right)_{\alpha\beta}^X$ and $\left(H_{\nu\lambda}^{(0,1)}\right)_\beta^X$ can be estimated from the conventional *ab initio* calculation, while $\left(P_{\nu\lambda}^{(1,0)}\right)_\alpha$ are determined by solving the first-order coupled-perturbed HF(CPHF) equation:

$$\sum_\lambda \left[\left(F_{\nu\lambda}^{(0)} - \epsilon_j^{(0)} S_{\nu\lambda}^{(0)}\right)\left(c_{j\lambda}^{(1,0)}\right)_\alpha + \left\{\left(F_{\nu\lambda}^{(1,0)}\right)_\alpha - \epsilon_j^{(0)}\left(S_{\nu\lambda}^{(1,0)}\right)_\alpha\right\} c_{j\lambda}^{(0)}\right] = 0. \tag{2.30}$$

Expanding eqs. (2.10) and (2.19) as Taylor series, separating orders, and equating with respect to $\mathbf{B}$, we can obtain the above CPHF equation. Note that $\left(c_{j\lambda}^{(1,0)}\right)_\alpha$, where j means the occupied orbitals, are required for $\left(P_{\nu\lambda}^{(1,0)}\right)_\alpha$. Suppose that $\left(c_{j\lambda}^{(1,0)}\right)_\alpha$ can be transformed to the unperturbed orbital $c_{j\lambda}^{(0)}$ as follows:

$$\left(c_{j\lambda}^{(1,0)}\right)_\alpha = \sum_k^{\text{occ}} U_{jk}^\alpha c_{k\lambda}^{(0)} + \sum_l^{\text{vir}} U_{jl}^\alpha c_{l\lambda}^{(0)}, \tag{2.31}$$

where U_{jk}^α is the transform matrix element. Substituting eq. (2.31) into eq. (2.30), and using the fact that unperturbed HF equation is already solved lead to

$$\sum_k^{\text{occ}} U_{jk}^\alpha \sum_\lambda \epsilon_k^{(0)} S_{\nu\lambda}^{(0)} c_{k\lambda}^{(0)} + \sum_l^{\text{vir}} U_{jl}^\alpha \sum_\lambda \epsilon_l^{(0)} S_{\nu\lambda}^{(0)} c_{l\lambda}^{(0)} - \sum_\lambda \epsilon_j^{(0)} S_{\nu\lambda}^{(0)} \left\{\sum_k^{\text{occ}} U_{jk}^\alpha c_{k\lambda}^{(0)} + \sum_l^{\text{vir}} U_{jl}^\alpha c_{l\lambda}^{(0)}\right\} + \sum_\lambda \left\{\left(F_{\nu\lambda}^{(1,0)}\right)_\alpha - \epsilon_j^{(0)}\left(S_{\nu\lambda}^{(1,0)}\right)_\alpha\right\} c_{j\lambda}^{(0)} = 0. \tag{2.32}$$

Multiplying the above equation on the left by $c_{m\nu}^{(0)}$, where m indicates the virtual orbitals, and summing up the equation with respect to ν, we can get

$$U_{jm}^\alpha = \frac{\sum_{\nu,\lambda} c_{m\nu}^{(0)} \left\{\left(F_{\nu\lambda}^{(1,0)}\right)_\alpha - \epsilon_j^{(0)}\left(S_{\nu\lambda}^{(1,0)}\right)_\alpha\right\} c_{j\lambda}^{(0)}}{\epsilon_j^{(0)} - \epsilon_m^{(0)}} \qquad \text{m: virtual orbitals.} \tag{2.33}$$

The first-order orthonormal conditions for the occupied orbitals, i and j, are written as

$$\sum_{\nu,\lambda}\left\{c_{i\nu}^{(0)}S_{\nu\lambda}^{(1,0)}c_{j\lambda}^{(0)}+\left(c_{i\lambda}^{(1,0)}\right)_{\alpha}S_{\nu\lambda}^{(0)}c_{j\lambda}^{(0)}+c_{i\nu}^{(0)}S_{\nu\lambda}^{(0)}\left(c_{j\lambda}^{(1,0)}\right)_{\alpha}\right\}=0. \tag{2.34}$$

Substituting eq. (2.31) into the above equation, we can obtain

$$U_{ji}^{\alpha}=-\frac{1}{2}\sum_{\nu,\lambda}c_{i\nu}^{(0)}S_{\nu\lambda}^{(1,0)}c_{j\lambda}^{(0)} \qquad \text{i: occupied orbitals.} \tag{2.35}$$

From eqs. (2.33) and (2.35), we can eventually reduce the expression for $\left(c_{j\lambda}^{(1,0)}\right)_{\alpha}$ as follows:

$$\begin{aligned}\left(c_{j\lambda}^{(1,0)}\right)_{\alpha}=&\sum_{k}^{\text{occ}}\left[-\frac{1}{2}\sum_{\zeta,\xi}c_{k\zeta}^{(0)}S_{\zeta\xi}^{(1,0)}c_{j\xi}^{(0)}\right]c_{k\lambda}^{(0)}\\&+\sum_{l}^{\text{vir}}\left[\frac{\sum_{\zeta,\xi}c_{l\zeta}^{(0)}\left\{\left(F_{\zeta\xi}^{(1,0)}\right)_{\alpha}-\epsilon_{j}^{(0)}\left(S_{\zeta\xi}^{(1,0)}\right)_{\alpha}\right\}c_{j\xi}^{(0)}}{\epsilon_{j}^{(0)}-\epsilon_{l}^{(0)}}\right]c_{l\lambda}^{(0)},\end{aligned} \tag{2.36}$$

where

$$(F_{\nu\lambda}^{(1,0)})_{\alpha}=(H_{\nu\lambda}^{(1,0)})_{\alpha}+(G_{\nu\lambda}^{(1,0)})_{\alpha}, \tag{2.37}$$

$$(H_{\nu\lambda}^{(1,0)})_{\alpha}=\frac{i}{2c}\langle(\mathbf{R}_{\nu\lambda}\times\mathbf{r})_{\alpha}\varphi_{\nu}\mid-\frac{1}{2}\nabla^{2}-\sum_{N}\frac{Z_{N}}{r_{N}}\mid\varphi_{\lambda}\rangle-\frac{i}{2c}\langle\varphi_{\nu}\mid L_{\alpha}^{\lambda}\mid\varphi_{\lambda}\rangle, \tag{2.38}$$

$$\begin{aligned}(G_{\nu\lambda}^{(1,0)})_{\alpha}=&\sum_{\zeta\xi}(P_{\zeta\xi}^{(1,0)})_{\alpha}\{(\varphi_{\nu}\varphi_{\lambda}|\varphi_{\zeta}\varphi_{\xi})-\frac{1}{2}(\varphi_{\nu}\varphi_{\xi}|\varphi_{\zeta}\varphi_{\lambda})\}\\&+\sum_{\zeta\xi}P_{\zeta\xi}^{(0)}\{\left((\chi_{\nu}\chi_{\lambda}|\chi_{\zeta}\chi_{\xi})^{(1,0)}\right)_{\alpha}-\frac{1}{2}\left((\chi_{\nu}\chi_{\xi}|\chi_{\zeta}\chi_{\lambda})^{(1,0)}\right)_{\alpha}\},\end{aligned} \tag{2.39}$$

$$\left((\chi_{\nu}\chi_{\lambda}|\chi_{\zeta}\chi_{\xi})^{(1,0)}\right)_{\alpha}=\frac{i}{2c}(\{(\mathbf{R}_{\nu\lambda}+\mathbf{R}_{\zeta\xi})\times\mathbf{r}\}_{\alpha}\varphi_{\nu}\varphi_{\lambda}|\varphi_{\zeta}\varphi_{\xi}), \tag{2.40}$$

$$(S_{\nu\lambda}^{(1,0)})_{\alpha}=\frac{i}{2c}\langle(\mathbf{R}_{\nu\lambda}\times\mathbf{r})_{\alpha}\varphi_{\nu}\mid\varphi_{\lambda}\rangle. \tag{2.41}$$

Using the above relations, the NMR shielding constants at the HF level can be evaluated. The GIAO method has been widely applied to the various problems and has given good results. The effect of the electron correlation in the NMR shielding constants have been investigated by many workers[5] and a development to the correlated method is straightforward. However, in this thesis, I am interested primarily in the relation between the

intermolecular(solute-solvent) interaction and the NMR shielding constants. Therefore the refinements in the intramolecular electronic structure for the NMR shielding constants remain as one of my future subjects. Additionally, the results in gas phase[5] suggest that the effect is less important at least for a water molecule which is treated as the solute molecule in this thesis.

II Theory of Molecular Liquids: RISM Theory

The characterization of liquid states, roughly speaking, is a more difficult problem than the characterization of the other states(gases and solids) of matter. In the gas phase, particles are moving randomly, and theory can treat the gas in ideal state analytically owing to this random motion. In the solid phase, on the other hand, particles(atoms or molecules) are placed periodically, and theory also can treat the solid in ideal state analytically owing to this periodic structure. However, in the liquid phase, particles are not moving randomly as in the gas phase, and particles are not placed periodically as in the solid phase. Due to this complexity, the characterization of liquid states is difficult. The positions of particles in the liquid phase vary from moment to moment, therefore, the statistical description, for example, the distribution of the position of the particle or the momentum of the particle, is essential to characterize the liquid state.

In section II.1, the distribution functions and the correlation functions, which characterize the liquid structure, are summarized briefly.[4] In section II.2, Ornstein-Zernike(OZ) equation for obtaining the structure of simple liquid is introduced.[4] Section II.3 is devoted to an introduction of the reference interaction site model(RISM) equation as the extension of the OZ equation for molecular liquids.[2, 4]

II.1 Distribution Function and Correlation Function

The distribution function(especially, the radial distribution function) plays a central role in the theory of liquid structure. There are two reasons for this. First, the distribution

function is directly measurable by radiation-scattering experiments. Second, thermodynamic properties of liquid can be expressed in simple formulas using the distribution function.

Consider a system of N particles in a volume V and at a temperature T(the canonical ensemble), the partition function Q_N is defined as follows:

$$Q_N = \frac{h^{-3N}}{N!} \int ... \int \exp\left[-\beta \mathcal{H}_N(\mathbf{r}_1, ..., \mathbf{r}_N, \mathbf{p}_1, ..., \mathbf{p}_N)\right] d\mathbf{r}_1 ... d\mathbf{r}_N d\mathbf{p}_1 ... d\mathbf{p}_N. \tag{2.42}$$

In the above equation, h is the Planck's constant. β is $\frac{1}{k_B T}$, where k_B is the Boltzmann constant. $\mathbf{r}_i$ and $\mathbf{p}_i$ are the position and the momentum of the particle i which has the mass of m, respectively. $\mathcal{H}_N$ is the Hamiltonian of the system, which is written in the sum of the kinetic and the potential energy

$$\mathcal{H}_N(\mathbf{r}_1, ..., \mathbf{r}_N, \mathbf{p}_1, ..., \mathbf{p}_N) = \sum_{i=1}^{N} \frac{\mathbf{p}_i^2}{2m} + U_N(\mathbf{r}_1, ..., \mathbf{r}_N). \tag{2.43}$$

The integrations over momenta in equation (2.42) can be carried out explicitly, and the partition function is then rewritten as

$$Q_N = \frac{1}{N! \Lambda^{3N}} Z_N. \tag{2.44}$$

Λ is the de Broglie thermal wavelength defined as follows:

$$\Lambda = \frac{h}{\sqrt{2\pi m k_B T}}, \tag{2.45}$$

and Z_N is the configuration integral

$$Z_N = \int ... \int \exp\left[-\beta U_N(\mathbf{r}_1, ..., \mathbf{r}_N)\right] d\mathbf{r}_1 ... d\mathbf{r}_N. \tag{2.46}$$

$\exp\left[-\beta U_N(\mathbf{r}_1, ..., \mathbf{r}_N)\right]$ is proportional to the probability of finding a certain configuration of particles, $\{\mathbf{r}_1, ..., \mathbf{r}_N\}$, and Z_N is the normalization factor of the probability. The probability density of finding arbitrary n particles of the system with coordinates in the elements $d\mathbf{r}_1 ... d\mathbf{r}_n$ of coordinate space, irrespective of the positions of the remaining

particles and irrespective of all momenta, is defined as follows:

$$\begin{aligned}\rho_N^{(n)}(\mathbf{r}_1,...,\mathbf{r}_n) &= \frac{N!}{(N-n)!}\frac{h^{-3N}}{N!}\frac{\int...\int \exp\left[-\beta\mathcal{H}_N\right]d\mathbf{r}_{n+1}...d\mathbf{r}_N d\mathbf{p}_1...d\mathbf{p}_N}{Q_N} \\ &= \frac{N!}{(N-n)!}\frac{\int...\int \exp\left[-\beta U_N(\mathbf{r}_1,...,\mathbf{r}_N)\right]d\mathbf{r}_{n+1}...d\mathbf{r}_N}{Z_N}. \end{aligned} \tag{2.47}$$

$N!/(N-n)!$ is the number of the ways of choosing n particles from N. The n-particle distribution function $\rho_N^{(n)}$ is normalized such that

$$\int...\int \rho_N^{(n)}(\mathbf{r}_1,...,\mathbf{r}_n)d\mathbf{r}_1...d\mathbf{r}_n = \frac{N!}{(N-n)!}. \tag{2.48}$$

In particular, 1-particle distribution function is normalized such that

$$\int \rho_N^{(1)}(\mathbf{r}_1)d\mathbf{r}_1 = N, \tag{2.49}$$

and for a homogeneous system,

$$\begin{aligned}\rho_N^{(1)}(\mathbf{r}_1) &= N/V \\ &= \rho. \end{aligned} \tag{2.50}$$

The n-particle distribution function $\rho_N^{(n)}(\mathbf{r}_1,...,\mathbf{r}_n)$ is rewritten in terms of the corresponding n-particle correlation function $g_N^{(n)}(\mathbf{r}_1,...,\mathbf{r}_n)$ by

$$\rho_N^{(n)}(\mathbf{r}_1,...,\mathbf{r}_n) = g_N^{(n)}(\mathbf{r}_1,...,\mathbf{r}_n)\prod_{i=1}^{n}\rho_N^{(1)}(\mathbf{r}_i), \tag{2.51}$$

or, for a homogeneous system, by

$$\rho_N^{(n)}(\mathbf{r}_1,...,\mathbf{r}_n) = g_N^{(n)}(\mathbf{r}_1,...,\mathbf{r}_n)\rho^n. \tag{2.52}$$

In the grand canonical ensemble(with volume V, temperature T, and chemical potential μ fixed), the n-particle distribution function is defined as

$$\rho^{(n)}(\mathbf{r}_1,...,\mathbf{r}_n) = \sum_{N\geq n}^{\infty} P(N)\rho_N^{(n)}(\mathbf{r}_1,...,\mathbf{r}_n), \tag{2.53}$$

where $P(N)$ is the probability that the system contains precisely N particles, irrespective of their coordinates and momenta, and is defined as

$$\begin{aligned} P(N) &= \frac{h^{-3N}}{N!}\int\cdots\int\frac{\exp[N\beta\mu]\exp[-\beta\mathcal{H}_N]}{\Xi}d\mathbf{r}_1...d\mathbf{r}_N d\mathbf{p}_1...d\mathbf{p}_N \\ &= \frac{1}{\Xi}\frac{z^N}{N!}Z_N. \end{aligned} \tag{2.54}$$

Ξ is the grand partition function

$$\Xi = \sum_{N=0}^{\infty}\frac{h^{-3N}}{N!}\exp[N\beta\mu]\int\cdots\int\exp[-\beta\mathcal{H}_N]d\mathbf{r}_1...d\mathbf{r}_N d\mathbf{p}_1...d\mathbf{p}_N \tag{2.55}$$

and z is the activity

$$z = \Lambda^{-3}\exp[\beta\mu]. \tag{2.56}$$

From the above equations, the n-particle distribution function is rewritten by

$$\rho^{(n)}(\mathbf{r}_1,...,\mathbf{r}_n) = \frac{1}{\Xi}\sum_{N\geq n}^{\infty}\int\cdots\int\exp[-\beta U_N(\mathbf{r}_1,...,\mathbf{r}_N)]d\mathbf{r}_{n+1}...d\mathbf{r}_N \tag{2.57}$$

The relation between the grand canonical n-particle distribution function and the corresponding distribution function is the same as in the canonical ensemble,

$$\rho^{(n)}(\mathbf{r}_1,...,\mathbf{r}_n) = g^{(n)}(\mathbf{r}_1,...,\mathbf{r}_n)\prod_{i=1}^{n}\rho^{(1)}(\mathbf{r}_i), \tag{2.58}$$

In the case that $n = 2$,

$$\rho^{(2)}(\mathbf{r}_1,\mathbf{r}_2) = g^{(2)}(\mathbf{r}_1,\mathbf{r}_2)\rho^{(1)}(\mathbf{r}_1)\rho^{(1)}(\mathbf{r}_2). \tag{2.59}$$

In the study of the liquid structure, in particular, $g^{(2)}(\mathbf{r}_1,\mathbf{r}_2)$ is important since it can be determined experimentally and thermodynamic properties of liquid can be written in simple formulas using the distribution function. If the system is isotropic as well as homogeneous, $g^{(2)}(\mathbf{r}_1,\mathbf{r}_2)$ is a function only of the separation $r = |\mathbf{r}_1-\mathbf{r}_2|$; it is then usually called the radial distribution function and written simply as $g(r)$. How can we estimate theoretically the radial distribution function, which characterizes the liquid structure? In the next section, the theoretical method for calculating the radial distribution function of simple liquids, which is called Ornstein-Zernike(OZ) equation, is introduced.

II.2 OZ Equation for Simple Liquids

Many years ago, Ornstein and Zernike proposed a division of the total correlation function $h(\mathbf{r}_1, \mathbf{r}_2) = g(\mathbf{r}_1, \mathbf{r}_2) - 1$, which is a measure of the total influence of molecule 1 on molecule 2 at distance $|\mathbf{r}_1 - \mathbf{r}_2|$, into two parts, a direct part and an indirect part. The direct part is given by a function $c(\mathbf{r}_1, \mathbf{r}_2)$ called the direct correlation function. The indirect part is the influence propagated directly from molecule 1 to a third molecule, 3, which in turn exerts its influence on 2, directly or indirectly through other particles. This effect is weighted by the density and averaged over all positions of molecules 3. With this decomposition of $h(\mathbf{r}_1, \mathbf{r}_2)$, we can write

$$h(\mathbf{r}_1, \mathbf{r}_2) = c(\mathbf{r}_1, \mathbf{r}_2) + \int c(\mathbf{r}_1, \mathbf{r}_3)\rho(\mathbf{r}_3)h(\mathbf{r}_2, \mathbf{r}_3)d\mathbf{r}_3 \tag{2.60}$$

Expanding the Eq. (2.60) as follows, one can see that the $h(\mathbf{r}_1, \mathbf{r}_2)$ includes the effect from the all particles in the liquid system:

$$\begin{aligned}
h(\mathbf{r}_1, \mathbf{r}_2) &= c(\mathbf{r}_1, \mathbf{r}_2) \\
&\quad + \int c(\mathbf{r}_1, \mathbf{r}_3)\rho(\mathbf{r}_3)c(\mathbf{r}_2, \mathbf{r}_3)d\mathbf{r}_3 \\
&\quad + \int\int c(\mathbf{r}_1, \mathbf{r}_3)\rho(\mathbf{r}_3)c(\mathbf{r}_2, \mathbf{r}_4)\rho(\mathbf{r}_4)h(\mathbf{r}_3, \mathbf{r}_4)d\mathbf{r}_3 d\mathbf{r}_4 \\
&= c(\mathbf{r}_1, \mathbf{r}_2) \\
&\quad + \int c(\mathbf{r}_1, \mathbf{r}_3)\rho(\mathbf{r}_3)c(\mathbf{r}_2, \mathbf{r}_3)d\mathbf{r}_3 \\
&\quad + \int\int c(\mathbf{r}_1, \mathbf{r}_3)\rho(\mathbf{r}_3)c(\mathbf{r}_2, \mathbf{r}_4)\rho(\mathbf{r}_4)c(\mathbf{r}_3, \mathbf{r}_4)d\mathbf{r}_3 d\mathbf{r}_4 \\
&\quad + \int\int\int c(\mathbf{r}_1, \mathbf{r}_3)\rho(\mathbf{r}_3)c(\mathbf{r}_2, \mathbf{r}_4)\rho(\mathbf{r}_4)c(\mathbf{r}_3, \mathbf{r}_5)\rho(\mathbf{r}_5)h(\mathbf{r}_4, \mathbf{r}_5)d\mathbf{r}_3 d\mathbf{r}_4 d\mathbf{r}_5 \\
&= \cdots .
\end{aligned} \tag{2.61}$$

This relation for the 2-particle correlation function is called the Ornstein-Zernike(OZ) equation. In this section, we derive the OZ equation for simple liquids from the analysis of the 2-particle distribution function in the grand canonical ensemble. Hereafter, we consider the homogeneous systems.

From eq. (2.57), 2-particle distribution function is written as an expansion in z:

$$\rho^{(2)}(\mathbf{r}_1,\mathbf{r}_2) = \frac{z^2\exp[-\beta u_{12}]}{\Xi}\{1+\sum_{N=3}^{\infty}\frac{z^{N-2}}{(N-2)!}\int\cdots\int\exp[-\beta U_N']d\mathbf{r}_3...d\mathbf{r}_N\}, \quad (2.62)$$

where U_N' indicates that the $u_{12}\equiv u(\mathbf{r}_1,\mathbf{r}_2)$ term has been omitted. Using the relation

$$\Xi = 1+\sum_{N=1}^{\infty}\frac{z^N}{N!}Z_N, \quad (2.63)$$

eq. (2.62) is expanded as follows:

$$\rho^{(2)}(\mathbf{r}_1,\mathbf{r}_2) = z^2\exp[-\beta u_{12}]\Big[1+z\{\int e^{-\beta U_3'}d\mathbf{r}_3 - Z_1\} + \frac{z^2}{2}\{\int\int e^{-\beta U_4'}d\mathbf{r}_3 d\mathbf{r}_4 + 2Z_1^2 - Z_2 - 2Z_1\int e^{-\beta U_3'}d\mathbf{r}_3\}+\cdots\Big]. \quad (2.64)$$

If we assume pair-wise additivity, we can write $\exp[-\beta U_3']$ as $\exp[-\beta u_{13}]\exp[-\beta u_{23}]$ ($\exp[-\beta u_{12}]$ is omitted from $\exp[-\beta U_3']$) . Now, we introduce the function,

$$f_{ij} = \exp[-\beta u_{ij}] - 1, \quad (2.65)$$

which is called as the Mayer f-function, and then we obtain

$$\exp[-\beta U_3'] = (1+f_{13})(1+f_{23}). \quad (2.66)$$

Using the above relations,

$$\begin{aligned}\int e^{-\beta U_3'}d\mathbf{r}_3 - Z_1 &= \int\{1+f_{13}+f_{23}+f_{13}f_{23}\}d\mathbf{r}_3 - Z_1\\ &= \int\{f_{13}+f_{23}+f_{13}f_{23}\}d\mathbf{r}_3. \end{aligned}\quad (2.67)$$

One can eventually get the relation for the 2-particle distribution function:

$$\begin{aligned}\rho^{(2)}(\mathbf{r}_1,\mathbf{r}_2) = z^2\exp[-\beta u_{12}]\Big[1 &+ z\int\{f_{13}+f_{23}+f_{13}f_{23}\}d\mathbf{r}_3\\ &+\frac{z^2}{2}\int\int\{2f_{13}f_{24}+2f_{13}f_{34}+2f_{24}f_{34}+f_{13}f_{14}+f_{23}f_{24}\\ &+f_{13}f_{14}f_{34}+f_{23}f_{24}f_{34}+4f_{13}f_{24}f_{34}+2f_{13}f_{14}f_{23}+2f_{13}f_{23}f_{24}\\ &+2f_{13}f_{23}f_{24}f_{34}+2f_{13}f_{14}f_{24}f_{34}+f_{13}f_{14}f_{23}f_{24}+f_{13}f_{14}f_{23}f_{24}f_{34}\}d\mathbf{r}_3 d\mathbf{r}_4\\ &+\cdots\Big]. \end{aligned}\quad (2.68)$$

In the next step, we expand the activity z in terms of the density $\rho = \langle N \rangle / V$. In order to obtain the relation between z and ρ, we consider the relation between the pressure p, the volume V, and the grand partition function Ξ:

$$\Xi = \exp\left[\frac{pV}{k_B T}\right]. \tag{2.69}$$

We now assume that the pressure can be expanded in powers of z according to

$$p = k_B T \sum_{j=1}^{\infty} b_j z^j. \tag{2.70}$$

Substituting eq. (2.70) into eq. (2.69), expanding the exponential, collecting the same powers of z, and equating the coefficient to those of eq. (2.63), we can obtain b_j in terms of Z_N:

$$\begin{aligned} b_1 &= \frac{1}{1!V} Z_1 \\ b_2 &= \frac{1}{2!V}(Z_1 - Z_1^2) \\ b_3 &= \frac{1}{3!V}(Z_3 - 3Z_2 Z_1 + 2Z_1^3) \\ &\cdots \end{aligned} \tag{2.71}$$

The density ρ is written as

$$\rho = \frac{z}{kT}\left(\frac{\partial p}{\partial z}\right)_{V,T}. \tag{2.72}$$

Substituting eq. (2.70) into eq. (2.72), we can obtain the relation between z and ρ

$$\rho = \sum_{j=1}^{\infty} j b_j z^j. \tag{2.73}$$

Since we wish to obtain the expression of z in terms of ρ, we assume that z is a power series in ρ

$$z = a_0 + a_1 \rho + a_2 \rho^2 + \cdots. \tag{2.74}$$

Substituting this into eq. (2.73) and equating coefficients of the same powers of ρ, we can get the expression:

$$z = \rho - 2b_2 \rho^2 + (8b_2^2 - 3b_3)\rho^3 + \cdots. \tag{2.75}$$

From eqs. (2.68) and (2.75), we can get the 2-particle distribution function as an expansion in ρ:

$$\begin{aligned}
\rho^{(2)}(\mathbf{r}_1,\mathbf{r}_2) &= e^{-\beta u_{12}}\rho^2 \\
&\quad + e^{-\beta u_{12}}\left(\int\{f_{13}+f_{23}+f_{13}f_{23}\}d\mathbf{r}_3 - 4b_2\right)\rho^3 \\
&\quad + e^{-\beta u_{12}}\Bigg(20b_2^2 - 6b_3 - 6\int\{f_{13}+f_{23}+f_{13}f_{23}\}d\mathbf{r}_3 b_2 \\
&\quad + \frac{1}{2}\int\int\{2f_{13}f_{24}+2f_{13}f_{34}+2f_{24}f_{34}+f_{13}f_{14}+f_{23}f_{24}+f_{13}f_{14}f_{34} \\
&\quad + f_{23}f_{24}f_{34}+4f_{13}f_{24}f_{34}+2f_{13}f_{14}f_{23}+2f_{13}f_{23}f_{24}+2f_{13}f_{23}f_{24}f_{34} \\
&\quad + 2f_{13}f_{14}f_{24}f_{34}+f_{13}f_{14}f_{23}f_{24}+f_{13}f_{14}f_{23}f_{24}f_{34}\}d\mathbf{r}_3 d\mathbf{r}_4\Bigg)\rho^4 \\
&\quad + \cdots. \qquad (2.76)
\end{aligned}$$

b_j can be also written in terms of f_{ij},

$$\begin{aligned}
b_2 &= \frac{1}{2!V}(Z_2 - Z_1^2) \\
&= \frac{1}{2!V}\left\{\int\int e^{-\beta U_2}d\mathbf{r}_1 d\mathbf{r}_2 - \left(\int d\mathbf{r}_1\right)^2\right\} \\
&= \frac{1}{2!V}\left\{\int\int f_{12}d\mathbf{r}_1 d\mathbf{r}_2\right\} \\
&= \frac{1}{2!V}\left\{\int d\mathbf{r}_1\int f_{12}d\mathbf{r}_{12}\right\} \\
&= \frac{1}{2}\int f_{12}d\mathbf{r}_{12}, \qquad (2.77) \\
b_3 &= \frac{1}{3!V}(Z_3 - 3Z_2Z_1 + 2Z_1^3) \\
&= \frac{1}{3!V}\left\{\int\int\int e^{-\beta U_3}d\mathbf{r}_1 d\mathbf{r}_2 d\mathbf{r}_3 - 3V\int\int e^{-\beta U_2}d\mathbf{r}_1 d\mathbf{r}_2 + 2V^3\right\} \\
&= \frac{1}{3!V}\Bigg\{\int\int\int(1+f_{12})(1+f_{13})(1+f_{23})d\mathbf{r}_1 d\mathbf{r}_2 d\mathbf{r}_3 \\
&\quad - 3V\int\int(1+f_{12})d\mathbf{r}_1 d\mathbf{r}_2 + 2V^3\Bigg\} \\
&= \frac{1}{6V}\int\int\int[f_{12}f_{13}f_{23}+f_{12}f_{13}+f_{12}f_{23}+f_{13}f_{23}]d\mathbf{r}_1 d\mathbf{r}_2 d\mathbf{r}_3 \\
&= \frac{1}{6V}\int d\mathbf{r}_1\int\int[f_{12}f_{13}f_{23}+f_{12}f_{13}+f_{12}f_{23}+f_{13}f_{23}]d\mathbf{r}_{12}d\mathbf{r}_{13}
\end{aligned}$$

$$= \frac{1}{6}\int\int [f_{12}f_{13}f_{23} + f_{12}f_{13} + f_{12}f_{23} + f_{13}f_{23}]d\mathbf{r}_{12}d\mathbf{r}_{13}, \tag{2.78}$$

$\cdots$

Substituting the above relations into eq. (2.76), we can eventually get the expression for the radial distribution function as an expansion in ρ:

$$\begin{aligned} g^{(2)}(\mathbf{r}_1,\mathbf{r}_2) &= \rho^{(2)}(\mathbf{r}_1,\mathbf{r}_2)/\rho^2 \\ &= e^{-\beta u_{12}}\Big[1 + \rho\int f_{13}f_{23}d\mathbf{r}_3 + \frac{\rho^2}{2}\int\int\{2f_{13}f_{24}f_{34} + 4f_{13}f_{23}f_{24}f_{34} \\ &\quad + f_{13}f_{14}f_{23}f_{24} + f_{13}f_{14}f_{23}f_{24}f_{34}\}d\mathbf{r}_3d\mathbf{r}_4 + \cdots\Big] \\ &= e^{-\beta u_{12}}[1 + \sum_{n=1}^{\infty}\rho^n\sum_i C_i(n+2)], \end{aligned} \tag{2.79}$$

where the coefficient $C_i(n+2)$ in the density expansion of the radial distribution function is called "1-2 irreducible cluster". The sum on i runs over all kinds of the clusters which consist of $n+2$ particles. In the case of $n = 2$, for example, $C_1(4)$ corresponds to the cluster $\int\int f_{13}f_{24}f_{34}d\mathbf{r}_3d\mathbf{r}_4$. Note that $\int f_{13}f_{23}d\mathbf{r}_3$ has the dimension of VN^{-1}, $\int\int f_{13}f_{23}f_{14}d\mathbf{r}_3d\mathbf{r}_4$ has the dimension of V^2N^{-2}, and so on. Therefore $g^{(2)}$ has no dimension. Note that $g^{(2)}(\mathbf{r}_1,\mathbf{r}_2) \to e^{-\beta u_{12}}$ as $\rho \to 0$.

The 1-2 irreducible cluster consists of two kinds of clusters, simple clusters and composite clusters. For example,

$$C_1(3) = \int f_{13}f_{23}d\mathbf{r}_3 \tag{2.80}$$

is the simple cluster, which cannot be decomposed into any simpler clusters. On the other hand,

$$C_3(4) = \frac{1}{2}\int\int f_{13}f_{14}f_{23}f_{24}d\mathbf{r}_3d\mathbf{r}_4 \tag{2.81}$$

is the composite cluster, since $C_3(4)$ can be decomposed into the product of the simple clusters as follows:

$$\begin{aligned} \int\int f_{13}f_{14}f_{23}f_{24}d\mathbf{r}_3d\mathbf{r}_4 &= \left(\int f_{13}f_{23}d\mathbf{r}_3\right)^2 \\ &= (C_1(3))^2. \end{aligned} \tag{2.82}$$

All of the composite clusters are included in the powers of the sum of all simple clusters. Using this relation, the radial distribution function(eq. (2.79)) can be rewritten as

$$\begin{aligned} g^{(2)}(\mathbf{r}_1,\mathbf{r}_2) &= e^{-\beta u_{12}}[1+\sum_{n=1}^{\infty}\rho^n\sum_i C_i(n+2)] \\ &= e^{-\beta u_{12}}[1+\left(\sum_{n=1}^{\infty}\rho^n\sum_i{}' C_i(n+2)\right)+\frac{1}{2!}\left(\sum_{n=1}^{\infty}\rho^n\sum_i{}' C_i(n+2)\right)^2 \\ &\quad +\frac{1}{3!}\left(\sum_{n=1}^{\infty}\rho^n\sum_i{}' C_i(n+2)\right)^3+\cdots]. \end{aligned} \tag{2.83}$$

In the above expression, $\sum_i{}'$ indicates that the composite clusters are omitted. Introducing the function S_{12},

$$S_{12}=\sum_{n=1}^{\infty}\rho^n\sum_i{}' C_i(n+2), \tag{2.84}$$

$g^{(2)}$ can be rewritten by simple form as

$$g^{(2)}(\mathbf{r}_1,\mathbf{r}_2) = \exp[-\beta u_{12}+S_{12}]. \tag{2.85}$$

Note that $u_{12}-\frac{1}{\beta}S_{12}$ is called the potential of mean force.

The simple cluster also consists of two kinds of cluster, series diagram and bridge diagram. The series diagram has the nodal points, through which all paths between the two particles at $\mathbf{r}_1$ and $\mathbf{r}_2$ pass, and the bridge diagram has no nodal points. For example,

$$\int\int f_{13}f_{24}f_{34}d\mathbf{r}_3d\mathbf{r}_4 \equiv \tag{2.86}$$

is the series diagram and the points at $\mathbf{r}_3$ and $\mathbf{r}_4$ are the nodal points. On the other hand,

$$\int\int f_{13}f_{14}f_{23}f_{24}f_{34}d\mathbf{r}_3d\mathbf{r}_4 \equiv \tag{2.87}$$

is the bridge diagram and there is no nodal points. In the above expression, the two fixed particles, 1 and 2, are called "root points"; the other particles, which are integrated over, are called "field points." S_{12} is re-expressed as

$$S_{12}=S_{12}^S+S_{12}^B \tag{2.88}$$

and

$$g^{(2)}(\mathbf{r}_1, \mathbf{r}_2) = \exp[-\beta u_{12} + S_{12}^S + S_{12}^B]. \tag{2.89}$$

S_{12}^S and S_{12}^B are the sum of the series diagrams and the sum of the bridge diagrams, respectively.

Consider the series diagrams which consist of an arbitrary number of nodal points, such as

$$\int\int f_{13} f_{23} f_{24} f_{34} d\mathbf{r}_3 d\mathbf{r}_4 \equiv$$ 

. (2.90)

When the field point 3 is assumed to be the closest nodal point to the root point 1 among all field points, the path between the field point 3 and the root point 2 always exists. In other words, one of the diagrams which are included in $g^{(2)}(\mathbf{r}_3, \mathbf{r}_2) - 1$ always exists between the field point 3 and the root point 2. Here, we define the two correlation functions. One is that the direct correlation function, $c(\mathbf{r}_1, \mathbf{r}_3)$, which gathers the contributions between the root point 1 and first nodal point 3 in all of the series diagrams. The other is that the total correlation function, $h(\mathbf{r}_3, \mathbf{r}_2) = g^{(2)}(\mathbf{r}_3, \mathbf{r}_2) - 1$, which gathers the contributions between the point 3 and root point 2 in all of the series diagrams. Using these correlation functions, the contribution between the root points 1 and 2 in the series diagram is expressed as follows:

$$S_{12}^S = \int c(\mathbf{r}_1, \mathbf{r}_3) \rho(\mathbf{r}_3) h(\mathbf{r}_3, \mathbf{r}_2) d\mathbf{r}_3. \tag{2.91}$$

Since $c(\mathbf{r}_1, \mathbf{r}_2)$ does not include the contribution from the series diagram S_{12}^S,

$$c(\mathbf{r}_1, \mathbf{r}_2) = h(\mathbf{r}_1, \mathbf{r}_2) - S_{12}^S. \tag{2.92}$$

Substituting eq. (2.92) into eq. (2.91), we can obtain the OZ equation:

$$h(\mathbf{r}_1, \mathbf{r}_2) = c(\mathbf{r}_1, \mathbf{r}_2) + \int c(\mathbf{r}_1, \mathbf{r}_3) \rho(\mathbf{r}_3) h(\mathbf{r}_3, \mathbf{r}_2) d\mathbf{r}_3. \tag{2.93}$$

The OZ equation can be considered to be a definition of the direct correlation function or, alternatively, it can be considered as a relation between h and c.

The relations obtained from the analysis of the 2-particle distribution function can be summarized as follows:

$$g^{(2)}(\mathbf{r}_1, \mathbf{r}_2) = \exp[-\beta u_{12} + S_{12}^S + S_{12}^B], \tag{2.94}$$

$$c(\mathbf{r}_1, \mathbf{r}_2) = g^{(2)}(\mathbf{r}_1, \mathbf{r}_2) - 1 - S_{12}^S, \tag{2.95}$$

$$g^{(2)}(\mathbf{r}_1, \mathbf{r}_2) - 1 = c(\mathbf{r}_1, \mathbf{r}_2) + \int c(\mathbf{r}_1, \mathbf{r}_3)\rho(\mathbf{r}_3)\{g^{(2)}(\mathbf{r}_3, \mathbf{r}_2) - 1\}d\mathbf{r}_3. \tag{2.96}$$

These three equations constitute exact equations within the pair-wise additive approximation for the potential U_N. If S_{12}^S or S_{12}^B were given, these three equations would give $g^{(2)}(\mathbf{r}_1, \mathbf{r}_2)$. The equations, however, are intractable because the f-function expansion for $g^{(2)}$ introduces an infinite series of many-dimensional integrals of products of f-functions. If we make the approximation of setting $S_{12}^B = 0$ in eq. (2.94),

$$g^{(2)}(\mathbf{r}_1, \mathbf{r}_2) = \exp[-\beta u_{12} + S_{12}^S] \tag{2.97}$$

we obtain an approximate integral equation for $g^{(2)}$ called the OZ/hypernetted-chain (HNC) equation:

$$g^{(2)}(\mathbf{r}_1, \mathbf{r}_2) = \exp[-\beta u_{12}] \exp\Big[\int \{g^{(2)}(\mathbf{r}_1, \mathbf{r}_3) - 1 - \log g^{(2)}(\mathbf{r}_1, \mathbf{r}_3) - \beta u_{13}\}\rho(\mathbf{r}_3)\{g^{(2)}(\mathbf{r}_3, \mathbf{r}_2) - 1\}\Big] d\mathbf{r}_3 \tag{2.98}$$

If we make the approximation of setting $S_{12}^B = 0$, and including only 1st-order in the expansion of $\exp[S_{12}^S]$ in eq. (2.94),

$$g^{(2)}(\mathbf{r}_1, \mathbf{r}_2) = \exp[-\beta u_{12}](1 + S_{12}^S) \tag{2.99}$$

we obtain instead an approximate integral equation for $g^{(2)}$ called the OZ/Percus-Yevick (PY) equation:

$$g^{(2)}(\mathbf{r}_1, \mathbf{r}_2)e^{\beta u_{12}} = 1 + \int g^{(2)}(\mathbf{r}_1, \mathbf{r}_3)\{1 - e^{\beta u_{13}}\}\rho(\mathbf{r}_3)\{g^{(2)}(\mathbf{r}_3, \mathbf{r}_2) - 1\}d\mathbf{r}_3. \tag{2.100}$$

In the above expressions, although the single-particle density is written as $\rho(\mathbf{r}_3)$ explicitly, it is equal to ρ in the homogeneous system which we consider hereafter.

If the pair potential u_{12}(hard-sphere, Lennard-Jones, and so on) is given, using eqs. (2.98) or (2.100), we can obtain the radial distribution function $g^{(2)}(\mathbf{r}_1, \mathbf{r}_2)$ and the thermodynamic properties of the simple liquids, and study liquid states theoretically. In the next section, we extend the OZ/HNC or OZ/PY equation for the molecular liquids.

II.3 RISM Equation for Molecular Liquids

In this section we introduce reference interaction site model(RISM) equation to obtain site-site pair correlation functions for molecular liquids. RISM equation can be derived from the statistical-mechanical partition function shown to be an exact equation. Here, however, we will give only outline of RISM equation in an intuitive manner.

One of the most important feature in molecular liquids is that the intermolecular interaction is a function not only of the separation of the molecules but also of their mutual orientation. Model potentials to treat molecular liquids are divided roughly into two types. The first type is described as follows:

$$u(\mathbf{1}, \mathbf{2}) = u(\mathbf{R}, \mathbf{\Omega}_1, \mathbf{\Omega}_2), \tag{2.101}$$

where **1** and **2** in the left hand side, respectively, are the coordinates of molecules 1 and 2 including their orientation. **R** is the coordinate vector between the centers of mass of the molecules, and $\mathbf{\Omega}_1$ and $\mathbf{\Omega}_2$ represent their orientation. This model includes, for example, the Stock-Mayer type potential,

$$u(\mathbf{1}, \mathbf{2}) = u_0(R) - \boldsymbol{\mu}_1 \cdot \mathbf{T}(\mathbf{R}) \cdot \boldsymbol{\mu}_2, \tag{2.102}$$

where $u_0(R)$ is the spherically symmetric term, $\boldsymbol{\mu}_i$ is the dipole moment vector of molecule i, and $\mathbf{T}(\mathbf{R})$ is the dipole-dipole interaction tensor. This model can be generalized by including the interactions of higher order, for example, dipole-quadrupole, quadrupole-quadrupole terms. The second type is a model in which each molecule is represented by a set of discrete interaction sites located usually at the sites of atomic nuclei. This model is called the interaction site model(ISM). The total potential energy of two interaction-site

molecules is obtained as the sum of spherically-symmetric interaction-site-potentials. Let $\mathbf{r}_{\alpha 1}$ be the coordinates of site α in molecule 1 and let $\mathbf{r}_{\beta_2}$ be the coordinates of site β in molecule 2, where 1 and 2 are different molecules. Then the total intermolecular potential energy is given by

$$u(\mathbf{1},\mathbf{2}) = \sum_{\alpha}\sum_{\beta} u_{\alpha_1\beta_2}(|\mathbf{r}_{\alpha 1} - \mathbf{r}_{\beta_2}|). \tag{2.103}$$

In the above expression, $u_{\alpha_1\beta_2}$ is a site-site potential and the sums on α and β run over all interaction sites in the respective molecules. The coordinates $\mathbf{r}_{\alpha 1}$ can be rewritten as

$$\mathbf{r}_{\alpha 1} = \mathbf{R}_1 + \mathbf{l}_{\alpha 1}(\Omega_1), \tag{2.104}$$

where $\mathbf{R}_1$ denotes the position of the center of molecule 1, and $\mathbf{l}_{\alpha 1}(\mathbf{\Omega}_1)$ is the displacement of the site α from that center. A diatomic ISM molecule is depicted schematically in Fig. 2.1.

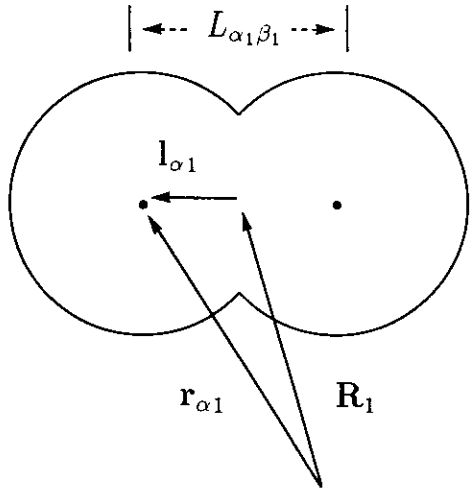

Figure 2.1: The shape of ISM molecule.

By using ISM, the dependence of $u(\mathbf{1},\mathbf{2})$ on the polar coordinates is replaced by the dependence on the intermolecular site-site separation. The two model potentials mentioned above are equivalent to each other in the sense that, given appropriate parameters, both of them can reproduce a potential determined by some other method such as the quantum

chemical calculation. The ISM has been used commonly in the molecular simulations of condensed phase properties for a large variety of chemical substances; electrostatic interactions are easily accounted by inclusion of Coulombic terms in the site-site potentials. Here, we utilize the ISM for constructing the integral equation theory of molecular liquids.

Before explaining the RISM equation, we reconsider the OZ equation in expanded form as shown in eq. (2.61)

$$\begin{aligned} h(\mathbf{r}_1,\mathbf{r}_2) = c(\mathbf{r}_1,\mathbf{r}_2) & \\ + \rho \int c(\mathbf{r}_1,\mathbf{r}_3)c(\mathbf{r}_3,\mathbf{r}_2)d\mathbf{r}_3 & \\ + \rho^2 \int\int c(\mathbf{r}_1,\mathbf{r}_3)c(\mathbf{r}_3,\mathbf{r}_4)c(\mathbf{r}_4,\mathbf{r}_2)d\mathbf{r}_3 d\mathbf{r}_4 & \\ + \rho^3 \int\int\int c(\mathbf{r}_1,\mathbf{r}_3)c(\mathbf{r}_3,\mathbf{r}_4)c(\mathbf{r}_4,\mathbf{r}_5)c(\mathbf{r}_5,\mathbf{r}_2)d\mathbf{r}_3 d\mathbf{r}_4 d\mathbf{r}_5 & \\ + \cdots . & \end{aligned} \tag{2.105}$$

In the diagrammatical representation, the above equation can be rewritten as:

$h(\mathbf{r}_1,\mathbf{r}_2) =$ 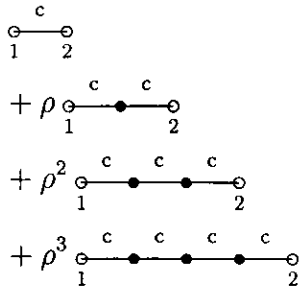

$+ \cdots ,$ (2.106)

where a full line is called a **c**-bond. The black circles, connected by **c**-bond, are the white circles which have been integrated over space, and have the number density of ρ. The above equation has the following physical interpretation. The total correlation between particles 1 and 2, represented by $h(\mathbf{r}_1,\mathbf{r}_2)$, is a sum of the direct correlation between 1 and 2 and the indirect correlation propagated via large numbers of intermediate black particles. The first term in the right hand side indicates the direct contribution from the two particles, and the second term from the three particles, and so on. The

key ingredient of the RISM equation is an OZ like relation between the site-site total correlation functions $h_{\alpha\beta}$ and the site-site direct correlation functions $c_{\alpha\beta}$. The above physical interpretation can be applied to site-site correlations with the allowance made for the fact that correlations also propagate via the intermolecular sites with geometrical constraints of the molecule. In the ISM framework, the constraint is represented by the intramolecular site-site pair distribution function $s_{\alpha_1\beta_1}$ for distinct site in the molecule 1, defined using the Dirac delta function as:

$$s_{\alpha_1\beta_1}(\mathbf{r},\mathbf{r}') = \frac{(1-\delta_{\alpha\beta})}{4\pi^2 L_{\alpha_1\beta_1}}\delta(|\mathbf{r}-\mathbf{r}'| - L_{\alpha_1\beta_1}), \tag{2.107}$$

where $L_{\alpha_1\beta_1}$ is the bond length between the sites α and β. $s_{\alpha_1\beta_1}$ represents the probability of finding site β of the molecule 1 at a position $\mathbf{r}'$ given that site α of the same molecule is at a position $\mathbf{r}$. Only the case that $|\mathbf{r}-\mathbf{r}'|$ is equal to $L_{\alpha_1\beta_1}$, $s_{\alpha_1\beta_1}$ has a certain value. By an analogy with the OZ equation for the simple liquids, the site-site total correlation functions $h_{\alpha\beta}$ consist of the **c**-bonds and the **s**-bonds which originate from the intramolecular site-site pair distribution function $s_{\alpha_1\beta_1}$,

$h(\mathbf{r}_1,\mathbf{r}_2) =$ 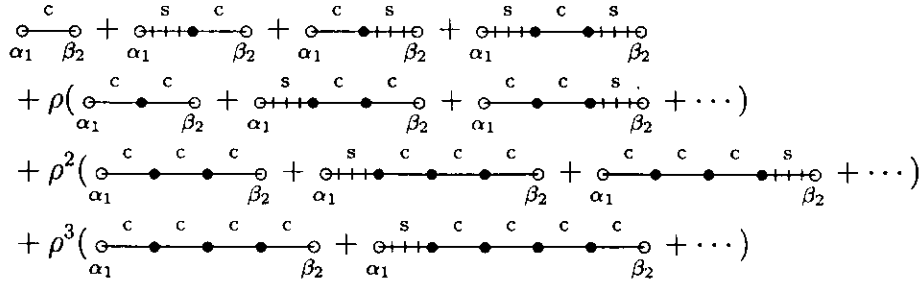

(2.108)

where a full line denotes a **c**-bond and 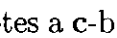 denotes an **s**-bond. It is noted that the black circles connected by **c**-bond or **s**-bond represent the intermediate ones to be integrated over space and summed over all sites in the molecule. For example, in the above expression,

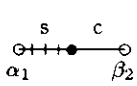
$$= \sum_{\gamma}^{\text{on 1}} \int s_{\alpha_1\gamma_1}(\mathbf{r},\mathbf{r}'')c_{\gamma_1\beta_2}(\mathbf{r}'',\mathbf{r}')d\mathbf{r}'', \tag{2.109}$$

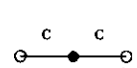
$$= \sum_{\gamma}^{\text{on 3}} \int c_{\alpha_1\gamma_3}(\mathbf{r},\mathbf{r}'')c_{\gamma_3\beta_2}(\mathbf{r}'',\mathbf{r}')d\mathbf{r}''. \tag{2.110}$$

Here, eq. (2.109) represents the indirect contribution between the site α on molecule 1 and the site β on molecule 2 through all the other sites on the molecule 1. While eq. (2.110) is the indirect contribution between the site α on molecule 1 and the site β on molecule 2 through all the sites on the molecule 3. If we define the total intramolecular site-site pair distribution function $\omega_{\alpha_1\beta_1}$(note that $\omega_{\alpha_1\beta_1}$ in denoted as $\mathrm{w}_{\alpha_1\beta_1}$ in some papers)

$$\omega_{\alpha_1\beta_1}(\mathbf{r},\mathbf{r}') = \delta_{\alpha\beta}\delta(\mathbf{r}-\mathbf{r}') + s_{\alpha_1\beta_1}(\mathbf{r},\mathbf{r}'), \tag{2.111}$$

we can rewrite, for instance, the terms of the zero-th order with the density in eq. (2.108) as

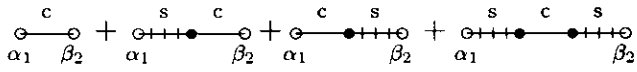

$$\begin{aligned} &= \sum_{\gamma}^{\text{on 1}}\sum_{\delta}^{\text{on 2}} \int\int \omega_{\alpha_1\gamma_1}(\mathbf{r},\mathbf{r}'')c_{\gamma_1\delta_2}(\mathbf{r}'',\mathbf{r}''')\omega_{\delta_2\beta_2}(\mathbf{r}''',\mathbf{r}')d\mathbf{r}''d\mathbf{r}''' \\ &\equiv \sum_{\gamma}^{\text{on 1}}\sum_{\delta}^{\text{on 2}} \omega_{\alpha_1\gamma_1} * c_{\gamma_1\delta_2} * \omega_{\delta_2\beta_2}(\mathbf{r},\mathbf{r}'). \end{aligned} \tag{2.112}$$

"$*$" denotes the spatial convolution integral over intermediate coordinates. Using the function ω, we can finally obtain the RISM equation for the molecular liquid system:

$$h_{\alpha_1\beta_2}(\mathbf{r},\mathbf{r}') = \sum_{\gamma}^{\text{on 1}}\sum_{\delta}^{\text{on 2}} \omega_{\alpha_1\gamma_1} * c_{\gamma_1\delta_2} * \omega_{\delta_2\beta_2}(\mathbf{r},\mathbf{r}') + \sum_{\gamma}^{\text{on 1}}\sum_{\zeta}^{\text{on 3}} \omega_{\alpha_1\gamma_1} * c_{\gamma_1\zeta_3} * \rho_{\zeta_3} h_{\zeta_3\beta_2}(\mathbf{r},\mathbf{r}'). \tag{2.113}$$

As is in the simple liquid theory, the site-site radial distribution function $g_{\alpha_1\beta_2}$ is equal to $h_{\alpha_1\beta_2}+1$. In order to obtain the site-site pair correlation functions, the RISM equation must be combined with a certain closure equation such as eq. (2.97) or eq. (2.99) for the OZ equation. Although several generalizations of these closure equations for molecular liquids have been proposed, the direct analogue of eq. (2.97)

$$g^{(2)}_{\alpha_1\beta_2}(\mathbf{r},\mathbf{r}') = \exp[-\beta u_{\alpha_1\beta_2}(\mathbf{r},\mathbf{r}') + S^S_{\alpha_1\beta_2}(\mathbf{r},\mathbf{r}')] \tag{2.114}$$

or eq. (2.99)

$$g^{(2)}_{\alpha_1\beta_2}(\mathbf{r},\mathbf{r}') = \exp[-\beta u_{\alpha_1\beta_2}(\mathbf{r},\mathbf{r}')](1 + S^S_{\alpha_1\beta_2}(\mathbf{r},\mathbf{r}')) \tag{2.115}$$

has been demonstrated by many examples to be very productive for describing structure of molecular liquids. The combination of eqs. (2.113) and (2.114) is called as the RISM/HNC equation, and the combination of eqs. (2.113) and (2.115) is called as the RISM/PY equation.

The RISM equation for a neat liquid can be readily generalized to a multi-component system using the matrix notations:

$$\mathbf{h} = \boldsymbol{\omega} * \mathbf{c} * \boldsymbol{\omega} + \boldsymbol{\omega} * \mathbf{c} * \boldsymbol{\rho}\mathbf{h}. \tag{2.116}$$

For a solute-solvent system, eq. (2.116) can be conveniently rewritten using the submatrices labeled with solutes(u) and solvents(v) as follows:

$$\begin{aligned}\begin{pmatrix} \mathbf{h}_{uu} & \mathbf{h}_{uv} \\ \mathbf{h}_{vu} & \mathbf{h}_{vv} \end{pmatrix} &= \begin{pmatrix} \boldsymbol{\omega}_u & \mathbf{0} \\ \mathbf{0} & \boldsymbol{\omega}_v \end{pmatrix} * \begin{pmatrix} \mathbf{c}_{uu} & \mathbf{c}_{uv} \\ \mathbf{c}_{vu} & \mathbf{c}_{vv} \end{pmatrix} * \begin{pmatrix} \boldsymbol{\omega}_u & \mathbf{0} \\ \mathbf{0} & \boldsymbol{\omega}_v \end{pmatrix} \\ &+ \begin{pmatrix} \boldsymbol{\omega}_u & \mathbf{0} \\ \mathbf{0} & \boldsymbol{\omega}_v \end{pmatrix} * \begin{pmatrix} \mathbf{c}_{uu} & \mathbf{c}_{uv} \\ \mathbf{c}_{vu} & \mathbf{c}_{vv} \end{pmatrix} * \begin{pmatrix} \boldsymbol{\rho}_u & \mathbf{0} \\ \mathbf{0} & \boldsymbol{\rho}_v \end{pmatrix} * \begin{pmatrix} \mathbf{h}_{uu} & \mathbf{h}_{uv} \\ \mathbf{h}_{vu} & \mathbf{h}_{vv} \end{pmatrix}, \end{aligned} \tag{2.117}$$

where the subscripts indicate the class of species included in the submatrix labels. Note that $\boldsymbol{\omega}$ is the block diagonal matrix and $\boldsymbol{\rho}$ is the diagonal matrix. With this notation, we have as an immediate consequence the set of equations, equivalent to eq. (2.113),

$$\mathbf{h}_{vv} = \boldsymbol{\omega}_v * \mathbf{c}_{vv} * \boldsymbol{\omega}_v + \boldsymbol{\omega}_v * \mathbf{c}_{vu} * \boldsymbol{\rho}_u\mathbf{h}_{vu} + \boldsymbol{\omega}_v * \mathbf{c}_{vv} * \boldsymbol{\rho}_v\mathbf{h}_{vv}, \tag{2.118}$$

$$\mathbf{h}_{uv} = \boldsymbol{\omega}_u * \mathbf{c}_{uv} * \boldsymbol{\omega}_v + \boldsymbol{\omega}_u * \mathbf{c}_{uu} * \boldsymbol{\rho}_u\mathbf{h}_{vu} + \boldsymbol{\omega}_u * \mathbf{c}_{uv} * \boldsymbol{\rho}_v\mathbf{h}_{vv}, \tag{2.119}$$

$$\mathbf{h}_{uu} = \boldsymbol{\omega}_u * \mathbf{c}_{uu} * \boldsymbol{\omega}_u + \boldsymbol{\omega}_u * \mathbf{c}_{uu} * \boldsymbol{\rho}_u\mathbf{h}_{uu} + \boldsymbol{\omega}_u * \mathbf{c}_{uv} * \boldsymbol{\rho}_v\mathbf{h}_{uv}. \tag{2.120}$$

We now consider the case in which all solute (u) species are at infinite dilution in the solvent mixture, i.e., $\boldsymbol{\rho}_u \to 0$. Then, in each of eqs. (2.118) - (2.120) the second term is vanishingly small compared to the others and we have

$$\mathbf{h}_{vv} = \boldsymbol{\omega}_v * \mathbf{c}_{vv} * \boldsymbol{\omega}_v + \boldsymbol{\omega}_v * \mathbf{c}_{vv} * \boldsymbol{\rho}_v\mathbf{h}_{vv}, \tag{2.121}$$

$$\mathbf{h}_{uv} = \boldsymbol{\omega}_u * \mathbf{c}_{uv} * \boldsymbol{\omega}_v + \boldsymbol{\omega}_u * \mathbf{c}_{uv} * \boldsymbol{\rho}_v\mathbf{h}_{vv}, \tag{2.122}$$

$$\mathbf{h}_{uu} = \boldsymbol{\omega}_u * \mathbf{c}_{uu} * \boldsymbol{\omega}_u + \boldsymbol{\omega}_u * \mathbf{c}_{uv} * \boldsymbol{\rho}_v\mathbf{h}_{uv}. \tag{2.123}$$

Now, we define the pure solvent site density pair correlation functions $\boldsymbol{\chi}_v$,

$$\boldsymbol{\chi}_v = \boldsymbol{\omega}_v + \boldsymbol{\rho}_v \mathbf{h}_{vv}, \tag{2.124}$$

then we can rewrite eq. (2.122) as

$$\mathbf{h}_{uv} = \boldsymbol{\omega}_u * \mathbf{c}_{uv} * \boldsymbol{\chi}_v, \tag{2.125}$$

or

$$h_{\alpha_u\beta_v} = \sum_{\gamma}\sum_{\gamma'} \omega_{\alpha_u\gamma_u} * c_{\gamma_u\gamma'_v} * \chi_{\gamma'_v\beta_v}. \tag{2.126}$$

This equation is the solute-solvent RISM equation in which the solute is at infinite dilution in solvents. This framework is suitable for the investigation of solute-solvent interactions in the systems. For an application of the theory to polar liquids in which the Coulombic interaction is essential, the equations (RISM/HNC or RISM/PY) should be renormalized to avoid divergence regarding the spatial integral.[6]

In the next section, we introduce the electronic structure theory coupled with RISM theory(RISM-SCF theory) through the electrostatic interaction between solute and solvents. Since it has been found that the RISM/HNC equation is appropriate for a highly polar system, the RISM/HNC equation is adopted for the description of molecular liquids in the RISM-SCF framework.

III Theory of Electronic Structure in Solution: RISM-SCF Theory

The development of theoretical methods to calculate the electronic structure in solution is one of the important issue in quantum chemistry in the last two decades. Since the quantum chemical calculation of the whole solute-solvent systems are intractable, hybrid approaches between the classical solvent and quantum solute have been developed. RISM self-consistent-field(RISM-SCF) method, which is introduced in this section, is one of such hybrid approaches. This method describes the solute-solvent interactions as the sum of

site-site interactions between the constituent atoms in solute and solvent molecules, and thus this method has an advantage in providing a microscopic picture of solute-solvent interaction. It is noted that the solute electronic structure and the statistical solvent distributions around the solute are treated in a self consistent manner.

Defining the energy of a molecule, E, by the sum of the electronic energy, $\langle \Psi \mid \mathcal{H} \mid \Psi \rangle$, and the nuclear repulsion energy, E_{nuc},

$$E = \langle \Psi \mid \mathcal{H} \mid \Psi \rangle + E_{nuc}, \tag{2.127}$$

where the total wave function $\mid \Psi \rangle$ is represented by a Slater determinant of molecular orbitals, ϕ_i, we can derive the Fock operator for an isolated molecule in gas phase from the variational principle,

$$\delta(E - \text{orthonormality condition for } \{\phi_i\}) = 0. \tag{2.128}$$

Similarly, the Fock operator for a solute molecule in solvent can be derived from the variational principle as follows. We define the solvation free energy as a sum of the electronic energy of a solute molecule E_{solute} and the excess chemical potential due to solute-solvent interactions $\Delta\mu$:

$$A = E_{solute} + \Delta\mu. \tag{2.129}$$

E_{solute} can be estimated by *ab initio* electronic structure methods such as the Hartree-Fock method:

$$E_{solute} = 2\sum_i \langle \phi_i \mid h \mid \phi_i \rangle + \sum_{i,j} (2\langle \phi_i\phi_i \mid \phi_j\phi_j \rangle - \langle \phi_i\phi_j \mid \phi_j\phi_i \rangle) + E_{nuc}, \tag{2.130}$$

where h is the one electron operator. On the other hand, for the chemical potential term we adopted the free energy[7] derived from RISM/HNC equation(eq. (2.113) and eq. (2.114)),

$$\begin{aligned}\Delta\mu = &-\frac{\rho}{\beta}\sum_{\alpha,s}\int\{\exp[-\beta u_{\alpha s} + t_{\alpha s}] - 1 - t_{\alpha s} - h_{\alpha s}t_{\alpha s} + \frac{1}{2}h_{\alpha s}^2\}d\mathbf{r} \\ &-\frac{1}{\beta}\int\{-\sum_{\alpha,s} c_{\alpha s}h_{\alpha s} + \frac{1}{2}\sum_{\alpha,\gamma,s',s} c_{\alpha s}\omega_{\alpha\gamma} * c_{\gamma s'} * \chi_{s's}\}d\mathbf{r}.\end{aligned} \tag{2.131}$$

In the above expression, β is equal to $\frac{1}{k_B T}$, where k_B and T are the Boltzmann constant and temperature, respectively. Note that ρ is the density of solvent. The Greek and Roman subscripts refer to the interaction sites of the solute and of the solvent molecules, respectively. $c_{\gamma s}$ and $h_{\gamma s}$ are the direct correlation functions and the total correlation functions, respectively. $t_{\alpha s}$ is equal to $h_{\alpha s} - c_{\alpha s}$. $\chi_{s's}$ is the pure solvent site density pair correlation functions(eq. (2.124)) and $\omega_{\alpha\gamma}$ is the total intramolecular correlation functions of the solute(eq. (2.111)). The solute-solvent interaction potentials $u_{\alpha s}$ are given as the sum of Coulombic and Lennard-Jones terms,

$$u_{\alpha s} = \frac{q_\alpha q_s}{r} + 4\epsilon_{\alpha s}\left[\left(\frac{\sigma_{\alpha s}}{r}\right)^{12} - \left(\frac{\sigma_{\alpha s}}{r}\right)^{6}\right]. \tag{2.132}$$

In this framework, the effective charges q_α assigned to the solute sites depend on the solute electronic wave function as

$$q_\alpha = q_\alpha^{(N)} - \sum_i 2\langle\phi_i \mid b_\alpha \mid \phi_i\rangle, \tag{2.133}$$

where b_α is the population operator generating the effective charge on the site α due to the electrons. $q_\alpha^{(N)}$ is the effective nuclear charge on the α site. In the case that the site is located at nucleus, $q_\alpha^{(N)}$ is equal to Z_α, where Z_α is the nuclear charge of the nucleus α. In the present case, q_α is determined by fitting to the electrostatic potential due to the solute electron distribution in the least square fashion.

The quantity A in eq. (2.129) can be regarded as a functional of the functions $h_{\alpha s}$, $c_{\alpha s}$, $t_{\alpha s}$, and ϕ_i. We define the following quantity I with the inclusion of the constraints to the orthonormality of molecular orbitals:

$$I = A[\mathbf{h}, \mathbf{c}, \mathbf{t}, \boldsymbol{\phi}] - \sum_{i,m} \epsilon_{im}(\langle\phi_i \mid \phi_m\rangle - \delta_{im}). \tag{2.134}$$

Taking the first variation with the basic quantities,

$$
\begin{aligned}
I+\delta I =& 2\sum_i \langle \phi_i+\delta\phi_i \mid h \mid \phi_i+\delta\phi_i\rangle \\
&+\sum_{i,j}(2\langle\{\phi_i+\delta\phi_i\}\{\phi_i+\delta\phi_i\} \mid \{\phi_j+\delta\phi_j\}\{\phi_j+\delta\phi_j\}\rangle \\
&-\langle\{\phi_i+\delta\phi_i\}\{\phi_j+\delta\phi_j\} \mid \{\phi_j+\delta\phi_j\}\{\phi_i+\delta\phi_i\}\rangle) + E_{nuc} \\
&-\frac{\rho}{\beta}\int\Big\{\sum_{\alpha,s}\exp[-\beta u_{\alpha s}+t_{\alpha s}] \\
&+2\sum_i\sum_\alpha\sum_{\alpha',s}\frac{\partial\exp[-\beta u_{\alpha' s}+t_{\alpha' s}]}{\partial q_\alpha}\Big(\frac{\partial q_\alpha}{\partial\phi_i}\delta\phi_i+\frac{\partial q_\alpha}{\partial\phi_i^*}\delta\phi_i^*\Big)+\cdots \\
&+\sum_{\alpha,s}\sum_{\alpha',s'}\frac{\partial\exp[-\beta u_{\alpha' s'}+t_{\alpha' s'}]}{\partial t_{\alpha s}}\delta t_{\alpha s}+\cdots \\
&-1-\sum_{\alpha,s}(t_{\alpha s}+\delta t_{\alpha s})-\sum_{\alpha,s}(h_{\alpha s}+\delta h_{\alpha s})(t_{\alpha s}+\delta t_{\alpha s})+\frac{1}{2}\sum_{\alpha,s}(h_{\alpha s}+\delta h_{\alpha s})^2\Big\}d\mathbf{r} \\
&-\frac{1}{\beta}\int\Big\{-\sum_{\alpha,s}(c_{\alpha s}+\delta c_{\alpha s})(h_{\alpha s}+\delta h_{\alpha s}) \\
&+\frac{1}{2}\sum_{\alpha,\gamma,s,s'}(c_{\alpha s}+\delta c_{\alpha s})(c_{\gamma s'}+\delta c_{\gamma s'})*\omega_{\alpha\gamma}*\chi_{s's}\Big\}d\mathbf{r} \\
&-\sum_{i,m}\epsilon_{im}(\langle\phi_i+\delta\phi_i \mid \phi_m+\delta\phi_m\rangle-\delta_{im}),
\end{aligned}
\tag{2.135}
$$

We obtain the variational principle as

$$
\begin{aligned}
\delta I =& 2\sum_i\langle\delta\phi_i \mid h \mid \phi_i\rangle + 2\sum_i\langle\delta\phi_i \mid \sum_j(2J_j-K_j) \mid \phi_i\rangle \\
&-2\frac{\rho}{\beta}\sum_i\sum_{\alpha,s}\langle\delta\phi_i \mid b_\alpha \mid \phi_i\rangle\int\beta\frac{q_s}{r}\exp[-\beta u_{\alpha s}+t_{\alpha s}]d\mathbf{r} \\
&-\frac{\rho}{\beta}\sum_{\alpha,s}\int(\exp[-\beta u_{\alpha s}+t_{\alpha s}]-h_{\alpha s}-1)\delta t_{\alpha s}d\mathbf{r} \\
&-\frac{\rho}{\beta}\sum_{\alpha,s}\int(-t_{\alpha s}+h_{\alpha s}-c_{\alpha s})\delta h_{\alpha s}d\mathbf{r} \\
&-\frac{1}{\beta}\sum_{\alpha,s}\int(h_{\alpha s}+\sum_{\gamma,s'}\omega_{\alpha\gamma}*c_{\gamma s'}*\chi_{s's})\delta c_{\alpha s}d\mathbf{r} \\
&-\sum_{i,m}\epsilon_{im}\langle\delta\phi_i \mid \phi_m\rangle \\
&+\text{complex conjugate} \\
=&0.
\end{aligned}
\tag{2.136}
$$

In the above equation, J_j and K_j are the Coulomb and exchange operator, respectively. The fourth, fifth, and sixth terms give the RISM/HNC equation. From the above relations, we can obtain the solvated Fock operator

$$\begin{aligned}\hat{F}_i &= h + \sum_j (2J_j - K_j) - \rho \sum_{\alpha,s} b_\alpha \int \frac{q_s}{r} \exp[-\beta u_{\alpha s} + t_{\alpha s}] d\mathbf{r} \\ &= h + \sum_j (2J_j - K_j) - \sum_\alpha b_\alpha V_\alpha, \end{aligned} \tag{2.137}$$

where

$$V_\alpha = \rho \sum_s \int q_s \frac{g_{\alpha s}}{r} d\mathbf{r}. \tag{2.138}$$

V_α is the microscopic mean field, which includes molecular level information as well as bulk properties of solvent. The RISM-SCF method can be much more informative compared to the usual self-consistent reaction field model based on the macroscopic dielectric continuum.

The rest of this section is devoted to the technique for the determination of effective charges assigned to the solute site, through which the RISM/HNC equation and the molecular orbital calculation are coupled. Although there can be several possibilities to define the effective charges, the least squares fitting technique is adopted in this work, so as to reproduce the electrostatic potential on the grids, defined arbitrary outside the solute molecule. The potential, $U(\mathbf{R}_k)$, which is generated by the solute molecule at the position $\mathbf{R}_k$ can be divided into two contributions: are from the nuclei, U_N, and the other from the electronic clouds, U_e:

$$U(\mathbf{R}_k) = U_N(\mathbf{R}_k) + U_e(\mathbf{R}_k), \tag{2.139}$$

where

$$U_N(\mathbf{R}_k) = \sum_A^N \frac{Z_A}{\mid \mathbf{R}_k - \mathbf{R}_A \mid}, \tag{2.140}$$

$$U_e(\mathbf{R}_k) = -\sum_{\nu,\lambda} P_{\nu\lambda} \langle \varphi_\nu \mid \frac{1}{\mid \mathbf{R}_k - \mathbf{r} \mid} \mid \varphi_\lambda \rangle \tag{2.141}$$

where Z_A is the nuclear charge of the nucleus A. $P_{\nu\lambda}$ is the density matrix, and φ_ν is the atomic orbital. While, the electrostatic potentials at the position $\mathbf{R}_k$ due to the effective charges on the interaction sites, which are identical to nucleus in the present case, are also written as

$$\tilde{U}(\mathbf{R}_k) = \tilde{U}_N(\mathbf{R}_k) + \tilde{U}_e(\mathbf{R}_k), \tag{2.142}$$

where

$$\tilde{U}_N(\mathbf{R}_k) = \sum_A^N \frac{q_A^{(N)}}{\mid \mathbf{R}_k - \mathbf{R}_A \mid}, \tag{2.143}$$

$$\tilde{U}_e(\mathbf{R}_k) = \sum_A^N \frac{q_A^{(e)}}{\mid \mathbf{R}_k - \mathbf{R}_A \mid}. \tag{2.144}$$

Therefore, in this case, the effective charges of nuclear part are given by $q_A^{(N)} = Z_A$. For the effective charge of electronic part, we carry out the usual procedure of minimizing the target functions with the constraints of preserving the total number of electrons as follows:

$$\frac{\partial}{\partial q_i^{(e)}} \left(\sum_{k=1}^{l} [U(\mathbf{R}_k) - \tilde{U}(\mathbf{R}_k)]^2 + 2\epsilon_e [\sum_A^N q_A^{(e)} - N_e] \right) = 0 \qquad \text{for all } q_i^{(e)}, \tag{2.145}$$

where k is the index of grid, and l is the total number of grid points. ϵ_e is Lagrange multipliers. N_e is the total number of electrons, $N_e = -\sum_{\nu,\lambda} P_{\nu\lambda} S_{\nu\lambda}$, and $S_{\nu\lambda}$ is the overlap integral between the atomic orbitals. $q_i^{(e)}$ are solved to be

$$q_i^{(e)} = -\sum_j a_{ij}^{-1} \sum_{\nu,\lambda} P_{\nu\lambda} D_{\nu\lambda,j} - \epsilon_e \sum_j a_{ij}^{-1}, \tag{2.146}$$

where

$$a_{ij} = \sum_k^l r_{ki}^{-1} r_{kj}^{-1}, \tag{2.147}$$

$$D_{\nu\lambda,j} = \sum_{k=1}^{l} \frac{1}{r_{kj}} \langle \varphi_\nu \mid \frac{1}{\mid \mathbf{R}_k - \mathbf{r} \mid} \mid \varphi_\lambda \rangle. \tag{2.148}$$

r_{ki} is the distance between the grid point k and the solute interaction site i. Using the relation,

$$\sum_i^N q_i^{(e)} = -\sum_{\nu,\lambda} P_{\nu\lambda} S_{\nu\lambda}, \tag{2.149}$$

we can obtain the Lagrange multiplier

$$\epsilon_e = \frac{-\sum_{i,j} a_{ij}^{-1} \sum_{\nu,\lambda} P_{\nu\lambda} D_{\nu\lambda,j} + \sum_{\nu,\lambda} P_{\nu\lambda} S_{\nu\lambda}}{\sum_{i,j} a_{ij}^{-1}}. \tag{2.150}$$

Finally, $q_i^{(e)}$ are given by

$$\begin{aligned} q_i^{(e)} &= \sum_{\nu,\lambda} P_{\nu\lambda} \langle \varphi_\nu \mid b_i \mid \varphi_\lambda \rangle \\ &= -\sum_j a_{ij}^{-1} \sum_{\nu,\lambda} P_{\nu\lambda} D_{\nu\lambda,j} \\ &\quad + \frac{\sum_j a_{ij}^{-1}}{\sum_{i,j} a_{ij}^{-1}} \left[\sum_{i,j} \{ a_{ij}^{-1} \sum_{\nu,\lambda} P_{\nu\lambda} D_{\nu\lambda,j} \} - \sum_{\nu,\lambda} P_{\nu\lambda} S_{\nu\lambda} \right]. \end{aligned} \tag{2.151}$$

From eqs. (2.137) and (2.151), the solvated Fock matrix element is written as follows:

$$\begin{aligned} F_{\nu\lambda} &= H_{\nu\lambda} + G_{\nu\lambda} - \sum_\alpha \langle \varphi_\nu \mid b_\alpha \mid \varphi_\lambda \rangle V_\alpha \\ &= H_{\nu\lambda} + G_{\nu\lambda} \\ &\quad - \sum_\alpha \left(\sum_\gamma a_{\alpha\gamma}^{-1} D_{\nu\lambda,\gamma} - \frac{\sum_\gamma a_{\alpha\gamma}^{-1}}{\sum_{\gamma,\gamma'} a_{\gamma\gamma'}^{-1}} \left[\sum_{\gamma,\gamma'} \{ a_{\gamma\gamma'}^{-1} D_{\nu\lambda,\gamma'} \} - S_{\nu\lambda} \right] \right) V_\alpha. \end{aligned} \tag{2.152}$$

As can be readily seen from the above equation, the microscopic mean field due to solvents interacts with the electronic structure of solute through the grid points. Note that the RISM/HNC equation is solved using $q_\alpha = Z_\alpha - q_\alpha^{(e)}$ as the effective charge of site α of the solute molecule.

Up to this point, the theoretical background of my work is reviewed briefly. In the next chapter, a new theory for the nuclear magnetic shielding in solution, based on the theories mentioned above, is explained.

References

[1] R. Ditchfield, Mol. Phys. **27**, 789 (1974).

[2] (a)D. Chandler and H.C. Andersen, J. Chem. Phys. **57**, 1930 (1972). (b)F. Hirata, P.J. Rossky, B.M. Pettitt, J. Chem. Phys. **78**, 4133 (1983) . (c)P. J. Rossky, Ann. Rev. Phys. Chem., **36**, 321 (1985). (d)F. Hirata, Bull. Chem. Soc. Jpn., **71**, 1483 (1998).

[3] (a)S. Ten-no, F. Hirata, and S. Kato, J. Chem. Phys. **100**, 7443 (1994). (b)H. Sato, F. Hirata, and S. Kato, J. Chem. Phys. **105**, 1546 (1996).

[4] (a)J. -P. Hansen and I. R. McDonald, *Theory of Simple Liquids* (Academic Press, London, 1986). (b)D. A. McQuarrie, *Statistical Mechanics* (HarperCollins, New York, 1976). (c)M. Toda, H. Matsuda, Y. Hiwatari, and M. Wadachi *EKITAI NO KOZO TO SEISHITU* (Iwanami, 1976) (in Japanese). (d)F. Yonezawa in *SURIKAGAKU* **444**, 76 (2000) (in Japanese).

[5] (a)A. C. de Dios, Prog. Nucl. Magn. Reson. Spectrosc., **29**, 229 (1996). (b)T. Helgaker, M. Jaszuński, and K. Ruud, Chem. Rev. **99**, 293 (1999). (c)U. Fleischer, C. van Wüllen, and W. Kutzelnigg in, *Encyclopedia of Computational Chemistry* edited by Paul von R. Schleyer, (Wiley, New York, 1998), p. 1827.

[6] (a)F. Hirata and P.J. Rossky, Chem. Phys. Lett. **83** (1981) 329. (b)F. Hirata, B.M. Pettitt, and P.J. Rossky, J. Chem. Phys. **77**, 509 (1982). (c)F. Hirata, P.J. Rossky, B.M. Pettitt, J. Chem. Phys. **78**, 4133 (1983) .

[7] S. J. Singer and D. Chandler, Mol. Phys. **55**, 621 (1985).

Chapter 3

Theory of NMR Shielding Constant in Solution

Related articles:

T. Yamazaki, H. Sato, and F. Hirata

"NMR chemical shifts in solution: a RISM-SCF approach"

Chemical Physics Letters, **325**, 668-674 (2000) ,

T. Yamazaki, H. Sato, and F. Hirata

"Solvent effect on the nuclear magnetic shielding: *ab initio* study by the combined reference interaction site model and electronic structure theories"

Journal of Chemical Physics, **115**, 8949-8957 (2001) .

Due to the site-specific sensitivity, the NMR spectroscopy is widely used for studying the structure and dynamics of chemical and biological systems ranging from small molecules to proteins and nucleic acids. Although many measurable parameters are of interest, such as spin-spin coupling constants, the nuclear Overhauser effect(NOE), and the spin relaxation time, chemical shift is the most commonly determined physical quantity and assigned in an essential step of NMR study. Since the most NMR measurements are carried out in solution, chemical shifts should probe not only the molecular structure but also the microscopic solvent effects, which are not separated in experiments. Therefore, it is of great importance to build a theory of the NMR chemical shift in solution, which

inevitably requires methods to treat the electronic structure of solute and the solvent distribution around the solute.

In the RISM-SCF framework, the nuclear magnetic shielding tensor $\boldsymbol{\sigma}^X$ of a nucleus X can be expressed as the mixed second derivative of the free energy A with respect to the external magnetic field $\mathbf{B}$ and the nuclear magnetic moment $\mathbf{m}^X$:

$$\sigma^X_{\alpha\beta} = \left.\frac{\partial^2 A(\mathbf{B},\mathbf{m})}{\partial B_\alpha \partial m^X_\beta}\right|_{\mathbf{B},\mathbf{m}=0} (\alpha,\beta = x,y,z)\,, \tag{3.1}$$

where B_α and m^X_β are the Cartesian components of $\mathbf{B}$ and of $\mathbf{m}^X$, respectively, and A is defined as a sum of the electronic energy of a solute molecule E_{solute} and the excess chemical potential due to solute-solvent interactions $\Delta\mu$:

$$A = E_{solute} + \Delta\mu. \tag{3.2}$$

In this thesis, E_{solute} is estimated in the Hartree-Fock (HF) level, and the gauge-invariant atomic orbitals (GIAO) method(see Section I in Chapter 2) is adopted to solve the gauge problem in the calculation of nuclear magnetic shielding. Each molecular orbital ϕ_i is expressed as a linear combination of GIAO $\chi_\nu(\mathbf{B})$:

$$\phi_i = \sum_\nu c_{i\nu}(\mathbf{B},\mathbf{m})\chi_\nu(\mathbf{B}), \tag{3.3}$$

where

$$\chi_\nu(\mathbf{B}) = \exp\left(-\frac{i}{c}\mathbf{A}_\nu \cdot \mathbf{r}\right)\varphi_\nu. \tag{3.4}$$

In the above expression, $\mathbf{A}_\nu = \frac{1}{2}\mathbf{B}\times\mathbf{R}_\nu$ is the vector potential at the nucleus position $\mathbf{R}_\nu$ of atomic orbital φ_ν. $\mathbf{r}$ is the position vector of an electron.

E_{solute} is given by

$$E_{solute} = \sum_{\nu\lambda} P_{\nu\lambda}(\mathbf{B},\mathbf{m})\left\{H_{\nu\lambda}(\mathbf{B},\mathbf{m}) + \frac{1}{2}G_{\nu\lambda}(\mathbf{B},\mathbf{m})\right\}. \tag{3.5}$$

The one electron term

$$H_{\nu\lambda}(\mathbf{B},\mathbf{m}) = \langle\chi_\nu \mid \frac{1}{2}\left\{-i\nabla + \frac{1}{c}\mathbf{A}(\mathbf{r})\right\}^2 - \sum_N \frac{Z_N}{r_N} \mid \chi_\lambda\rangle, \tag{3.6}$$

depends on the magnetic vector potential

$$\mathbf{A}(\mathbf{r}) = \frac{1}{2}\mathbf{B} \times \mathbf{r}_O + \sum_N \frac{\mathbf{m}^N \times \mathbf{r}_N}{r_N^3}, \tag{3.7}$$

where $\mathbf{r}_O$ is the position of an electron with respect to an arbitrarily chosen gauge origin $\mathbf{O}$, and $\mathbf{r}_N$ is the position of an electron relative to the nucleus with charge Z_N. Using the commutator

$$[-i\nabla + \frac{1}{c}\mathbf{A}(\mathbf{r}), \exp(-\frac{i}{c}\mathbf{A}_\lambda \cdot \mathbf{r})] = -\frac{1}{c}\mathbf{A}_\lambda \exp(-\frac{i}{c}\mathbf{A}_\lambda \cdot \mathbf{r}), \tag{3.8}$$

one can see that the $H_{\nu\lambda}$ is independent of $\mathbf{O}$.

The density matrix $P_{\nu\lambda}(\mathbf{B}, \mathbf{m})$ and the two electron term $G_{\nu\lambda}(\mathbf{B}, \mathbf{m})$ are given by

$$P_{\nu\lambda}(\mathbf{B}, \mathbf{m}) = 2\sum_j^{occ} c_{j\nu}^*(\mathbf{B}, \mathbf{m}) c_{j\lambda}(\mathbf{B}, \mathbf{m}), \tag{3.9}$$

$$\begin{aligned} G_{\nu\lambda}(\mathbf{B}, \mathbf{m}) &= \sum_{\zeta\xi} P_{\zeta\xi}(\mathbf{B}, \mathbf{m})\{(\chi_\nu\chi_\lambda|\chi_\zeta\chi_\xi) - \frac{1}{2}(\chi_\nu\chi_\xi|\chi_\zeta\chi_\lambda)\} \\ &= \sum_{\zeta\xi} P_{\zeta\xi}(\mathbf{B}, \mathbf{m}) G_{\nu\lambda\zeta\xi}(\mathbf{B}), \end{aligned} \tag{3.10}$$

where

$$(\chi_\nu\chi_\lambda|\chi_\zeta\chi_\xi) = \int\int d\tau_1 d\tau_2 \chi_\nu^*(1)\chi_\lambda(1)\frac{1}{r_{12}}\chi_\zeta^*(2)\chi_\xi(2). \tag{3.11}$$

For the chemical potential term $\Delta\mu$, the equation derived by Singer and Chandler(eq. (2.131)) is employed:

$$\Delta\mu = -\rho k_B T \sum_{\gamma s} \int d\mathbf{r}\left[c_{\gamma s}(r) - \frac{1}{2}h_{\gamma s}^2(r) + \frac{1}{2}h_{\gamma s}(r)c_{\gamma s}(r)\right], \tag{3.12}$$

where ρ, k_B and T are the density of solvent, the Boltzmann constant and temperature, respectively. The subscripts γ and s refer to the interaction sites of the solute and of the solvent molecules, respectively. The direct correlation functions $c_{\gamma s}$ and the total correlation functions $h_{\gamma s}$ are obtained by the RISM theory with the hypernetted-chain (HNC) type of closure(eq. (2.113) and eq. (2.114)):

$$h_{\gamma s}(r) = \sum_{\gamma' s'} \omega_{\gamma\gamma'} * c_{\gamma' s'} * \chi_{s' s}(r), \tag{3.13}$$

$$g_{\gamma s}(r) = \exp\left[-\frac{1}{k_B T}u_{\gamma s}(r) + h_{\gamma s}(r) - c_{\gamma s}(r)\right], \tag{3.14}$$

where $g_{\gamma s} = h_{\gamma s} + 1$ is the radial distribution function of the s-th site of solvent molecules around the γ-th site of the solute molecule. $\omega_{\gamma\gamma'}$ is the intramolecular correlation function containing the geometrical information of the solute. $\chi_{s's}$ is the pure solvent site density pair correlation function. Here "$*$" denotes the spatial convolution. The solute-solvent interaction potential $u_{\gamma s}$ is assumed to be the sum of Coulombic and Lennard-Jones terms:

$$u_{\gamma s} = \frac{q_\gamma q_s}{r} + 4\epsilon_{\gamma s}\left[\left(\frac{\sigma_{\gamma s}}{r}\right)^{12} - \left(\frac{\sigma_{\gamma s}}{r}\right)^{6}\right]. \tag{3.15}$$

The standard mixing rules $\epsilon_{\gamma s} = (\epsilon_\gamma \epsilon_s)^{1/2}$ and $\sigma_{\gamma s} = (\sigma_\gamma + \sigma_s)/2$ are employed for calculating the Lennard-Jones potential parameters. Note that the effective charges q_γ assigned to the solute sites depend on the solute electronic wave function as follows:

$$q_\gamma = \sum_{\nu\lambda} P_{\nu\lambda}(\mathbf{B},\mathbf{m})\langle\chi_\nu(\mathbf{B}) \mid b_\gamma \mid \chi_\lambda(\mathbf{B})\rangle, \tag{3.16}$$

where b_γ is the population operator for the solute site γ. The Fock operator with solvent effect derives naturally from the variational procedure:

$$F_{\nu\lambda} = H_{\nu\lambda} + G_{\nu\lambda} - \sum_\gamma \langle\chi_\nu \mid b_\gamma \mid \chi_\lambda\rangle \rho \sum_s q_s \int d\mathbf{r}\frac{g_{\gamma s}}{r}. \tag{3.17}$$

First, differentiating eq. (3.2) with respect to m_β^X leads to

$$\begin{aligned}
\frac{\partial A}{\partial m_\beta^X} &= \frac{\partial E_{solute}}{\partial m_\beta^X} + \frac{\partial \Delta\mu}{\partial m_\beta^X} \\
&= \sum_{\nu\lambda}\left[\frac{\partial P_{\nu\lambda}}{\partial m_\beta^X}\{H_{\nu\lambda} + G_{\nu\lambda}\} + P_{\nu\lambda}\frac{\partial H_{\nu\lambda}}{\partial m_\beta^X}\right] + \sum_\gamma \frac{\partial q_\gamma}{\partial m_\beta^X}\rho\sum_s q_s\int d\mathbf{r}\frac{g_{\gamma s}}{r} \\
&= \sum_{\nu\lambda} P_{\nu\lambda}\frac{\partial H_{\nu\lambda}}{\partial m_\beta^X}.
\end{aligned} \tag{3.18}$$

Secondly, differentiating the eq. (3.18) with respect to B_α leads to the final expression for the nuclear magnetic shielding tensor

$$\sigma_{\alpha\beta}^X = \sum_{\nu\lambda}\left\{P_{\nu\lambda}^{(0)}\left(H_{\nu\lambda}^{(1,1)}\right)_{\alpha\beta}^X + \left(P_{\nu\lambda}^{(1,0)}\right)_\alpha\left(H_{\nu\lambda}^{(0,1)}\right)_\beta^X\right\}. \tag{3.19}$$

Note that this equation is the same form as in the gas phase derived in section I. In the above equation, for example,

$$\left(P_{\nu\lambda}^{(1,0)}\right)_\alpha = \left.\frac{\partial P_{\nu\lambda}}{\partial B_\alpha}\right|_{\mathbf{B},\mathbf{m}=0}, \tag{3.20}$$

$$\left(H_{\nu\lambda}^{(1,1)}\right)_{\alpha\beta}^{X} = \left.\frac{\partial^2 H_{\nu\lambda}}{\partial B_\alpha \partial m_\beta^X}\right|_{\mathbf{B},\mathbf{m}=0}. \tag{3.21}$$

$P_{\nu\lambda}^{(0)}$ can be calculated from the field-independent RISM-SCF method. $\left(H_{\nu\lambda}^{(1,1)}\right)_{\alpha\beta}^{X}$ and $\left(H_{\nu\lambda}^{(0,1)}\right)_{\beta}^{X}$ are the same expressions as those from the conventional *ab initio* electronic structure theory in gas phase, while $\left(P_{\nu\lambda}^{(1,0)}\right)_\alpha$ are determined by solving the first-order coupled-perturbed HF equation in the RISM-SCF framework:

$$\sum_\lambda \left[\left(F_{\nu\lambda}^{(0)} - \epsilon_j^{(0)} S_{\nu\lambda}^{(0)}\right)\left(c_{j\lambda}^{(1,0)}\right)_\alpha + \left\{\left(F_{\nu\lambda}^{(1,0)}\right)_\alpha - \epsilon_j^{(0)}\left(S_{\nu\lambda}^{(1,0)}\right)_\alpha\right\} c_{j\lambda}^{(0)}\right] = 0. \tag{3.22}$$

The derivative of the interaction term between solute and solvents with respect to the external magnetic field is required for calculating $\left(F_{\nu\lambda}^{(1,0)}\right)_\alpha$:

$$\begin{aligned}\left(F_{\nu\lambda}^{(1,0)}\right)_\alpha &= \left(H_{\nu\lambda}^{(1,0)}\right)_\alpha + \sum_{\zeta\xi}\left\{P_{\zeta\xi}^{(0)}\left(G_{\nu\lambda\zeta\xi}^{(1,0)}\right)_\alpha + \left(P_{\zeta\xi}^{(1,0)}\right)_\alpha G_{\nu\lambda\zeta\xi}^{(0)}\right\} \\ &\quad - \sum_\gamma \left(\langle\chi_\nu \mid b_\gamma \mid \chi_\lambda\rangle^{(1,0)}\right)_\alpha \rho \sum_s q_s \int d\mathbf{r}\frac{g_{\gamma s}}{r}.\end{aligned} \tag{3.23}$$

The effective charges of solute are determined by the least square fitting procedure in the present work. The derivative of the elements for the population operator is, then, given by

$$\begin{aligned}\left(\langle\chi_\nu \mid b_\gamma \mid \chi_\lambda\rangle^{(1,0)}\right)_\alpha &= -\sum_{\gamma'} a_{\gamma\gamma'}^{-1}\left(D_{\nu\lambda,\gamma'}^{(1,0)}\right)_\alpha \\ &\quad + \frac{\sum_{\gamma'} a_{\gamma\gamma'}^{-1}}{\sum_{\gamma'\gamma''} a_{\gamma'\gamma''}^{-1}}\left[\sum_{\gamma'\gamma''}\left\{a_{\gamma'\gamma''}^{-1}\left(D_{\nu\lambda,\gamma''}^{(1,0)}\right)_\alpha\right\} - \left(S_{\nu\lambda}^{(1,0)}\right)_\alpha\right].\end{aligned} \tag{3.24}$$

where

$$a_{\gamma\gamma'} = \sum_k r_{k\gamma}^{-1} r_{k\gamma'}^{-1}, \tag{3.25}$$

$$\left(D_{\nu\lambda,\gamma'}^{(1,0)}\right)_\alpha = \sum_k \frac{1}{r_{k\gamma'}}\langle\frac{i}{2}\left\{(\mathbf{R}_\nu - \mathbf{R}_\lambda)\times\mathbf{r}\right\}_\alpha \varphi_\nu \mid \frac{1}{\mathbf{R}_k - \mathbf{r}} \mid \varphi_\lambda\rangle, \tag{3.26}$$

$\mathbf{R}_k$ is the position vector of grid, and $r_{k\gamma}$ is the distance between the grid point k and the solute interaction site γ. In eq. (3.23), the contribution from the derivative of the radial

distribution function with respect to the external magnetic field does not appear. The radial distribution function, in the present framework, depends on the external magnetic field only through the effective charges of solute, and therefore, the derivative of the radial distribution function depends only on the derivative of the effective charge of solute with respect to the external magnetic field. Differentiating the effective charge of solute with respect to the external magnetic field leads to the trace of the products of Hermitian and anti-Hermitian matrices(see eq. (3.16)). Since the trace of these products is equal to zero, the derivative of the effective charge also vanishes. For this reason, the contribution does not appear.

The present method has two outstanding features. One can obtain the nuclear magnetic shielding constant in solution nonempirically in the sense that the theory is free from macroscopic empirical parameters such as dielectric constant, and study the nuclear magnetic shielding by the relationship with the solvation structure. Another advantage of the present method is that electron correlation can be taken into account by the standard procedures.

Chapter 4

Results and Discussion

T. Yamazaki, H. Sato, and F. Hirata

"NMR chemical shifts in solution: a RISM-SCF approach"

Chemical Physics Letters, **325**, 668-674 (2000) ,

T. Yamazaki, H. Sato, and F. Hirata

"Solvent effect on the nuclear magnetic shielding: *ab initio* study by the combined reference interaction site model and electronic structure theories"

Journal of Chemical Physics, **115**, 8949-8957 (2001) .

I Chemical Shifts of a Water Molecule Solvated in Water

In this section, the numerical results of chemical shifts obtained using the RISM-SCF procedure are presented. Here, the chemical shift of a water molecule in water is calculated to demonstrate the validity of the present method. An isolated water molecule in gas phase is adopted as the reference material for the chemical shift. The results in the following tables and figures are obtained by using the TIP3P[1]-like model for solvent molecules. The geometry of both solute water molecule in liquid phase and isolated water molecule in gas phase are fixed at that of the TIP3P model except for the case that the effect of geometry change to the chemical shift is examined. The values σ=1.0 Å and ϵ=0.056 kcal/mol

are assigned to the van der Waals parameters of the hydrogen site.[2] The electronic wave functions of the solute water molecule and of the isolated water molecule were calculated in the Hartree-Fock level with 6-311G** basis set using the GAUSSIAN 94[3] incorporated in the RISM-SCF method. In case of the nuclear magnetic shieldings in gas phase, it is reported that the results obtained using the basis set of this level are reasonably close to the estimated Hartree-Fock limit.[4]

Table 1
Nuclear magnetic shieldings and chemical shifts of water molecule (ppm)

	Nuclear magnetic shielding		Chemical shift
	Gas phase	Liquid phase	
Hydrogen			
Mikkelsen et al.	30.91	29.96	0.95
present work	31.49	29.68	1.81
exp.	30.05	25.79	4.26
Oxygen			
Mikkelsen et al.	336.6	346.0	-9.4
present work	343.5	366.5	-23.0
exp.	344.0	307.9	36.1

I.1 Chemical shifts of hydrogen

The results for the nuclear magnetic shielding of the atoms in a water molecule in gas phase and in aqueous solutions (25 ℃, 1.0g/cm^3), obtained by the present method, are shown in Table 1 along with the experimental data[5] and the theoretical results based on the continuum model.[6] Also presented in the table are the results for the chemical shift associated with transferring the water molecule from gas to aqueous environment. The result obtained by the present method for the chemical shift of hydrogen is in qualitative

accord with the experiment. The theoretical result based on the continuum model also shows a reasonable account for the chemical shift of hydrogen. However, it is worthwhile to remark at this point that our result was obtained entirely in a non-empirical manner unlike the other approach. I believe this is the essential requirement for theoretical treatments to be predictive.

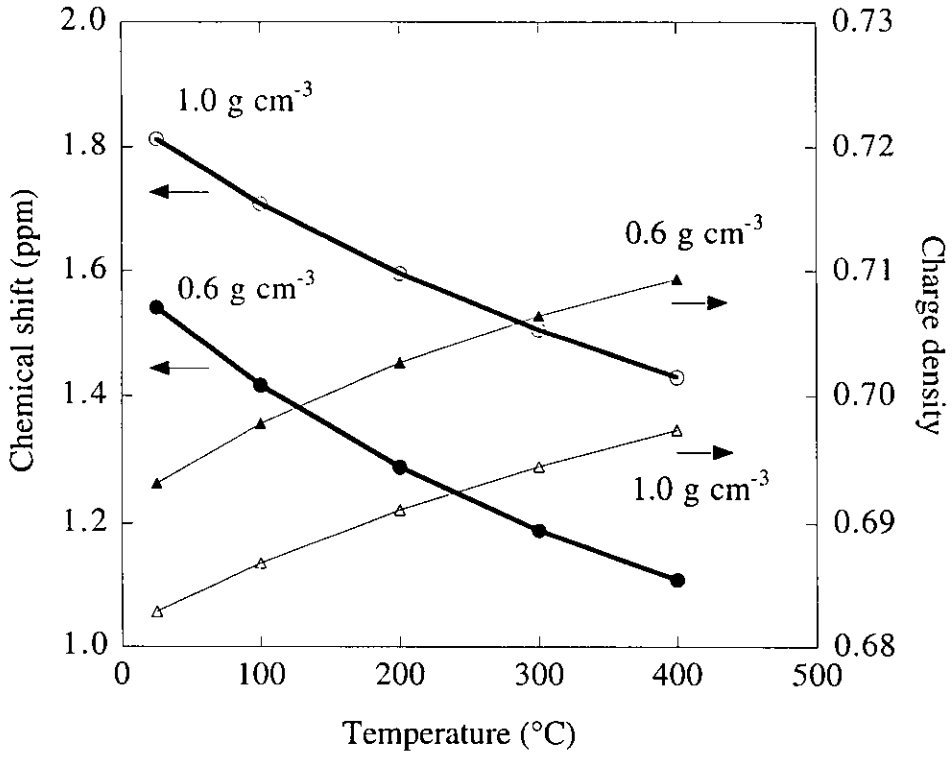

Figure 4.1: Temperature dependence of the chemical shift(left hand side) and of the charge density(right hand side) of hydrogen atom at the normal($1.0g/cm^3$) and the low($0.6g/cm^3$) density.

In Fig. 4.1, the chemical shift and the charge density of hydrogen are plotted as a function of temperature for the normal ($1.0g/cm^3$) and low density ($0.6g/cm^3$). First, let us analyze temperature dependence of the chemical shift. It is found that the charge density increases with rising temperature, while the chemical shift decreases. The temperature dependence of the chemical shift is in accordance with the experimentally observed trend

.[7] Considering the increase in charge density and the decrease in the height of the first peak of the pair correlation functions (PCF) around 1.8Å shown in Fig. 4.2, it is clear that the decrease the chemical shift with increasing temperature is caused by weakening of hydrogen-bonds. Such an interpretation regarding the temperature dependence of the hydrogen chemical shift has been given rather intuitively in the field of solution NMR. However, this is the first *ab initio* theory to relate the two observables, the chemical shift and the PCFs, which probe the degree of hydrogen-bonding in water.

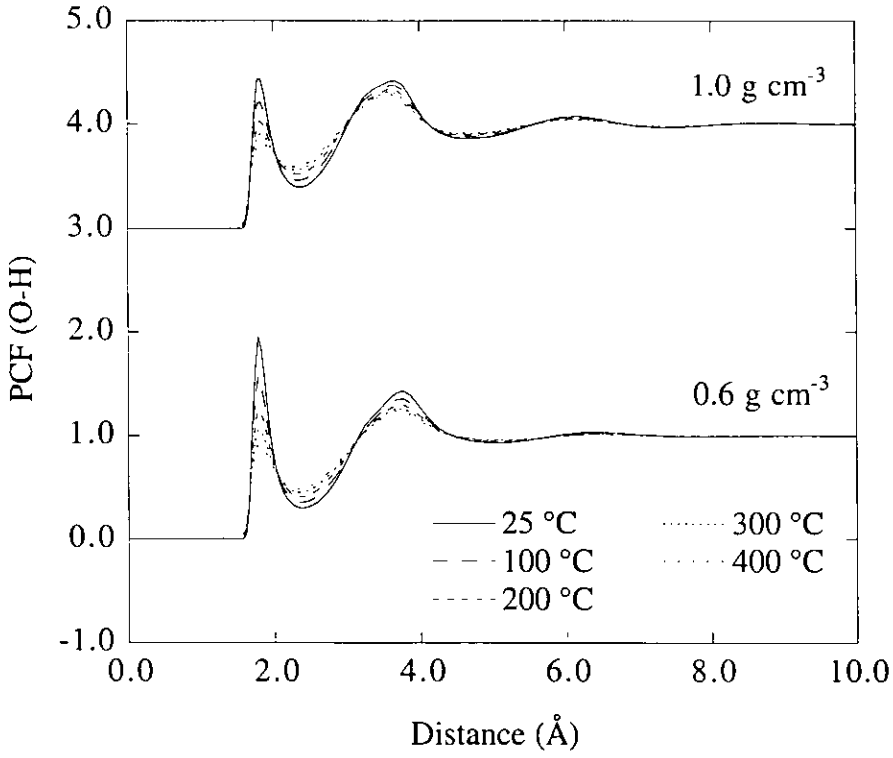

Figure 4.2: Temperature dependence of O-H PCF in liquid water at the normal($1.0 g/cm^3$) and the low($0.6 g/cm^3$) density.

Next, let us discuss the density dependence. It is seen from the results of the chemical shift and of the charge density that the strength of hydrogen-bond in the low density is weaker than that in the normal density. On the other hand, the results for PCFs and their difference between the two density cases, which are shown in Fig. 4.2 and Fig. 4.3, respectively, also suggest that the correlation between oxygen and hydrogen in the low

density is stronger than that in the normal density.

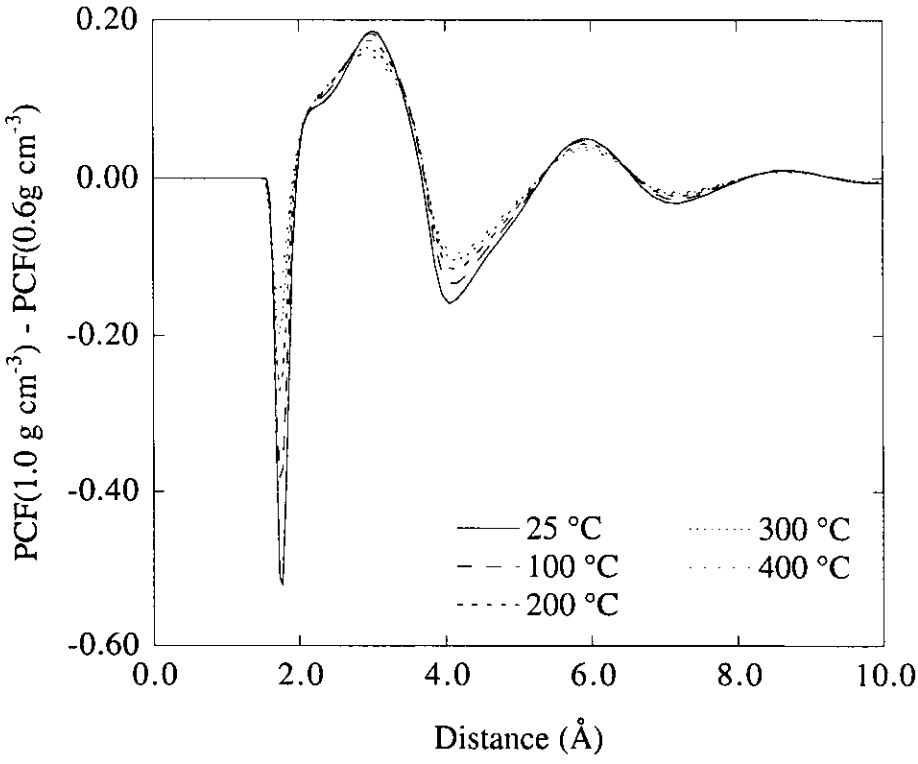

Figure 4.3: Response of O-H PCF to temperature change at the normal($1.0g/cm^3$) and the low($0.6g/cm^3$) density.

These observations are apparently contradictory. Why is the O-H correlation at the low density stronger? The problem was already discussed by Sato and Hirata.[8] According to their discussion, the density increase will give rise to two effects on the correlation between oxygen and hydrogen. One of those is the increase in the molecular polarization, which promotes the correlation. The other is the enhancement of the packing effect, which disturbs the correlation. The correlation between oxygen and hydrogen is determined by an interplay between their two effects with increasing density: the packing effect dominates and weakens the correlation in the normal density, while the electronic polarization effect dominates over the packing effect to make the correlation stronger in the low density. The strength of hydrogen-bond would be related not only to the height of the peak of the PCFs but to the number of hydrogen-bond. The number of hydrogen-bond is given by

$N = \rho_H \int_0^R g_{OH} 4\pi r^2 dr$, where ρ_H is the number density of hydrogen atoms, g_{OH} is the O-H PCF, and R is the first minimum of O-H PCF which is most commonly employed, respectively. Sato and Hirata. also reported that the number of hydrogen-bond increases with increasing density. We can say from these discussions that the total electrostatic potential on the solute molecule induced by the hydrogen-bond is stronger in the normal density, though the correlation is less. Therefore, the results of the chemical shift suggest that the hydrogen-bond is stronger in the normal density.

Table 2

Temperature and density dependence of hydrogen chemical shifts in water(ppm)

Temp. / Dens.	Calc.		Exp.
	Sheilding constant	Chemical shift	Chemical shift
30 / 1.00	29.69	1.80	4.27
200 / 0.86	29.99	1.50	2.84
300 / 0.71	30.21	1.28	2.12 ± 0.02
400 / 0.60	30.38	1.11	1.64 ± 0.05

The shielding constant and the chemical shift of water hydrogen are presented in Table 2 for a wide range of temperature and density in comparison with the experimental results.[7] It is seen that the present method reproduces the order of magnitude and tendency of the experimental chemical shifts reasonably well. It can be concluded that the method is valid not only for the temperature dependence, but also for the density dependence of chemical shift of hydrogen.

Quantitatively speaking, however, the agreement with experiments is not always satisfactory. The conceivable sources of the disagreement can be classified roughly into the following three: electronic structure of solute, solvent distribution, and intermolecular interaction. In the present framework, the electron correlation is disregarded. Although

the results in gas phase[4, 9] suggest that the effect is less important for hydrogen, it is not necessarily clear whether the same statement applies to liquid phase. The solvent distribution, which affects the electronic structure through the electrostatic reaction field, depends on the closure relation employed in the integral equation. Making use of the other closure relations may improve the results. Contributions from the electronic overlap[10] in the solute-solvent repulsive interaction are not taken into account in the present method. Despite that the effect is reported to be small for hydrogen,[10, 11, 12] the present calculation indicates that such effect may not be entirely negligible. If such effect is negligibly small, the disagreement between the theory and experiments will not depend on temperature and density of solvent. However, our results indicate that the disagreement enlarges with increasing density and/or decreasing temperature, in which the electronic overlap becomes more significant.

I.2 Chemical shifts of oxygen

It can be seen from Table 1 that the present results of the chemical shift of oxygen disagrees with the experiment[13] not only for the absolute value but also for their direction (sign). The same trend is seen in the continuum model.[4, 6, 14, 15] Although the present theory describes the hydrogen-bond in molecular level, the classical description may not be sufficient for the chemical shift of oxygen in water. One may also be concerned with the molecular geometry. Several geometries of the "solute" water molecule, including the one optimized in liquid phase, were examined. However, the result was not improved appreciably. Since the RISM theory is known to give reasonable account for the statistical distribution of solvent around solute, and thereby for the reaction field, the qualitative error observed in the calculation of the oxygen chemical shift may not be due merely to the approximations involved in the classical nature of the theory. It can be due rather to some quantum effects which are disregarded in the present treatment. It is worthwhile in this respect to note that the *ab initio* calculation gives good account for the chemical shift of oxygen of water in a molecular cluster.[16, 17] This suggests that the chemical shift of

oxygen is extremely sensitive to subtle details of the intermolecular interaction. The most conspicuous element, which is included in the cluster treatment but not in the present theory, is the exchange or overlap of electrons between solute and solvent. Generally speaking, thermodynamic quantities will not distinguish such a subtle effect in the intermolecular interaction or the electronic structure: the NMR chemical shift, on the other hand, could be sensitive enough to probe such subtlety. In this regard, the NMR chemical shift can be a good candidate as an experimental criterion for further improvement of the theories. Concerning the intermolecular effect for the nuclear magnetic shielding, a more detailed discussion is given in section III.

II Chemical Shifts of a Water Molecule Solvated in Various Solvents

Recently, the proton chemical shifts of a water molecule in dilute organic solvents have been obtained by Nakahara *et al.*[18, 19] over a wide temperature range using a modern NMR machine. On the basis of the experiment, the proton chemical shifts of a solute water molecule in a variety of solvents, over the temperature range studied, are in the sequence, in water > in acetone > in chloroform > in carbon tetrachloride. The proton chemical shifts decrease with increasing temperature. In this section, I study solvent and temperature dependence of the proton chemical shifts of a water molecule in a variety of solvent; water, acetone, chloroform, and carbon tetrachloride, used in the above experiment. An isolated water molecule in gas phase is adopted as the reference material for the chemical shifts. The TIP3P-like[1] model (including core repulsion for the hydrogen site) is used to describe solute and solvent water. The OPLS parameters are used for acetone (methyl group is treated as a united atom centered on the carbon atom)[20] and carbon tetrachloride solvents.[21] For chloroform, the parameters proposed by Dietz *et al*[22] are employed. The geometric and potential parameters for the solute and solvent are summarized in Table 3. The geometric parameters for acetone are taken from experimental results in gas phase.[23] The solvent densities for water, acetone, chloroform, and carbon tetrachloride are, respectively, fixed at 0.03336, 0.008187, 0.007480, and 0.006238 molecules/Å^3, which are measured at 1 atm and 20 ℃,[24] and the temperature is changed from 10 to 50 ℃ for every 10 ℃. The electronic wave functions of a water molecule in solvent and in gas phase were calculated in the Hartree-Fock level with 6-311G** basis set using the GAUSSIAN 94[3] incorporated in the RISM-SCF method. The effective charges are parametrized so as to reproduce the electrostatic potential around the solute molecule by using 26 angular grids ((100),(110),(111) and so on), which originates from the center of mass of the solute molecule. In each direction, four radial grids are equally spaced from 2 to 30 Bohr. The excess grids inside the van der Waals radius are discarded. As in the

pervious section, total number of the grids is 78.

TABLE 3. Geometric and Lennerd-Jones parameters

Molecule	Geometric parameter(Å and degree)		Site	q(e)	σ(Å)	ε(kcal/mol)
H_2O	r (O-H)	0.9572	H	0.400	3.216	0.1188
	∠ H-O-H	104.52	O	-0.800	1.000	0.0560
CH_3CH_3CO	r (CH_3-C)	1.507	CH_3	0.062	3.910	0.1600
	r (C=O)	1.222	C	0.300	3.750	0.1050
	∠ CH_3-C-CH_3	117.20	O	-0.424	2.960	0.2100
$CHCl_3$	r (C-H)	1.100	C	0.179	3.400	0.1017
	r (C-Cl)	1.758	H	0.082	2.200	0.0199
	∠ Cl-C-Cl	111.30	Cl	-0.087	3.440	0.2993
CCl_4	r (C-Cl)	1.769	C	0.248	3.800	0.0500
	∠ Cl-C-Cl	109.47	Cl	-0.062	3.470	0.2660

The proton chemical shifts in each solvent, obtained by the present procedure, are plotted as a function of temperature in Fig. 4.4. The nuclear magnetic shielding constants and the chemical shifts of the hydrogen atom of the solute water molecule in the four solvents at 20 ℃ are shown in Table 4. The radial distribution functions(RDF) and the response of RDFs to temperature change for each solvent are shown in Figs. 4.5 - 4.8.

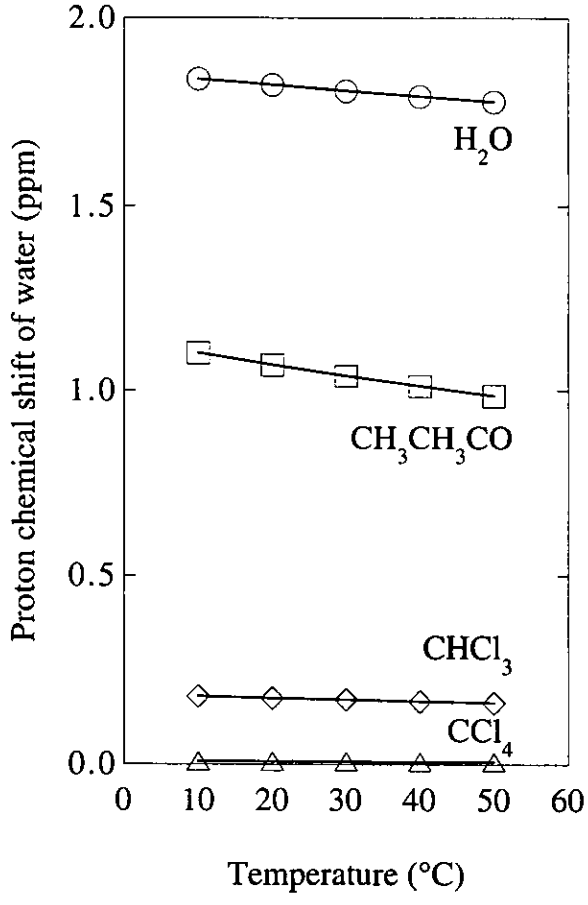

Figure 4.4: Temperature dependence of the chemical shift of a water molecule in water, acetone, chloroform, and carbon tetrachloride. The chemical shifts are given relative to the isolated water molecule in gas phase.

TABLE 4. Nuclear magnetic shieldings and chemical shifts(ppm) for the hydrogen atom of the solute water molecule.

Solvent	Nuclear magnetic shieldings	Chemical shifts
H_2O	29.6710	1.821
CH_3CH_3CO	30.4219	1.070
$CHCl_3$	31.3145	0.178
CCl_4	31.4851	0.007

As is shown in Fig. 4.4, the present method qualitatively reproduces the two observations in the experiment.[18, 19] First, the proton chemical shifts of the solute water molecule are in the sequence over the temperature range studied,

in water > in acetone > in chloroform > in carbon tetrachloride.

Secondly, the proton chemical shifts decrease with increasing temperature. These results demonstrate capability of the theory to predict experimental results at least qualitatively. Fig. 4.4 is the principal result of this thesis. In the following paragraphs, I discuss the relationship between the solvation structures and the proton chemical shifts.

The solvation structure is governed by two factors, the electrostatic interaction(EI) between solute and solvents and the packing effect(PE). The electrostatic potential induced by solvent affects the electronic structure of solute molecule, and changes the nuclear magnetic shieldings. Therefore, on discussing the relation between the solvation structures and the proton chemical shifts, the following decomposition of the RDF into two terms is useful: RDF "g^{PE}" concerns about the packing effect and is defined by neglecting the electrostatic interactions between solute and solvents, RDFs "g^{EI}" associated with the

electrostatic interactions, which can be defined by

$$g^{\mathrm{EI}}(r) = g(r; \mathrm{EI} \neq 0) - g^{\mathrm{PE}}(r; \mathrm{EI} = 0), \tag{4.1}$$

where $g(r; \mathrm{EI} \neq 0)$ is the RDF with full solute-solvent interactions.

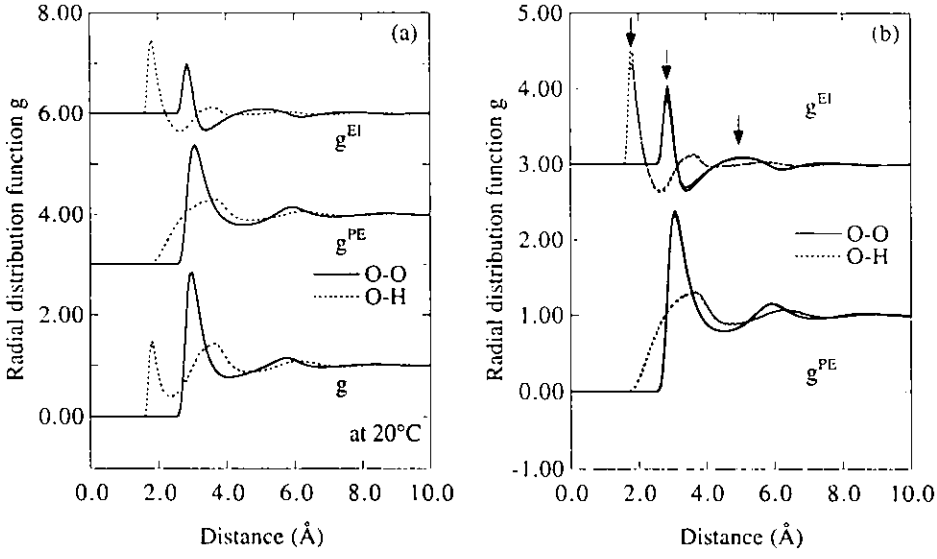

Figure 4.5: RDFs and response of RDFs to the temperature change for the water(solute)-water(solvent) system. (a) Decomposition of g into g^{PE} and g^{EI} with their origin at the oxygen atom of the water molecule at 20 ℃. (b) Response of g^{PE} and g^{EI} to the temperature change. The RDFs obtained at 10 and 50 ℃ are shown. The arrow indicates the direction of change in the peak height of $g^{\mathrm{EI}}(r)$ due to temperature increase.

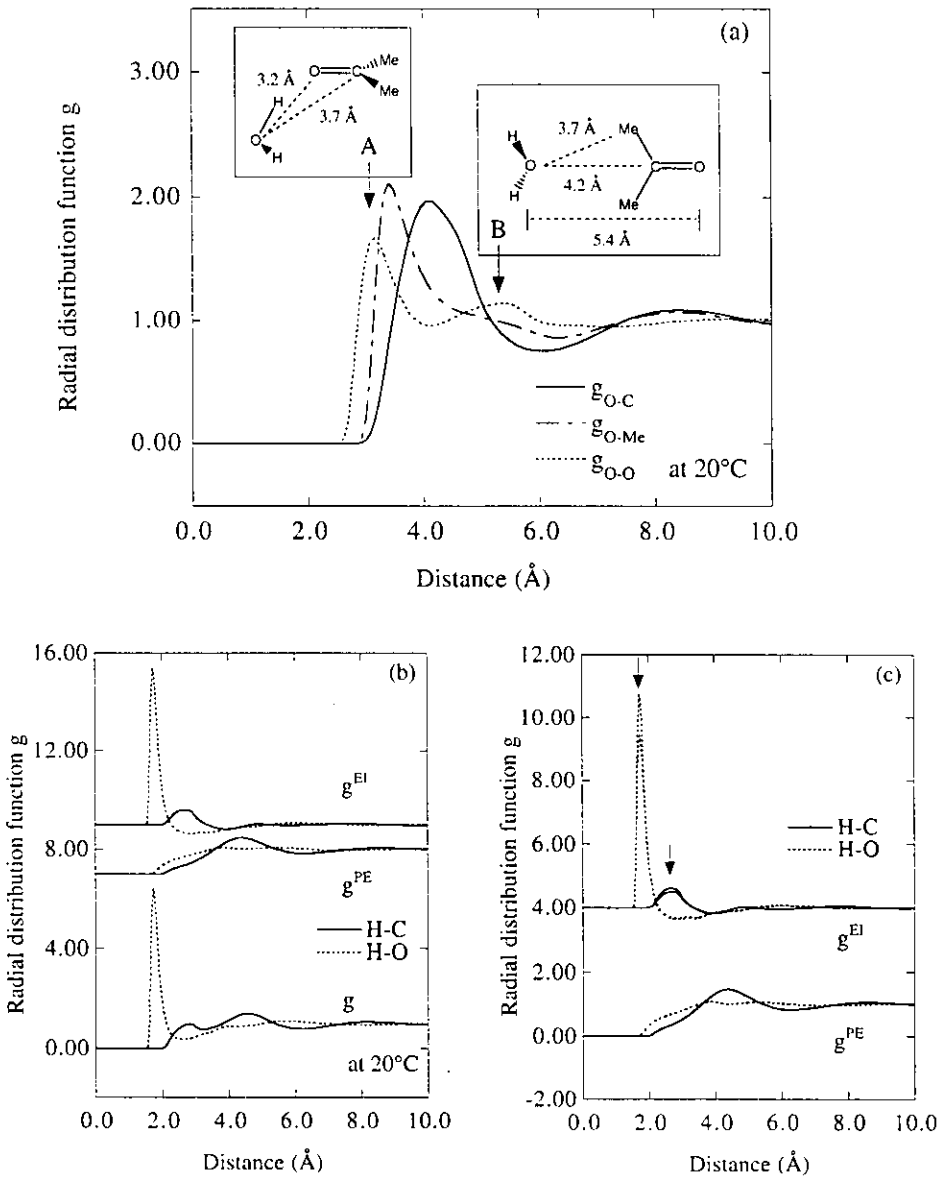

Figure 4.6: RDFs and response of RDFs to the temperature change for the water(solute)-acetone(solvent) system. (a) RDFs with their origin at the oxygen atom of the water molecule. The arrow indicates the peak positions which are characteristic of the two solvation structures "A" and "B". (b) Decomposition of g into g^{PE} and g^{EI} with their origin at the hydrogen atom of the water molecule at 20 ℃. (c) Response of g^{PE} and g^{EI} to the temperature change. The RDFs obtained at 10 and 50 ℃ are shown. The arrow indicates the direction of change in the peak height of $g^{\mathrm{EI}}(r)$ due to temperature increase.

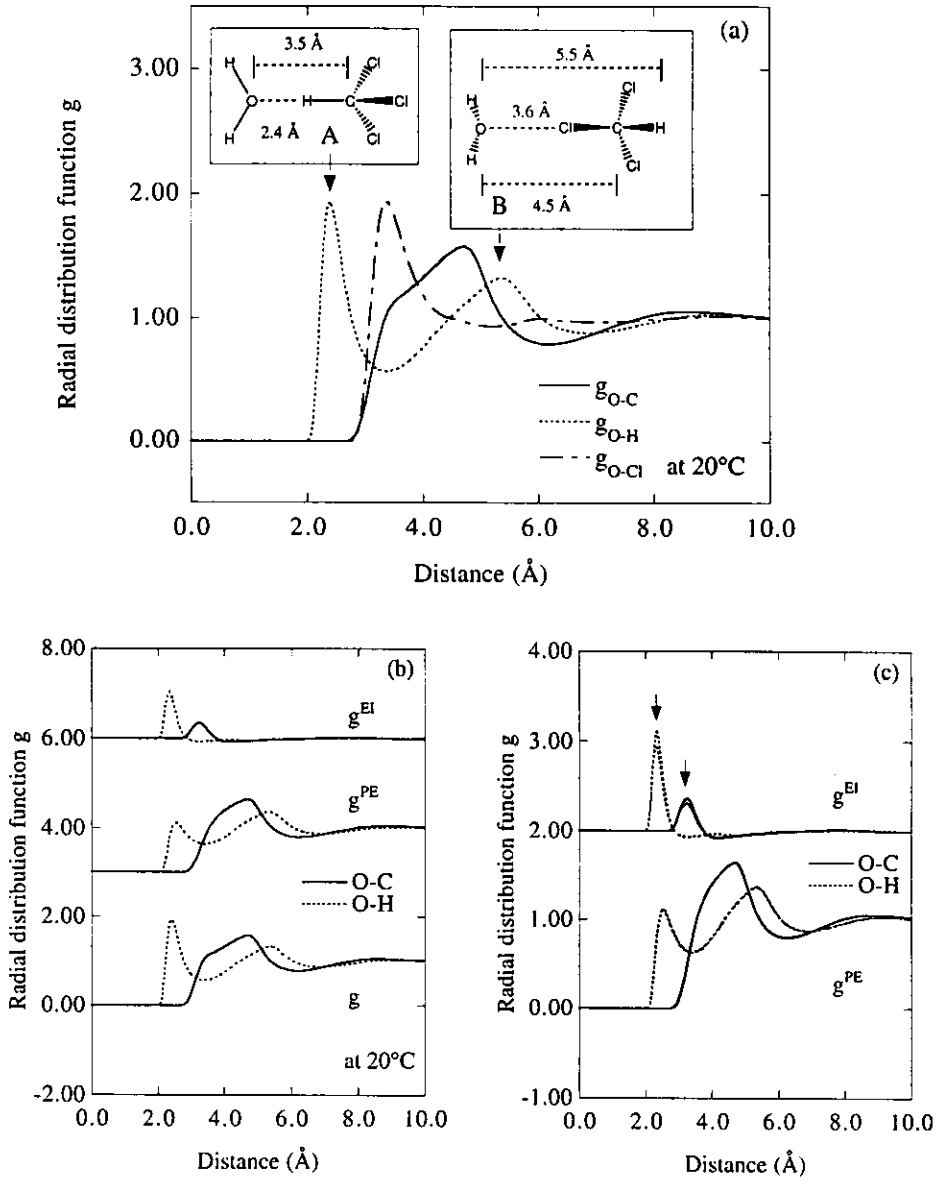

Figure 4.7: RDFs and response of RDFs to the temperature change for the water(solute)-chloroform(solvent) system. (a) RDFs with their origin at the oxygen atom of the water molecule. The arrow indicates the peak positions which are characteristic of the two solvation structures "A" and "B". (b) Decomposition of g into g^{PE} and g^{EI} with their origin at the oxygen atom of the water molecule at 20 ℃. (c) Response of g^{PE} and g^{EI} to the temperature change. The RDFs obtained at 10 and 50 ℃ are shown. The arrow indicates the direction of change in the peak height of $g^{\mathrm{EI}}(r)$ due to temperature increase.

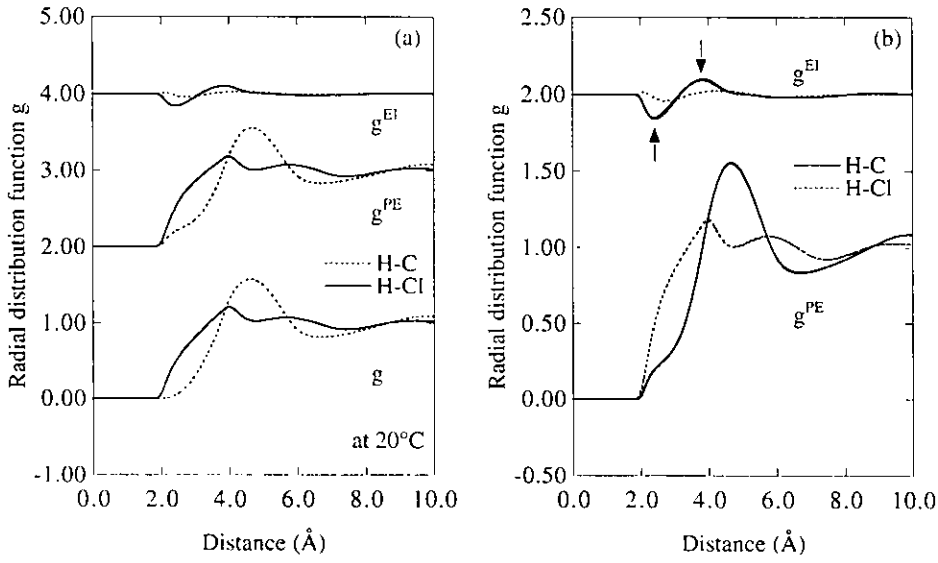

Figure 4.8: RDFs and response of RDFs to the temperature change for the water(solute)-carbon tetrachloride(solvent) system. (a) Decomposition of g into g^{PE} and g^{EI} with their origin at the oxygen atom of the water molecule at 20 ℃. (b) Response of g^{PE} and g^{EI} to the temperature change. The RDFs obtained at 10 and 50 ℃ are shown. The arrow indicates the direction of change in the peak height of $g^{\mathrm{EI}}(r)$ due to temperature increase.

First, I discuss the relationship between the solvation structures and the proton chemical shifts at 20 ℃. For the case of water as solvent shown in Fig. 4.5(a), the first peak of $g_{\mathrm{O\text{-}H}}$ appearing at about 1.8 Å represents hydrogen bonds with nearest neighbors. As can be readily seen from $g^{\mathrm{EI}}_{\mathrm{O\text{-}H}}$, the electrostatic interaction is dominant for this peak. Peculiar to water is the peak in $g^{\mathrm{EI}}_{\mathrm{O\text{-}O}}$ located at around 4.5 Å, indicative of a significant population of second neighbors in the tetrahedral ice-like structure. These solvation structures affect the chemical shift of solute water. Since both hydrogen and oxygen atoms of the solute water form hydrogen bonds with solvent water, the solute water molecule polarizes strongly, and the proton chemical shift shows the largest value. For the case of acetone shown in Fig. 4.6(a), $g_{\mathrm{O\text{-}O}}$ has two peaks around at 3.2 Å and 5.4 Å, which are desig-

nated by the arrows A and B. Their two peaks, respectively, correspond to the solvation structures in the first solvation shell in which the electronic structure of solute would be perturbed largely by the solvent molecules around. The first peak of $g_{\text{O-C}}$ is located at the radial distance in between the positions of the two peaks in $g_{\text{O-O}}$ stated above. The structure that the oxygen of acetone faces the water molecule, forming hydrogen bond, is named "A-structure", and the other is called "B-structure" in which the methyl groups of acetone direct toward the water molecule. These two solvation structures are schematically shown in the figure. Dimers are schematically drawn such that distances between the sites of water and acetone are almost coincident with the peak positions of the RDFs. Considering the RDFs originated in the hydrogen atom of water solute shown in Fig. 4.6(b), one can clearly understand how these solvation structures affect the chemical shift. The two peaks in $g_{\text{H-C}}$ present at positions within 5 Å correspond to the A- and B-structures, respectively, and can be decomposed into the peaks in $g^{\text{EI}}_{\text{H-C}}$ and in $g^{\text{PE}}_{\text{H-C}}$ distinctly. Besides, the first sharp peak in $g_{\text{H-O}}$ located at 2 Å represents the hydrogen bond in the A-structure. This suggests that the A-structure dominates the proton chemical shift of water molecule in acetone.

For the case of chloroform in Fig. 4.7(a), the shoulder and the peak located at about 3.5 Å and 4.5 Å, respectively, in $g_{\text{O-C}}$ fall in between the positions of the two peaks, designated by the arrows A and B, in $g_{\text{O-H}}$. The peaks are assigned to the two solvation structures "A" and "B", respectively, shown in the figure. The structure in which the hydrogen of chloroform forms hydrogen bond with the oxygen of water is the A-structure, the peak of which appears in $g^{\text{EI}}_{\text{O-H}}$ at around 2.4 Å in Fig. 4.7(b), and that in which the chlorines of chloroform face a water molecule is the B-structure. Similar to the case of acetone, the A-structure seems to dominate the proton chemical shift of water molecule in chloroform solvent.

Although both acetone and chloroform solvents form hydrogen bonds with water molecules, the charges on the atoms of both solvents, forming hydrogen bonds, are less

than those in solvent water molecules, and the electrostatic interaction affects only one(H or O) site of the solute water molecule. Therefore, the solute water is not polarized in those solvents as much as in water solvent, and the proton chemical shifts are less in those solvents than those in water. The difference between the proton chemical shifts in acetone and in chloroform depends on the difference between their dipole moments.

In the case of carbon tetrachloride shown in Fig. 4.8(a), the distinct solvation structure reflecting the electrostatic interaction does not appear, since each site of carbon tetrachloride has little charge, and the packing effect dominates its solvation structure. The electronic structure of water in carbon tetrachloride almost retains that in isolated molecule and therefore the proton chemical shift is nearly 0 ppm.

Next, I discuss the relationship between the temperature dependence of the proton chemical shifts and of the solvation structures. In Figs. 4.5(b), 4.6(c), 4.7(c), and 4.8(b), the RDFs at 10 ℃ and at 50 ℃ are shown. The arrows indicate the direction of change in the peak height of $g^{\mathrm{EI}}(r)$ at the radial distance due to temperature increase. For water solvent in Fig. 4.5(b), the decrease in the height of the first peaks of $g^{\mathrm{EI}}_{\mathrm{O\text{-}O}}$ and $g^{\mathrm{EI}}_{\mathrm{O\text{-}H}}$ with increasing temperature is caused by weakening of the hydrogen bonds with the nearest neighbors. In addition, the height of the peak of $g^{\mathrm{EI}}_{\mathrm{O\text{-}O}}$ around 4.5 Å decreases as temperature increases. This change indicates "melting" of the ice-like structure. As a result of these changes in the solvation structure, the proton chemical shift decreases with increasing temperature. For acetone and chloroform solvents in Figs. 4.6(c) and 4.7(c), the height of the peaks of g^{EI}, which correspond to the A-structure forming hydrogen bond with solute water, decreases as temperature increases. This change in the solvation structure with increasing temperature causes decrease in the proton chemical shifts. On the other hand, the height of the peaks in g^{PE} which correspond to the B-structure is almost retained constant with rising temperature. For carbon tetrachloride in Fig. 4.8(b), the solvation structure of g^{EI} disappears with increasing temperature.

The previous and present sections for the proton chemical shift for solvent effects

have demonstrated capability of predicting experimental results, and of discussing its temperature and density dependence in molecular level. From the quantitative viewpoint, on the other hand, the agreement of the temperature and solvent dependence of the chemical shifts with experiments are not always satisfactory. The chemical shift in each solvent is underestimated compared to that of experiments. In other words, the magnetic shielding is overestimated. Furthermore, the experimental results[18, 19] indicate that the gradients of the chemical shifts plotted as a function of temperature are proportional to their magnitudes. Concerning the relationship between the gradients of water and acetone solvents, the present method failed to reproduce the experiment. In the previous section, I have calculated the nuclear magnetic shielding constant for an oxygen atom of a water molecule solvated in water. The theory overestimated the magnetic shielding compared to the experimental value. The conclusion was not altered when the molecular geometry of water was changed. As a result, the direction of the chemical shift for oxygen atom relative to the gas phase was opposite to the empirical result. Why does the present theory overestimate the magnetic shieldings? From the analysis of the intermolecular interaction on the nuclear magnetic shielding using a molecular cluster, which is described in the following section, I conclude that the defect of our theory stated above is due to neglecting the overlap of electron clouds, e.g. the Pauli repulsion, between solute and solvent molecules. As shown in eq. (3.15), this overlap is disregarded in the present theory. This intermolecular effect on the chemical shifts is called the overlap effect,[10, 25, 26] and its importance on calculating the chemical shifts has been discussed in the recent studies.[15, 27, 28] In the next section, I examine how the overlap of electron clouds affects the nuclear magnetic shieldings.

III Intermolecular Effect on NMR Shielding Constant

In this section, I discuss the intermolecular effect including the Pauli repulsion on the nuclear magnetic shielding to verify the theory. I utilize a molecular cluster consisting of five water molecules that are arranged in a tetrahedral fashion shown in Fig. 4.9. The distance between oxygen atom of central molecule and those of surrounding molecules is 2.8 Å. The geometry of a water molecule is taken from that of the SPC model.[29]

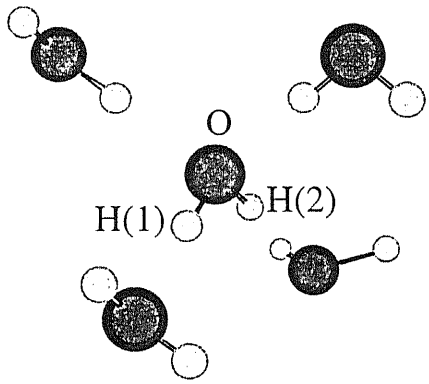

Figure 4.9: Geometrical arrangement of the water pentamer.

Two types of calculations are carried out for the nuclear magnetic shieldings of the pentamer. In one of them, the central molecule of the pentamer is treated by quantum chemistry and the surrounding molecules are treated as point charges centered at each nucleus. Hereafter, this model is called as "PC model". The other model treats all water molecules by quantum chemistry. This model is called as "QC model". For the point charges, the Mulliken charges estimated in the QC model are employed. Although the point charges determined by the least square fitting procedure in the RISM-SCF theory are also examined, the trend of the results, discussed as follows, is similar to that of the Mulliken charges. The PC model disregards the overlap of electrons between the central molecule and surrounding molecules, and the QC model includes the overlap. The interaction between the central molecule and the surrounding molecules in the PC model

is expected to be similar to that in the RISM-SCF theory, although the former model neglects both of the thermal averaging of solvent configurations and bulk solvent effect. Comparing these two results, one can examine how the overlap of electron clouds affects the nuclear magnetic shielding of the central molecule, and can inspect the accuracy of the RISM-SCF theory. For the basis set super position error in the nuclear magnetic shieldings of the QC model, the counterpoise correction[30] is made.[27, 31, 32] The calculations were carried out in the Hartree-Fock level with 6-311G** basis set. The nuclear magnetic shielding constants obtained for the two models are shown in Table 5.

TABLE 5. Nuclear magnetic shielding constants (ppm) obtained from the two different models.

Site	σ (PC)	σ (QC)	$\Delta\sigma^{a)}$
H(1)	28.2234	25.3773	2.846
H(2)	28.0615	25.2611	2.800
O	336.1045	315.3761	20.728

[a)] $\Delta\sigma = \sigma$ (PC) $- \sigma$ (QC)

From this result, it is found that the nuclear magnetic shieldings of both hydrogen and oxygen atoms in the PC model are larger than those in the QC model. This is caused by the insufficient description of the electronic structure due to the neglect of overlap of electron clouds.

One can decompose the equation (3.19) as follows:

$$\begin{aligned}
\sigma^X_{\alpha\beta} &= \sum_{\nu\lambda}\left\{P^{(0)}_{\nu\lambda}\left(H^{(1,1)}_{\nu\lambda}\right)^X_{\alpha\beta} + \left(P^{(1,0)}_{\nu\lambda}\right)_\alpha\left(H^{(0,1)}_{\nu\lambda}\right)^X_\beta\right\} \\
&= \sum_{\nu\lambda\in \mathrm{CM}}\left\{P^{(0)}_{\nu\lambda}\left(H^{(1,1)}_{\nu\lambda}\right)^X_{\alpha\beta} + \left(P^{(1,0)}_{\nu\lambda}\right)_\alpha\left(H^{(0,1)}_{\nu\lambda}\right)^X_\beta\right\} \\
&\quad +\sum_{\nu\lambda}{}'\left\{P^{(0)}_{\nu\lambda}\left(H^{(1,1)}_{\nu\lambda}\right)^X_{\alpha\beta} + \left(P^{(1,0)}_{\nu\lambda}\right)_\alpha\left(H^{(0,1)}_{\nu\lambda}\right)^X_\beta\right\} \\
&= \sigma^X_{\alpha\beta}(\text{polarization}) + \sigma^X_{\alpha\beta}(\text{softness}) + \sigma^X_{\alpha\beta}(\text{mix}), \qquad (4.2)
\end{aligned}$$

where CM indicates the central molecule which has nucleus X. $\sum'$ represents the rest of the summation, which is not included in the first and second terms. I have defined the following three terms:

$$\sigma^X_{\alpha\beta}(\text{polarization}) = \sum_{\nu\lambda\in \mathrm{CM}} P^{(0)}_{\nu\lambda}\left(H^{(1,1)}_{\nu\lambda}\right)^X_{\alpha\beta}, \qquad (4.3)$$

$$\sigma^X_{\alpha\beta}(\text{softness}) = \sum_{\nu\lambda\in \mathrm{CM}} \left(P^{(1,0)}_{\nu\lambda}\right)_\alpha\left(H^{(0,1)}_{\nu\lambda}\right)^X_\beta, \qquad (4.4)$$

$$\sigma^X_{\alpha\beta}(\text{mix}) = \sum_{\nu\lambda}{}'\left\{P^{(0)}_{\nu\lambda}\left(H^{(1,1)}_{\nu\lambda}\right)^X_{\alpha\beta} + \left(P^{(1,0)}_{\nu\lambda}\right)_\alpha\left(H^{(0,1)}_{\nu\lambda}\right)^X_\beta\right\}, \qquad (4.5)$$

$\boldsymbol{\sigma}^X$(polarization) corresponds essentially to the contribution from the spatial polarization of the electron cloud in the central molecule to the magnetic shielding, while $\boldsymbol{\sigma}^X$(softness) signifies that from the response of the electron cloud to the magnetic field. In other words, $\boldsymbol{\sigma}^X$(softness) gages how easily the electron cloud to change its shape for shielding responding to the magnetic field. $\boldsymbol{\sigma}^X$(mix) is the remaining contribution which is not contained in the PC model. The difference between the nuclear magnetic shieldings for the PC and QC models can be decomposed into the three terms:

$$\begin{aligned}
\Delta\sigma^X_{\alpha\beta} &= \sigma^X_{\alpha\beta}(\text{PC model}) - \sigma^X_{\alpha\beta}(\text{QC model}) \\
&= \Delta\sigma^X_{\alpha\beta}(\text{polarization}) + \Delta\sigma^X_{\alpha\beta}(\text{softness}) + \Delta\sigma^X_{\alpha\beta}(\text{mix}). \qquad (4.6)
\end{aligned}$$

From the first and second terms, one can understand the changes in the polarization of the electron cloud and in the softness of the electron cloud for the magnetic shieldings due

to neglecting of the electron overlap, respectively. Note that $\Delta\sigma^X_{\alpha\beta}(\mathrm{mix}) = 0 - \sigma^X_{\alpha\beta}(\mathrm{mix})$. The values of these three terms are shown in the Fig. 4.10.

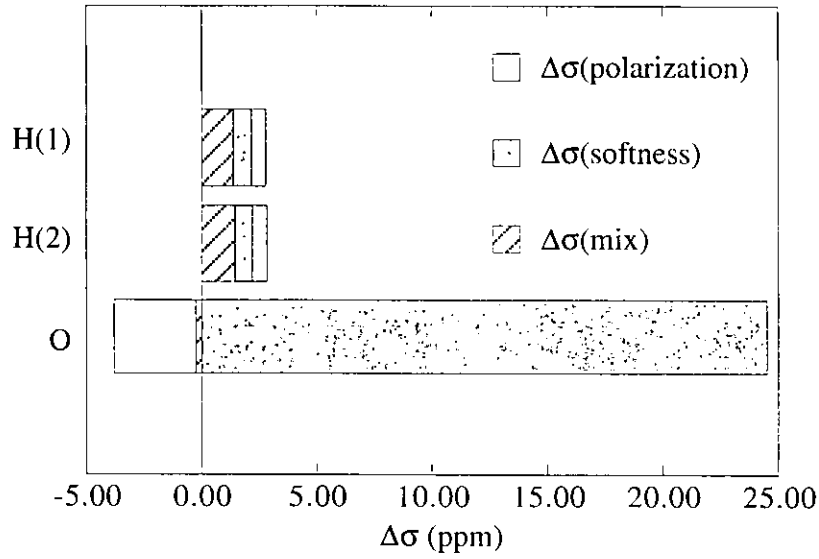

Figure 4.10: Changes in the components of the nuclear magnetic shielding for the central molecule in the pentamer due to missing of the electron overlap. $\Delta\boldsymbol{\sigma}^X$(polarization) and $\Delta\boldsymbol{\sigma}^X$(softness) correspond to the changes in the polarization of electron cloud and in the softness of the electron cloud for the nuclear magnetic shieldings, respectively. $\Delta\boldsymbol{\sigma}^X$(mix) is the remaining contribution to the nuclear magnetic shielding in the QC model, which is not contained in the PC model.

For both oxygen and hydrogen atoms, it is found that the lack of the overlap increases $\boldsymbol{\sigma}^X$(softness). It suggests that the electron cloud of the PC model can change easily its shape for shielding in comparison with that of the QC model. Particularly, the change in $\boldsymbol{\sigma}^X$(softness) is remarkable for the oxygen atom, and therefore, it is necessary for the theory to take the overlap effect into account. Although the theory takes reasonable account for solvent effect to the magnetic shielding as long as hydrogen atoms are concerned, the overlap effect should be included in the theory for discussion in quantitative level.

The softness of the electron cloud in the PC model can lead to the overestimation of the nuclear magnetic shielding obtained by the theories(the continuum, the QM/MM, and the RISM-SCF theory) in which the overlap of electron clouds between solute and

solvent molecules is disregarded. A new theory which includes the overlap effect is highly desired for the NMR chemical shifts in solution.

References

[1] W.L. Jorgensen, J. Am. Chem. Soc. **103**, 335 (1981).

[2] S. Ten-no, F. Hirata, S. Kato, J. Chem. Phys. **100**, 7443 (1994).

[3] Gaussian 94, Revision D.3, M. J. Frisch, G. W. Trucks, H. B. Schlegel, P. M. W. Gill, B. G. Johnson, M. A. Robb, J. R. Cheeseman, T. Keith, G. A. Petersson, J. A. Montgomery, K. Raghavachari, M. A. Al-Laham, V. G. Zakrzewski, J. V. Ortiz, J. B. Foresman, J. Cioslowski, B. B. Stefanov, A. Nanayakkara, M. Challacombe, C. Y. Peng, P. Y. Ayala, W. Chen, M. W. Wong, J. L. Andres, E. S. Replogle, R. Gomperts, R. L. Martin, D. J. Fox, J. S. Binkley, D. J. Defrees, J. Baker, J. P. Stewart, M. Head-Gordon, C. Gonzalez, and J. A. Pople, Gaussian, Inc., Pittsburgh PA, 1995.

[4] T. Helgaker, M. Jaszuński, K. Ruud, Chem. Rev. **99**, 293 (1999).

[5] W.T. Raynes, Nucl. Magn. Reson. **7**, 1 (1978).

[6] K. V. Mikkelsen, K. Ruud, T. Helgaker, Chem. Phys. Lett. **253**, 443 (1996).

[7] N. Matubayasi, C. Wakai, M. Nakahara, J. Chem. Phys. **107**, 9133 (1997).

[8] H. Sato, F. Hirata, J. Chem. Phys. **111**, 8545 (1999).

[9] J. Gauss, Chem. Phys. Lett. **229**, 198 (1994).

[10] J.C. Hindman, J. Chem. Phys. **44**, 4582 (1966).

[11] J. Homer, M.S. Mohammadi, J. Chem. Soc., Faraday Trans. 1 **84**, 2959 (1988).

[12] I. M. Svishchev, P. G. Kusalik, J. Am. Chem. Soc. **115**, 8270 (1993).

[13] R.E. Wasylishen, S. Mooibroek, J.B. Macdonald, J. Chem. Phys. **81**, 1057 (1984).

[14] K. V. Mikkelsen, P. Jϕrgensen, K. Ruud, T. Helgaker, J. Chem. Phys. **106**, 1170 (1997).

[15] T. M. Nymand, P. -O. Åstrand, K. V. Mikkelsen, J. Phys. Chem. B **101**, 4105 (1997).

[16] D.B. Chesnut, B.E. Rusiloski, J. Mol. Struct. (*THEOCHEM*) **314**, 19 (1994).

[17] V.G. Malkin, O.L. Malkina, G. Steinebrunner, H. Huber, Chem. Eur. J. **2**, 452 (1996).

[18] M. Nakahara and C. Wakai, Chem. Lett. 809 (1992).

[19] M. Nakahara, DENKI KAGAKU (presently Electrochemistry) **62**, 108 (1994) (in Japanese).

[20] W. L. Jorgensen, J. M. Briggs, and M. L. Contreras, J. Phys. Chem. **94**, 1683 (1990).

[21] E. M. Duffy, D. L. Severance, and W. L. Jorgensen, J. Am. Chem. Soc. **114**, 7535 (1992).

[22] W. Dietz and K. Heinzinger, Ber. Bunsenges. Phys. Chem. **89**, 968 (1985).

[23] M. D. Harmony, V. W. Laurie, R. L. Kuczkowski, R. H. Schwendeman, D. A. Ramsay, F. J. Lovas, W. J. Lafferty, and A. G. Maki, J. Phys. Chem. Ref. Data **8**, 619 (1979).

[24] *Handbook of Chemistry and Physics*, 76th ed., edited by D. R. Lide (CRC, Boca Raton,1995).

[25] A. D. Buckingham and K. P. Lawley, Mol. Phys. **3**, 219 (1960).

[26] P. J. Berkeley, Jr., and M. W. Hanna, J. Chem. Phys. **41**, 2530 (1964).

[27] Q. Cui and M. Karplus, J. Phys. Chem. B **104**, 3721 (2000).

[28] T. Yamazaki, H. Sato, and F. Hirata, Chem. Phys. Lett. **325**, 668 (2000).

[29] H. J. C. Berendsen, J. P. M. Postma, W. F. van Gunsteren, and J. Hermans, *Intermolecular Forces*, edited by B. Pullman (Reidel, Dordrecht, 1981), p.331.

[30] S. F. Boys and F. Bernardi, Mol. Phys. **19**, 553 (1970).

[31] S. Ferchiou and C. Giessner-Prettre, Chem. Phys. Lett. **103**, 156 (1983).

[32] D. B. Chesnut and B. E. Rusiloski, J. Phys. Chem. **97**, 2839 (1993).

Chapter 5

Conclusions

In this thesis, I have proposed a new method for the theoretical treatment of the nuclear magnetic shielding in solution. In this chapter, I summarize my work, and present the prospects of my future study.

In order to investigate the relation between the NMR shielding constants and solvation structure, a new theory of the nuclear magnetic shielding in solution was proposed, based on the *ab initio* electronic structure theory combined with the reference interaction site model in statistical mechanics for molecular liquids(RISM-SCF). The RISM-SCF method treats both solute and solvent molecules in atomic level, and determines the solute electronic structure and the statistical solvent distribution in a self-consistent manner. Thus, the method provides a microscopic picture for the solvent effect on the electronic structure of a solute molecule within reasonable computation cost. Furthermore, this approach is suitable for studying the relationship between the chemical shifts and solute-solvent interactions, because the RISM-SCF method treats a solute-solvent system, in which a solute molecule is at infinite dilution in solvent.

In the RISM-SCF framework, the nuclear magnetic shielding tensor $\boldsymbol{\sigma}^X$ of a nucleus X can be expressed as the mixed second derivative of the free energy. The final expression of the nuclear magnetic shielding tensor based on the RISM-SCF is as follows:

$$\sigma^X_{\alpha\beta} = \sum_{\nu\lambda} \left\{ P^{(0)}_{\nu\lambda} \left(H^{(1,1)}_{\nu\lambda} \right)^X_{\alpha\beta} + \left(P^{(1,0)}_{\nu\lambda} \right)_\alpha \left(H^{(0,1)}_{\nu\lambda} \right)^X_\beta \right\}. \tag{5.1}$$

$P^{(0)}_{\nu\lambda}$ can be calculated from the field-independent RISM-SCF method. $\left(H^{(1,1)}_{\nu\lambda}\right)^{X}_{\alpha\beta}$ and $\left(H^{(0,1)}_{\nu\lambda}\right)^{X}_{\beta}$ are the same expressions with those from the conventional *ab initio* calculation in gas phase, while $\left(P^{(1,0)}_{\nu\lambda}\right)_{\alpha}$ are determined by solving the first-order coupled-perturbed Hartree-Fock equation in the RISM-SCF framework.

First, I implemented this method to a water molecule solvated in water, and confirmed that the method is valid not only for the temperature dependence, but also for the density dependence of the proton chemical shift of a water molecule in water. Next, I implemented this method to a water molecule solvated in water, acetone, chloroform, and carbon tetrachloride. As a result, the present method qualitatively reproduces the two observations in experiment. First, solvent effects on the proton chemical shifts of a solute water molecule are in the following sequence over the temperature range studied,

$$\text{in water} > \text{in acetone} > \text{in chloroform} > \text{in carbon tetrachloride}.$$

Secondly, the proton chemical shifts decrease with increasing temperature. These results demonstrate capability of the theory to predict experimental results at least qualitatively. In order to discuss the relation between the solvation structures and the proton chemical shifts, the solvation structure was decomposed into two terms described as follows. The first is the radial distribution function(RDF) "g^{PE}" concerned with the packing effect defined by neglecting the electrostatic interactions between solute and solvents. The second is the RDFs "g^{EI}" associated with the electrostatic interactions and is defined by the following equation,

$$g^{\mathrm{EI}}(r) = g(r; \mathrm{EI} \neq 0) - g^{\mathrm{PE}}(r; \mathrm{EI} = 0). \tag{5.2}$$

where $g(r; \mathrm{EI} \neq 0)$ is the RDF with full solute-solvent interactions. From the decomposition analysis, I clarified the relation between solvation structures and the proton chemical shifts. Furthermore, from a separate calculation using a molecular cluster, I confirmed that inclusion of the overlap effect in the intermolecular interaction is necessary for quantitative prediction. It is found that the electron cloud becomes soft in terms of response

to the magnetic field due to the missing of the electronic overlap, which in turn causes the overestimation of the nuclear magnetic shielding.

As can be understood from the analysis using the molecular cluster, it is difficult for the present method to handle the solute-solvent system in which the overlap is not negligible, such as the nuclear magnetic shielding for the oxygen atom of a water molecule in aqueous environment. Nevertheless, the present method is promising in some application in which the overlap is not significant. Such applications can include the proton chemical shift, which is studied in extremely wide range of fields in science. For example, in biochemistry, it would be of great interest to investigate a relation between the chemical shift and the conformational change of a biomolecule in solution. Considering the importance of pressure effect on protein conformation as mentioned in Introduction, the study on the pressure dependence of the chemical shifts of amino acids in solution would also be an intriguing problem. It is expected that the theory would be applied successfully to a wide variety of problems in solution.

One of my next subjects is building up a new electronic structure theory in solution including the quantum mechanical solute-solvent interaction corresponding to the overlap effect for the NMR shielding constants. The theory will open up a new horizon in the investigation of solute-solvent interactions in solution. Such investigations include the chemical shifts of noble gases in solutions, which are recently utilized for investigating protein structures, and the spectra of a solvated electron in solution. The study is now in progress.

Appendix

Elucidating the mechanism of solvation effect on molecules is of great importance, because most chemical processes of interest occur in solution. It is essential for this purpose to develop theoretical methods for evaluating the electronic structure in solution. In order to elucidate chemical properties of solute molecules, which originate from electrons in molecules, quantum chemical treatments are required. On the other hand, in order to understand properties of solution, which consists of huge number of molecules, statistical treatments are needed. Constructing an electronic structure theory in solution requires to unite the two different theoretical frameworks stated above. The difficulty is concentrated in a problem how we describe the solute-solvent interaction. The majority of theories developed in the last two decades adopts a combination of the electrostatic and classical short-range interactions as the solute-solvent interaction. Obviously, these theories lack short-range quantum effects such as the exchange repulsion between solutes and solvents.

In the recent development of the theoretical method for solution, theories for the NMR chemical shift in solution have been proposed by some workers.[1, 2, 3] In their papers, they have confirmed that the short-range quantum mechanical effects, which is referred to as the overlap effect on the nuclear magnetic shielding,[4, 5, 6] is indispensable for estimating the NMR chemical shift in solution not only quantitatively but also qualitatively sometimes. Therefore, a new theory which accounts the overlap effect is highly desired for the NMR chemical shift in solution. Such theory will not only provide valuable insight into the chemical shifts but also open up a new horizon in the investigation of various chemical processes in solutions.

In this appendix, we propose an electronic structure theory in solution including the quantum solute-solvent interaction for an atomic molecule solvated in atomic solvent molecules as the first step. This theory consists of two theoretical frameworks: the Ornstein-Zernike(OZ) equation for simple liquids and the *ab initio* electronic structure theory. In this framework, the solute-solvent interaction is described by using the "environmental potential" method proposed by Katsuki *et al.*,[7] which accounts for the short-range quantum effect exerted on a solute from solvent molecules along with usual long-range interactions.

The organization of this chapter is as follows. In Sec. A.I, we review the effective hamiltonian method for the environmental effect. The effective hamiltonian method is originally developed by Huzinaga *et al.*,[8] and the environmental potential method is a revised form of the effective hamiltonian method.[7] In Sec. A.II, we propose a new electronic structure theory in solution including the quantum chemical solute-solvent interaction. We follow the strategy[9] developed in the RISM-SCF theory for deriving the equations. In Sec. A.III, we show preliminary results concerning the electronic structure of a neon molecule solvated in neon liquid, which is obtained by using the new method.

A.I Effective Hamiltonian Method for Environmental Effect

The Fock operator for the molecular cluster consisting of many atomic molecules, is expressed as follows:

$$F^{\mathrm{All}} = -\frac{1}{2}\Delta - \sum_{N}\frac{Z^{N}}{r} + \sum_{r,s}(2J_{rs} - K_{rs})\sum_{j} c_{rj}c_{sj}, \tag{A1}$$

where Z^N is the nuclear charge of nucleus N. r is the distance between an electron and nucleus. J_{rs} and K_{rs} are the Coulomb and exchange integrals, respectively. c_{rj} is the molecular orbital coefficient. r and s indicate the atomic orbitals, and j means the molecular orbital. We divide the system into one central molecule(Cent) and environmental

molecules(Env). Then, the Fock operator in eq. (A1) can be written as

$$F^{\mathrm{All}} = -\frac{1}{2}\Delta - \frac{Z^{\mathrm{Cent}}}{r} + \sum_{r,s}^{\text{on Cent}} (2J_{rs} - K_{rs}) \sum_{j} c_{rj}c_{sj} - \sum_{D}^{\text{on Env}} \frac{Z^{D}}{r} + \sum_{t,u}^{\text{Rest of sum}} (2J_{tu} - K_{tu}) \sum_{j} c_{tj}c_{uj}. \quad \text{(A2)}$$

On the basis of eq. (A2), the Fock operator of the central molecule including the effects from the environmental molecules can be written as:

$$F \cong -\frac{1}{2}\Delta - \frac{Z^{\mathrm{Cent}}}{r} + \sum_{r,s}^{\text{on Cent}} (2J_{rs} - K_{rs}) \sum_{j} c_{rj}c_{sj} + \sum_{D}^{\mathrm{Env}} \bar{V}^{D}, \quad \text{(A3)}$$

where

$$\bar{V}^{D} = -\frac{Z^{D}}{r} + \sum_{r,s}^{\text{on } D} (2J_{rs} - K_{rs}) \sum_{j} c^{D}_{rj}c^{D}_{sj}. \quad \text{(A4)}$$

Note that c^{D}_{rj} is the molecular orbital coefficient of the environmental molecule D. The coefficient is determined variationally using isolated molecule D. This approximation can be called as a "frozen environment approximation." The element of the above Fock operator is written as follows:

$$F_{pq} \cong H_{pq} + G_{pq} + \sum_{D}^{\mathrm{Env}} \langle \chi_p | \bar{V}^{D} | \chi_q \rangle, \quad \text{(A5)}$$

where

$$\langle \chi_p | \bar{V}^{D} | \chi_q \rangle = \langle \chi_p | \frac{-Z^{D}}{r} | \chi_q \rangle + \sum_{r,s}^{\text{on } D} P^{D}_{rs} \left[(\chi_p \chi_q | \chi_r \chi_s) - \frac{1}{2} (\chi_p \chi_s | \chi_r \chi_q) \right]. \quad \text{(A6)}$$

Note that p and q correspond to the atomic orbitals of the central molecule. On the other hand, r and s indicate the environmental molecule. H_{pq} and G_{pq} are the one- and two-electron terms of the central molecule, respectively. In order to compute $\{F_{pq}\}$ from equation (A5), we still need to calculate a majority of molecular integrals in eq. (A1). To avoid this difficulty, we replace the operator $\bar{V}^{D}$ by an appropriate spectral representation:

$$\bar{V}^{D} \rightarrow \Omega^{D} \bar{V}^{D} \Omega^{D}, \quad \text{(A7)}$$

where

$$\Omega^D = \sum_{a,b}^{\text{on } D} |f_a\rangle (\mathrm{S}^{-1})_{ab} \langle f_b|. \tag{A8}$$

Then,

$$F_{pq} \sim H_{pq} + G_{pq} + \sum_{D}^{\text{Env}} \langle \chi_p | \Omega^D \bar{V}^D \Omega^D | \chi_q \rangle. \tag{A9}$$

In this framework, since only molecular orbitals of the central molecule are treated explicitly, those of the environmental molecules should be prevented from collapsing into the environmental region. In this work, we solve this problem by simply adding the following projection operator, so-called the shift operator, to eq. (A9):

$$P^D_{\text{shift}} = \sum_{j}^{\text{occ on } D} \sum_{r,s}^{\text{on } D} -n\epsilon^D_j |\chi_r\rangle c^D_{rj} c^D_{sj} \langle \chi_s|, \tag{A10}$$

where ϵ^D_j is the j-th molecular orbital energy of the isolated molecule D, and n is an arbitrary parameter. In the present stage, n is determined so as to reproduce the results obtained by all-electron calculation. Finally, we obtain the approximated Fock matrix with the environmental effect:

$$F_{pq} = H_{pq} + G_{pq} + \sum_{D}^{\text{Env}} \langle \chi_p | V^D | \chi_q \rangle, \tag{A11}$$

where

$$\begin{aligned} \langle \chi_p | V^D | \chi_q \rangle &= \langle \chi_p | \Omega^D \{ \bar{V}^D + P^D_{\text{shift}} \} \Omega^D | \chi_q \rangle \\ &= \langle \chi_p | \Omega^D \{ \frac{-Z^D}{r} + \sum_{j}^{\text{on } D} (2J_j - K_j) + P^D_{\text{shift}} \} \Omega^D | \chi_q \rangle. \end{aligned} \tag{A12}$$

This is the "environmental potential" in the spectral representation.

Explicit form of each matrix element is summarized as follows for convenience. Nucleus-electron attraction part:

$$\langle \chi_p | \Omega^D \{ \frac{-Z^D}{r} \} \Omega^D | \chi_q \rangle = \sum_{a,b,c,d}^{\text{on } D} \langle \chi_p | f_a \rangle (\mathrm{S}^{-1})_{ab} \langle f_b | \frac{-Z^D}{r} | f_c \rangle (\mathrm{S}^{-1})_{cd} \langle f_d | \chi_q \rangle. \tag{A13}$$

Two electron part:

$$\langle\chi_p|\Omega^D\{\sum_j^{\text{on } D}(2J_j - K_j)\}\Omega^D|\chi_q\rangle$$

$$= \sum_{a,b,c,d}^{\text{on } D} \langle\chi_p|f_a\rangle(\mathrm{S}^{-1})_{ab}\langle f_b|\sum_j^{\text{on } D}(2J_j - K_j)|f_c\rangle(\mathrm{S}^{-1})_{cd}\langle f_d|\chi_q\rangle$$

$$= \sum_{a,b,c,d}^{\text{on } D} \langle\chi_p|f_a\rangle(\mathrm{S}^{-1})_{ab}(\sum_{r,s}^{\text{on } D} P^D_{rs}G'_{bcrs})(\mathrm{S}^{-1})_{cd}\langle f_d|\chi_q\rangle, \quad \text{(A14)}$$

where

$$\sum_{r,s}^{\text{on } D} P^D_{rs}G'_{bcrs} = \sum_{r,s}^{\text{on } D} P^D_{rs}\left[(f_bf_c|\chi_r\chi_s) - \frac{1}{2}(f_b\chi_s|\chi_rf_c)\right]. \quad \text{(A15)}$$

Shift operator:

$$\langle\chi_p|\Omega^D\{P^D_{\text{shift}}\}\Omega^D|\chi_q\rangle$$

$$= \sum_{a,b,c,d}^{\text{on } D} \langle\chi_p|f_a\rangle(\mathrm{S}^{-1})_{ab}\langle f_b|P^D_{\text{shift}}|f_c\rangle(\mathrm{S}^{-1})_{cd}\langle f_d|\chi_q\rangle$$

$$= \sum_{a,b,c,d}^{\text{on } D} \langle\chi_p|f_a\rangle(\mathrm{S}^{-1})_{ab}\sum_{r,s}^{\text{on } D}\langle f_b|\chi_r\rangle W^D_{rs}\langle\chi_s|f_c\rangle(\mathrm{S}^{-1})_{cd}\langle f_d|\chi_q\rangle, \quad \text{(A16)}$$

where

$$W^D_{rs} = \sum_j^{\text{occ on } D} -n\epsilon^D_j c^D_{rj}c^D_{sj}. \quad \text{(A17)}$$

A.II New Electronic Structure Theory in Solution

In this section, an electronic structure theory in solution including quantum intermolecular interaction is proposed. The solute-solvent interaction is described by using the "environmental potential" mentioned in the previous section. Construction of the theory is carried out for the simplest system, an infinite dilute solute(atom)-solvent(atom) system as the first step.

In this framework, the interaction potential between solute and solvent, $u_{uv}(R)$, separated by the distance R along with an arbitrary axis in the 3-dimensional coordinate, is described by using the environmental potential as follows:

$$u_{uv}(R) = 2\sum_i \langle \varphi_i \mid V^{\text{solv}} \mid \varphi_i \rangle$$
$$= \sum_{p,q}^{\text{on solv}} \sum_{a,b,c,d} P_{pq}\langle \chi_p | f_a \rangle (\mathbf{S}^{-1})_{ab} \langle f_b | \{ \frac{-Z}{r} + \sum_j^{\text{on solv}} (2J_j - K_j) + P_{\text{shift}} \} | f_c \rangle (\mathbf{S}^{-1})_{cd} \langle f_d | \chi_q \rangle. \tag{A18}$$

where φ_i are the molecular orbitals of solute, which are expressed as a linear combination of the atomic orbitals χ_p. r is the separation between an electron and a solvent nucleus which has the charge Z. J_j and K_j are the Coulomb and exchange operator, respectively. P_{shift} is the shift operator. f_a are the basis sets on which the quantum chemical effects of solvent are projected, and $\mathbf{S}$ is the overlap matrix between the basis sets. Note that f_a have the same origin with the solvent nucleus. Therefore the overlap matrix element $\langle \chi_p | f_a \rangle$ is the function of $\mathbf{R} = (R, \theta, \phi)$. The solvated Fock operator can be derived by the variation of the solvation free energy A in the same sprit as in the RISM-SCF framework. A is expressed as

$$A = E_{solute} + \Delta\mu. \tag{A19}$$

E_{solute} can be estimated by the Hartree Fock(HF) method, and the free energy derived from the OZ/HNC equation is adopted:

$$E_{solute} = 2\sum_i \langle \varphi_i \mid h \mid \varphi_i \rangle + \sum_{i,j} (2\langle \varphi_i\varphi_i \mid \varphi_j\varphi_j \rangle - \langle \varphi_i\varphi_j \mid \varphi_j\varphi_i \rangle) + E_{nuc}, \tag{A20}$$

$$\Delta\mu = -\frac{\rho}{\beta}\int \{\exp[-\beta u_{uv}(R) + t_{uv}(R)] - 1 - t_{uv}(R) - h_{uv}(R)t_{uv}(R) + \frac{1}{2}h_{uv}(R)^2\} d\mathbf{R}$$
$$-\frac{1}{\beta}\int \{-c_{uv}(R)h_{uv}(R) + \frac{1}{2}c_{uv}(R)c_{uv}(R) * \chi_{vv}\} d\mathbf{R}. \tag{A21}$$

In the above expression, β is equal to $\frac{1}{k_B T}$, where k_B and T are the Boltzmann constant and temperature, respectively. ρ is the density of solvent. c_{uv} and h_{uv} are the direct and total correlation functions, respectively. t_{uv} is equal to $h_{uv} - c_{uv}$. χ_{vv} is the pure solvent site

density pair correlation functions. Note that χ_{vv} is evaluated by the OZ/HNC equation for solvent-solvent system with the Lennard-Jones(LJ) interaction in the present stage. The quantity A can be regarded as a functional of the functions $h_{\alpha s}$, $c_{\alpha s}$, $t_{\alpha s}$, and φ_i. We define I with the constrains to the orthonormality of the molecular orbitals as

$$I = A[\mathbf{h}, \mathbf{c}, \mathbf{t}, \boldsymbol{\varphi}] - \sum_{i,m} \epsilon_{im}(\langle \varphi_i \mid \varphi_m \rangle - \delta_{im}), \tag{A22}$$

Variations with respect to the functions yield

$$\begin{aligned}
\delta I =& 2\sum_i \langle \delta\varphi_i \mid h \mid \varphi_i \rangle + 2\sum_i \langle \delta\varphi_i \mid \sum_j (2J_j - K_j) \mid \varphi_i \rangle \\
&- \rho \int 2\sum_i \langle \delta\varphi_i \mid V^{\text{solv}} \mid \varphi_i \rangle \exp[-\beta u_{uv}(R) + t_{uv}(R)] d\mathbf{R} \\
&- \frac{\rho}{\beta} \int (\exp[-\beta u_{uv}(R) + t_{uv}(R)] - h_{uv}(R) - 1)\delta t_{uv} d\mathbf{R} \\
&- \frac{\rho}{\beta} \int (-t_{uv}(R) + h_{uv}(R) - c_{uv}(R))\delta h_{uv} d\mathbf{R} \\
&- \frac{1}{\beta} \int (h_{uv}(R) + c_{uv}(R) * \chi_{vv})\delta c_{uv} d\mathbf{R} \\
&- \sum_{i,m} \epsilon_{im} \langle \delta\varphi_i \mid \varphi_m \rangle.
\end{aligned} \tag{A23}$$

The fourth, fifth, and sixth terms give the OZ/HNC equation. One can eventually obtain the expression for the solvated Fock matrix element:

$$F_{pq} = H_{pq} + G_{pq} + \rho \int \langle \chi_p \mid V^{\text{solv}} \mid \chi_q \rangle g_{uv}(R) d\mathbf{R}, \tag{A24}$$

where H_{pq} and G_{pq} are the usual one- and two-electron terms, respectively. The last term in the right hand side of the above equation is rewritten explicitly as

$$\begin{aligned}
&\int \langle \chi_p \mid V^{\text{solv}} \mid \chi_q \rangle g_{uv}(R) d\mathbf{R} \\
&= \int \sum_{a,b,c,d}^{\text{on solv}} \langle \chi_p | f_a \rangle (\mathbf{S}^{-1})_{ab} \langle f_b | \{ \frac{-Z}{r} + \sum_j^{\text{on solv}} (2J_j - K_j) + P_{\text{shift}} \} | f_c \rangle (\mathbf{S}^{-1})_{cd} \langle f_d | \chi_q \rangle g_{uv}(R) d\mathbf{R},
\end{aligned} \tag{A25}$$

and therefore, $\Upsilon_{pq} \equiv \langle \chi_p \mid V^{\text{solv}} \mid \chi_q \rangle$ is the function of $\mathbf{R}$. In the present stage, we adopt the simple manner for evaluating $\Upsilon_{pq}(R, \theta, \phi)$ as follows.

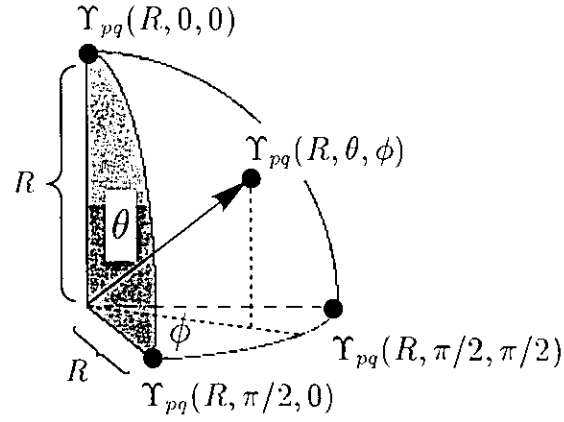

Figure A-1: Octant with the radius R.

Considering the sphere with the radius R and dividing the sphere into octant, each point in the spherical surface has the value of $\Upsilon_{pq}(R,\theta,\phi)$, as shown in Fig. A-1. Then, the value at each point can be represented by using the values of the three vertices. In the case of the first octant, for example, three vertices have the values of $\Upsilon_{pq}(R,0,0)$, $\Upsilon_{pq}(R,\pi/2,0)$, and $\Upsilon_{pq}(R,\pi/2,\pi/2)$, therefore, the values of $\Upsilon_{pq}(R,\theta,\phi)$ in the first octant can be represented by using these three values as follows:

$$\Upsilon_{pq}(R,\theta,\phi) = \sin\theta\cos\phi\Upsilon_{pq}(R,\pi/2,0) + \sin\theta\sin\phi\Upsilon_{pq}(R,\pi/2,\pi/2) + \cos\theta\Upsilon_{pq}(R,0,0). \tag{A26}$$

Adapting the same treatment for the rest of octants, finally, we can get the relation:

$$\begin{aligned}
&\rho\int\langle\chi_p \mid V^{\mathrm{solv}} \mid \chi_q\rangle g_{uv}(R)d\mathbf{R} \\
&= \rho\int\int\int \Upsilon_{pq}(R,\theta,\phi)g_{uv}(R)R^2\sin\theta dRd\theta d\phi \\
&= \rho\int \pi\Big[\Upsilon_{pq}(R,0,0) + \Upsilon_{pq}(R,\pi/2,0) + \Upsilon_{pq}(R,\pi/2,\pi/2) + \Upsilon_{pq}(R,\pi,0) \\
&\quad + \Upsilon_{pq}(R,\pi/2,\pi) + \Upsilon_{pq}(R,\pi/2,3\pi/2)\Big]R^2 g_{uv}(R)dR.
\end{aligned} \tag{A27}$$

In the case of the evaluation of the atomic orbital(AO) integrals, generally speaking, eq. (A27) is an approximation. Only the case that the AOs consist of the s-type and p-type

functions, the relation in eq. (A27) is exact. Preserving the values at each grid point used for the integration of the correlation functions for each axis, namely, $\Upsilon_{pq}(R,0,0)$, $\Upsilon_{pq}(R,\pi/2,0)$, $\Upsilon_{pq}(R,\pi/2,\pi/2)$, $\Upsilon_{pq}(R,\pi,0)$, $\Upsilon_{pq}(R,\pi/2,\pi)$, and $\Upsilon_{pq}(R,\pi/2,3\pi/2)$, we can evaluate the solvated Fock matrix elements. We thus obtained a set of equations for the electronic structure in solution, i.e., the solute-solvent OZ equation, the HNC equation, and the modified HF equation incorporating the solvation effect, which are required to determine by a self-consistent procedure.

A.III Electronic Structure of a Neon Molecule Solvated in Neon Liquid

In this section, we show preliminary results obtained by using the electronic structure theory in solution formulated in the previous sections. Here, the electronic structure of a neon molecule solvated in neon liquid is calculated to demonstrate the validity of the new method. On the calculation of the density pair correlation function in pure solvent(eq. (2.124)), the values σ=2.79 Å and ϵ=0.07318 kcal/mol are assigned to the LJ parameters of the neon solvent site[10]. The electronic wave functions of the solute neon molecule were calculated in the HF level with 6-311G basis set. The environmental potential was generated by projecting the electronic wave functions of the solvent neon molecule, which were calculated in the HF level with 6-311G basis set, on the deconstructed 6-311G basis set. In the present work, the parameter for the shift operator is determined so as to reproduce the interaction energy of the neon dimer obtained by all-electron calculation with 6-311G basis set qualitatively, considering the fact that the liquid structure, roughly speaking, is dominated by the behavior in the beginning of the repulsive part of the intermolecular interaction: $n = 4.0$. The results for the interaction energy of neon dimer by using the environmental potential method with the parameter $n = 4.0$ are shown in Fig. A-2 along with the results from the all-electron calculation. Note that the electronic structure of a neon molecule solvated in neon liquid can not be treated by the theories

which lack the short-range quantum mechanical effects such as the exchange repulsion between the solutes and solvents.

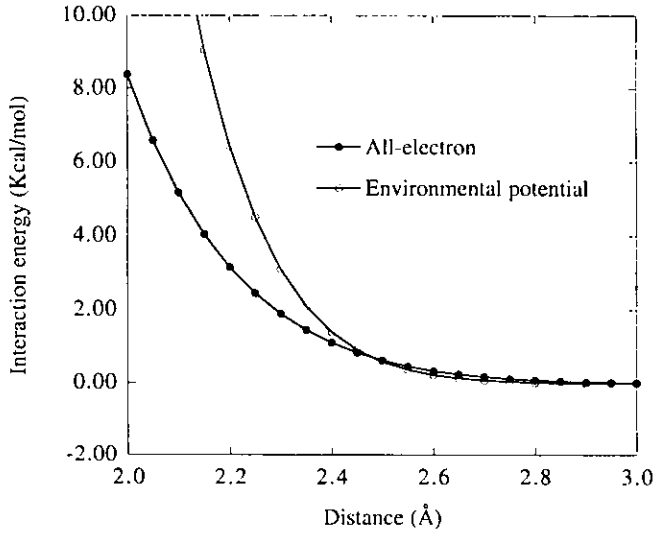

Figure A-2: The results for the interaction energy of neon dimer by using the environmental potential method using the parameter $n = 4.0$ and the all-electron calculation.

The results for the radial distribution functions(RDFs) between the solute and solvent neons obtained by the new method are shown in Fig. A-3 along with those from the OZ/HNC equation using the LJ interactions with the same parameters for χ_{vv}. The density dependence of the RDFs at 100 K is shown in Fig. A-3(a) and at 300 K is in (b). Note that the density is scaled by the LJ parameter σ. As shown in the figures, the present method reasonably reproduces the density dependence of the RDFs obtained by using LJ interaction potential: decrease in the solvation structure around the neon solute with decreasing the density. These results demonstrate capability of the present theory to investigate the solvation structure at least in the qualitative level. The environmental potential in the HF framework, the attractive part of the interaction potential cannot be described. Therefore, the solvation structure is more readily destructured than that obtained by using the LJ interactions.

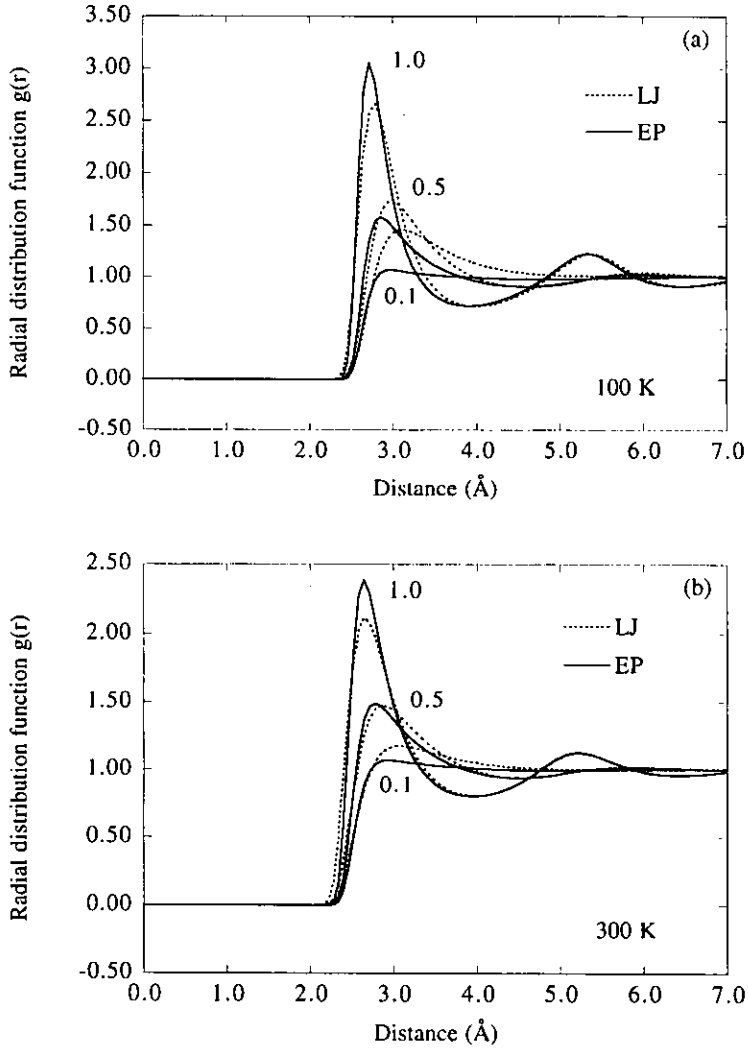

Figure A-3: The results for the radial distribution functions(RDFs) between the solute neon and solvent neon obtained by the two methods. LJ indicates the OZ/HNC equation with the Lennard-Jones(LJ) interaction. EP indicates the present method using the environmental potential. (a) is the results at 100 K, and (b) is at 300 K.

In Fig. A-4, the density dependence of the electronic spatial extent, which are the expected values of r^2, of a solute neon molecule is shown along with that of an isolated neon molecule. Fig. A-4 is the principal result in this Appendix. As can be readily seen from the figure, the extent decreases with increasing the density. Additionally, the electronic extent of solute neon molecule at 300 K is more sensitive to the density change

than that at 100 K. These results are in accord with our intuition, strongly indicating that our attempt is promising.

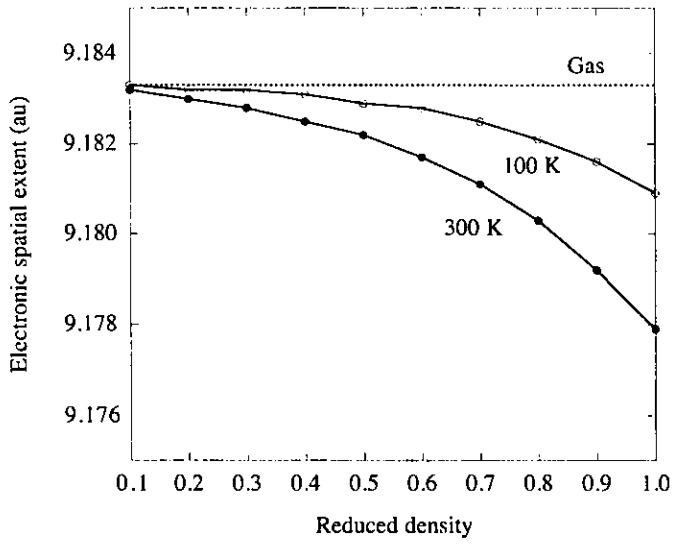

Figure A-4: The density dependence of the electronic spatial extents of solute neon molecule, along with the electronic spatial extent of isolated neon molecule.

The methodology proposed in this appendix has in principle a great prospect to be extended to molecular liquids. Following two phases in the extension are conceivable. In the first phase, we employ the RISM theory to describe the pair density correlation functions between molecules, giving the molecular geometry. The intermolecular atomic-interactions can be calculated using the pseudo potential method described in this appendix with some approximation: in case of water, only electrons in oxygen atoms are treated quantum chemically. The second phase is much more difficult and challenging. There, all atoms in the system is treated with quantum chemistry, thereby, the molecular geometry along with the liquid structure should be produced entirely from the electronic structure theory combined with the OZ type equation for atomic liquids. We are confident in achieving such a goal in near future.

References

[1] T. M. Nymand, P. -O. Åstrand, and K. V. Mikkelsen, J. Phys. Chem. B **101**, 4105 (1997).

[2] Q. Cui and M. Karplus, J. Phys. Chem. B **104**, 3721 (2000).

[3] T. Yamazaki, H. Sato, and F. Hirata, J. Chem. Phys. **115**, 8949 (2001).

[4] A. D. Buckingham and K. P. Lawley, Mol. Phys. **3**, 219 (1960).

[5] P. J. Berkeley, Jr., and M. W. Hanna, J. Chem. Phys. **41**, 2530 (1964).

[6] J.C. Hindman, J. Chem. Phys. **44**, 4582 (1966).

[7] S. Katsuki, Can. J. Chem. **70**, 285 (1992).

[8] S. Huzinaga, Can. J. Chem. **73**, 619 (1995).

[9] H. Sato, F. Hirata, and S. Kato, J. Chem. Phys. **105**, 1546 (1996).

[10] J. J. Morales and M. J. Nuevo, J. Comput. Chem. **16**, 105 (1995).